Year : 2020

IMPROVING HYDROLOGIC MODEL REALISM USING STABLE WATER ISOTOPES IN THE SWISS ALPS

Beria Harsh

Beria Harsh, 2020, IMPROVING HYDROLOGIC MODEL REALISM USING STABLE WATER ISOTOPES IN THE SWISS ALPS

Originally published at : Thesis, University of Lausanne

Posted at the University of Lausanne Open Archive http://serval.unil.ch
Document URN : urn:nbn:ch:serval-BIB_F160C96E90306

UNIL | Université de Lausanne

Faculté des géosciences et de l'environnement
Institut des dynamiques de la surface terrestre

IMPROVING HYDROLOGIC MODEL REALISM USING STABLE WATER ISOTOPES IN THE SWISS ALPS

Thèse de doctorat

Présentée à la
Faculté des géosciences et de l'environnement
Institut des dynamiques de la surface terrestre
de l'Université de Lausanne

pour l'obtention du grade de
Doctorat en sciences de l'environnement

par

Harsh Beria

Titulaire d'un
Master of Technology
Indian Institute of Technology Kharagpur (India)

JURY

Prof. Bettina Schaefli	Directeur de thèse
Prof. Grégoire Mariéthoz	co-directeur de thèse
Prof. Torsten Vennemann	Expert interne
Prof. Jan Seibert	Expert externe
Prof. Markus Hrachowitz	Expert externe

Sous la présidence de
Prof. Christian Kull

Lausanne, 2020

UNIL | Université de Lausanne
Faculté des géosciences et de l'environnement
bâtiment Géopolis bureau 4631

IMPRIMATUR

Vu le rapport présenté par le jury d'examen, composé de

Président de la séance publique :	M. le Professeur Christian Kull
Président du colloque :	M. le Professeur Christian Kull
Directeur de thèse :	M. le Professeur Grégoire Mariéthoz
Co-directrice de thèse :	Mme la Professeure Bettina Schaefli
Expert interne :	M. le Professeur Torsten Vennemann
Expert externe :	M. le Professeur Jan Seibert
Expert externe :	M. le Professeur Markus Hrachowitz

Le Doyen de la Faculté des géosciences et de l'environnement autorise l'impression de la thèse de

Monsieur Harsh BERIA

Titulaire d'un
Master of Technology in Land and Water Resources Engineering
de l'Indian Institute of Technology Kharagpur

intitulée

IMPROVING HYDROLOGIC MODEL REALISM USING STABLE WATER ISOTOPES IN THE SWISS ALPS

Lausanne, le 30 septembre 2020

Pour le Doyen de la Faculté des géosciences et de l'environnement

Professeur Christian Kull

Table of Contents

Dedicated to my late father

Jai Prakash Beria

Acknowledgement

This work would not have been possible without the constant guidance, support and encouragement from Bettina. Thank for you giving me this wonderful opportunity, the last four years have been a lot fun. Thank you to my jury members for giving your valuable time to review my thesis and the very interesting discussions that followed.

Thank you to Anthony, Natalie, and Josh for providing the great working environment and the awfully cramped up office space. It continues to amaze me how Anthony can run on the hillslope with a solar panel on his back, how Josh knows almost everything there is to know in hydrology, and how Natalie can fit so many languages in her head. You guys are amazing!

I will always remember the monumentally long coffee breaks every day at 10:00, 14:00, 16:00, …., with the whole gang (Lionel, Mathieu, Moctar, Stylianos, Fatemeh, Inigo, Gustavo, Fabio, Andrea, Manuel, Elisa, Tom, Joanne, Lilly, Philipp, Leanne, Sassi, Thibault, Raphaël, ……..). It was incredibly hard to get anything done! And thanks Gregoire for adopting me to your group and for the innumerous path breaking research ideas every time I saw you at an isle during AGU (I hope one of them fructifies at some point!). A special shout out to Lionel for working with me during his holidays, this would not have been possible without you.

And finally my family, thank you for being there through the thick and thin. This would not have been possible without you mom, thanks for being there. And papa, I finally made it.

Thank you!

Harsh

अभी तो सफ़र शुरू हुआ है

मंजिल ज़रा दूर है ।

Abstract

Climate change is modifying global precipitation patterns and bringing about unprecedented changes in the different facets of the water cycle. In order to be better prepared for the potentially adverse impacts of climate change on water resources, we need to improve our understanding of the water cycle. Environmental tracers such as stable water isotopes provide a useful medium to help untangle the complex web of Earth System processes. Stable water isotopes are naturally present in rainfall and snowfall, making them an ideal environmental tracer to track the journey of a water particle along its entire hydrologic life cycle.

In this thesis, I use stable water isotopes to improve the representation of hydrological processes occurring within mountainous landscapes in rainfall-runoff models. In the first chapter, I undertake a comprehensive review of ways in which stable water isotopes have been used in snow hydrology, with a special focus on mountainous environments. This review explains the different transformations that a water particle undergoes once it enters the landscape through rainfall or snowfall. In the second chapter, I build a novel Bayesian mixing model that derives valuable information from stable water isotope data, while taking into account the numerous limitations of field hydrology. In the third chapter, I propose a new hydrologic modeling framework that uses information derived from stable water isotopes, as illustrated in Chapter 2, to build more reliable rainfall-runoff models by constraining both the celerity and velocity behavior of catchments. This modeling framework is comprehensively evaluated in a Swiss Alpine catchment called Vallon de Nant. Finally, in the fourth chapter, I use stable water isotopes, streamflow recession analysis, and a conceptual groundwater model to show how climate change may increase groundwater recharge in the Swiss Alps.

This thesis therefore improves our understanding of the dominant hydrologic processes occurring in mountainous environments, and provides a novel approach to parameterize these processes within rainfall-runoff models. The key findings are summarized in the final chapter, where I also highlight practical challenges in isotope hydrology, and propose future research directions.

Résumé

Le changement climatique modifie mondialement les schémas de précipitation et entraîne des changements sans précédent dans les différentes facettes du cycle de l'eau. Afin d'être préparés aux potentiels effets négatifs dus au changement climatique sur les ressources en eau, nous devons améliorer notre compréhension du cycle de l'eau. Les traceurs environnementaux tels que les isotopes stables de l'eau constituent un moyen pour démêler le complexe réseau des processus du système terrestre. Ces isotopes stables de l'eau sont naturellement présents aussi bien dans la pluie que dans les chutes de neige, ce qui en fait un traceur idéal pour suivre le parcours d'une particule d'eau tout au long de son cycle de vie.

Dans cette thèse, j'utilise les isotopes stables de l'eau pour améliorer la représentation des processus hydrologiques se produisant dans les paysages montagneux dans les modèles de pluie et de ruissellement. Dans le premier chapitre, j'entreprends un examen complet des différentes façons dont les isotopes stables de l'eau ont été utilisés dans l'hydrologie et en particulier de la neige, en mettant l'accent particulier sur les environnements montagneux. Cette revue explique les différentes transformations qu'une particule d'eau subit une fois dans le paysage, par la pluie ou par les chutes de neige. Dans le deuxième chapitre, je construis un nouveau modèle mixte bayésien qui tire de précieuses informations des données isotopiques de l'eau, tout en tenant compte des nombreuses limites des données de terrain. Dans le troisième chapitre, je propose un nouveau cadre de modélisation hydrologique qui utilise les informations dérivées des isotopes stables de l'eau, comme illustré dans le chapitre 2, pour construire des modèles fiables de précipitations et de ruissellement, ceci en limitant à la fois la célérité et la vitesse des bassins versants. Ce cadre de modélisation est évalué de manière exhaustive dans Vallon de Nant, un bassin versant des Alpes suisse. Enfin, dans le quatrième chapitre j'utilise les isotopes stables de l'eau, l'analyse par récession du débit des cours d'eau et un modèle conceptuel des eaux souterraines pour montrer comment le changement climatique pourrait augmenter la recharge souterraine en eaux dans les Alpes suisses.

Cette thèse améliore donc notre compréhension des processus hydrologiques dominants qui se produisent dans les environnements montagneux, et fournit une nouvelle approche pour paramétrer ces processus dans les modèles de pluie et de ruissellement. Les principales conclusions sont résumées dans le dernier chapitre, où je souligne également les défis pratiques de l'hydrologie isotopique et propose des orientations de recherche pour l'avenir.

General Introduction

Background and rationale for the study

Climate change modifies atmospheric circulation dynamics resulting in significant changes in precipitation patterns, with ensuing impacts on the hydrosphere and biosphere (Malhi et al., 2020). We are already experiencing the climate repercussions with large scale species extinction (Ceballos et al., 2017), increased instances of floods and droughts (Stott, 2016), and major issues in food security (Schmidhuber and Tubiello, 2007). In order to protect the biosphere from the potentially adverse impacts of climate change, we need to have a very good understanding of the different facets of the water cycle. This will allow building reliable hydrological models that make robust predictions about future water resources.

Mountain environments are at the forefront of this change, with their average temperatures projected to rise by 0.25 - 0.4 °C/decade (Nogués-Bravo et al., 2007) resulting in higher amount of rainfall at the cost of snow and an earlier onset of snowmelt (Clow, 2010; Dudley et al., 2017). The propagation of these changes across mountainous regions is expected to reduce streamflow (Berghuijs et al., 2014), increase the frequency of stream droughts (Jenicek et al., 2018), and adversely impact tree growth (Campbell, 2019). This is particularly relevant for the global economy as snowmelt from mountainous regions sustain critical water supplies for the various needs (such as irrigation, hydroelectric power generation, etc.) of over one-sixth of the global population (Barnett et al., 2005; Kapnick et al., 2018; Viviroli et al., 2007).

Mountain landscapes are extremely complex in terms of their geological features and their hydrologic behavior. For instance, water in the Alpine catchments is stored in the form of glacier, snow, soil, and groundwater, creating multiple flow paths among different storage compartments. The interactions between these compartments add substantial complexity to the hydrology in these regions. Resolving this level of complexity requires large amount of hydrometeorological measurements. However, such measurements are difficult to obtain because of the remote location and the harsh winter conditions, with frequent avalanches making the job of systematic data collection incredibly difficult. Also, such catchments

respond very quickly to rainfall or snowmelt events, in the time scale of a few minutes, often triggering flash floods downstream. It becomes imperative to better understand mountain hydrology and develop reliable hydrological models for these regions.

Traditionally, most hydrological models that are used in mountainous landscapes are calibrated against streamflow, as streamflow data are widely available (Hrachowitz et al., 2016). However, streamflow data alone cannot constrain all the hydrologic fluxes, limiting the predictive power of such models. This leads to scenarios where the model reproduces streamflow hydrographs, but at the cost of errors in other flux estimates. For example, hydrological models often overestimate evaporation flux by underestimating soil moisture content, while simulating streamflow reasonably well (Sutanudjaja et al., 2014). This becomes especially relevant in a scenario when a large rainfall event follows, and the model is unable to reproduce the high streamflow because the antecedent soil moisture conditions within the model domain was much lower than reality. Other examples include incorrect partitioning between tree water uptake and groundwater recharge. These sorts of model conflicts arise when the model fails to correctly simulate the internal system dynamics such as flux partitioning (Hrachowitz and Clark, 2017). This has been also referred to as equifinality in the hydrologic literature, where multiple model parameter states lead to similar model performance (Beven and Freer, 2001; Khatami et al., 2019), making it difficult to identify the most reliable parameter set. Equifinality can lead to a breach in confidence in the results of a hydrological model, limiting its usage for future climate evaluations.

Including auxiliary datasets such as remote sensing based estimates of evapotranspiration (Odusanya et al., 2019; Rajib et al., 2018), snow cover (Nijzink et al., 2018; Parajka and Blöschl, 2008; Salvatore et al., 2018), groundwater (Bai et al., 2018; Dembélé et al., 2020), and soil moisture (Kunnath-Poovakka et al., 2016; Sutanudjaja et al., 2014) have been proposed to improve the parameter identifiability problem. More recently, calibration based on hydrologic signatures such as flow duration curves has gained traction to get around the problem of overfitting, while aptly constraining the hydrological model (Addor et al., 2018; Branger and McMillan, 2020; Jayathilake and Smith, 2019; Kelleher et al., 2017; Shafii and Tolson, 2015). A detailed review linking hydrologic signatures to hydrologic processes is given in McMillan, (2020).

Another reason for poorly constrained hydrological models is that a lot of these models do not adequately differentiate celerity from velocity (Mcdonnell and Beven, 2014). Celerity represents the speed of propagation of a large rainfall or snowmelt event through a catchment, whereas velocity represents the speed at which a water particle traverses through the catchment. A hydrological model calibrated against streamflow captures the celerity (i.e. the fast response behavior) of a catchment, which is mainly controlled by storage deficit. However, such a model fails to resolve the velocity aspect, which is largely controlled by the geomorphological characteristics of subsurface storage (Mcdonnell and Beven, 2014), and the catchment moisture state (Harman, 2015). Accounting for both celerity and velocity is especially relevant in mountainous catchments, where large convective summer rains trigger flash floods (Brunner et al., 2018; Stoffel et al., 2016; Weingartner et al., 2003). However, during such flash floods, most of the stream water still comes from pre-event water (Kirchner, 2003; Klaus and McDonnell, 2013; Obradovic and Sklash, 1986; Pearce et al., 1986), i.e. the rainfall event only helps mobilize older water that was already stored within the catchment. This distinction is often not made in hydrological models.

Naturally occurring environmental tracers such as stable water isotopes, conservative solutes, etc. capture the velocity response of a catchment, which if used with streamflow data, can help in constraining both celerity and velocity responses of the catchment. This distinction can help resolve conflicts in the internal partitioning within hydrological models, hence improving hydrologic realism. A detailed overview of the basics of stable water isotopes is provided in Section 1.3.

Stable water isotopes have usually been used to learn about the dominant hydrologic processes occurring within a catchment (Birkel and Soulsby, 2015; Son and Sivapalan, 2007; Vaché and McDonnell, 2006), thereby helping inform the model structure. Additionally, they have been used in water quality modeling. In such applications, a solute transport equation is solved in addition to the water balance equation and the isotopic ratio aids in calibrating parameters of the solute transport model (Birkel and Soulsby, 2015; Hrachowitz et al., 2013; Tetzlaff et al., 2015). However, the number of parameters in such a transport model is much higher than in regular hydrological models. Hence, due to the enhanced model complexity, it

is unclear if information gained by using additional data compensates for the subsequent increase in model complexity (Kelleher et al., 2019). In the absence of sufficient data to constrain the model, issues related to equifinality might occur, where the observed dataset is insufficient to constrain the most likely model parameter state (Beven and Freer, 2001; Shafii et al., 2019), reducing confidence in the predictive power of such a model.

Transit time modeling is another way to incorporate isotope data to help inform the internal flux partitioning within the hydrological model. Transit time of water is the time taken by a water particle to exit a catchment after being first introduced (Benettin et al., 2015). In this modeling approach, a Master equation which estimates the average residence time of water within a catchment is solved (Botter et al., 2011), yielding the expected (or mean) transit time, which is a catchment specific property. Such an approach uses the flux estimates from a hydrological model, and estimates the degree of mixing occurring within the different catchment storages (Harman, 2015). Transit time modeling provides a stochastic alternative to modeling solute transport and hence can be used in water quality modeling (Hrachowitz et al., 2016).

In this work, I use stable water isotopes to learn about the dominant hydrological processes within a Swiss Alpine catchment, Vallon de Nant, and use this information to build more reliable hydrological models. I also demonstrate that stable water isotopes provide valuable information about complex hydrological processes such as groundwater recharge, and can be used to estimate the impact of climate change on groundwater recharge in the Alps. The specific objectives of this project are summarized in the following section.

Research Objectives

The research goals can be summarized as:

- To identify ways in which stable water isotopes have been used in order to learn about the dominant hydrological processes, with a special focus on snow-influenced Alpine catchments.

- To develop a mixing model that works with small sample sizes (a common limitation in isotope hydrology), and provides flexibility to incorporate transformations made by different hydrological processes.
- To develop a novel approach of integrating stable water isotopes within a continuous hydrological model and test it in a Swiss Alpine catchment, Vallon de Nant.
- To use the insights gained by the last two objectives to better understand the impact of climate change on groundwater recharge in snow-dominated regions in the Alps.

Structure of the thesis

The first chapter summarizes the current state of knowledge of how different hydro-meteorological processes affect the isotopic composition of snow in its different forms (snowfall, snowpack, snowmelt), and through selected examples, discusses how stable water isotopes can provide a better understanding of snow hydrological processes, both through a qualitative and a quantitative lens. The synthesis summarizes the journey of a snow particle along its entire hydrologic life cycle, and highlights the major practical challenges remaining in snow hydrology and proposes future research directions.

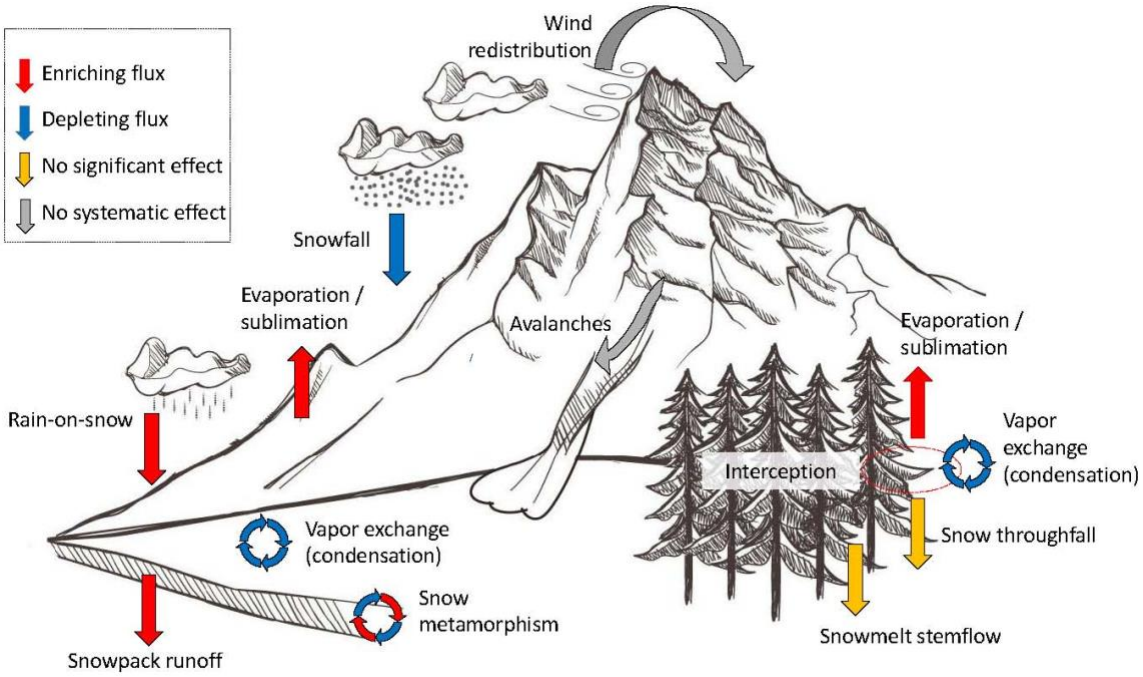

Figure I1. Life cycle of snow seen through the eyes of a hydrologist highlighting fluxes that lead to an enrichment or depletion in stable water isotopes of the snowpack (on the ground or intercepted by canopy); fluxes for which there is no systematic effect or no significant effect are also identified. (Graphic based on original work from www.freepik.com)

In the second chapter, a novel Bayesian mixing model is developed that solves the classical linear mixing problem in a Bayesian inference framework, while addressing problems of small sizes. Conventional mixing models require large amount of data which is generally not available in isotope hydrology. This new mixing approach works even with limited data availability. Additionally, the model accounts for an often overlooked bias that arises due to unweighted mixing. The efficacy of the model is established using a series of statistical benchmarking tests, a virtual hydrological experiment and a real case study where the proportion of groundwater recharge coming from summer vs winter precipitation is estimated within a Swiss Alpine catchment, Vallon de Nant.

In the third chapter, a semi-distributed hydrological model is developed to simulate streamflow in Vallon de Nant at very high temporal resolution (10-minutes). The stable water isotope data are then incorporated within the hydrological model using a novel Bayesian calibration scheme and the mixing model developed in Chapter 2. The coupling strategy

ensures that both celerity and velocity components of the catchment are appropriately represented within the model domain, without significant increasing model complexity.

In the final chapter, the Bayesian mixing model which was developed in Chapter 2 is used with a recession analysis to show that the extent of groundwater recharge in the high elevation regions of the Swiss Alps will increase in a warming climate. Higher winter streamflow might lead to reduced summer flows, with ensuing negative consequences for freshwater ecosystems and more broader concerns about water security and aquatic ecosystem resilience.

I then conclude the thesis with a summary of the key takeaways from this project followed by an open discussion about future possible work.

1. Understanding snow hydrological processes through the lens of stable water isotopes

Harsh Beria, Joshua R. Larsen, Natalie C. Ceperley, Anthony Michelon, Torsten Vennemann, Bettina Schaefli

Published[1] in *Wiley Interdisciplinary Reviews: Water.*

[1] Beria, H., Larsen, J. R., Ceperley, N. C., Michelon, A., Vennemann, T. and Schaefli, B.: Understanding snow hydrological processes through the lens of stable water isotopes, Wiley Interdiscip. Rev. Water, 5(6), e1311, doi:10.1002/wat2.1311, 2018.

Abstract

Snowfall may have different stable isotopic compositions compared to rainfall, allowing its contribution to potentially be tracked through the hydrological cycle. This review summarizes the state of knowledge of how different hydro-meteorological processes affect the isotopic composition of snow in its different forms (snowfall, snowpack, snowmelt), and, through selected examples, discusses how stable water isotopes can provide a better understanding of snow hydrological processes. A detailed account is given of how the variability in isotopic composition of snow changes from precipitation to final melting. The effect of different snow ablation processes (sublimation, melting, and redistribution by wind or avalanches) on the isotope ratios of the underlying snowpack are also examined. Insights into the role of canopy in snow interception processes, and how the isotopic composition in canopy underlying snowpacks can elucidate the exchanges therein are discussed, as well as case studies demonstrating the usefulness of stable water isotopes to estimate seasonality in the groundwater recharge. Rain-on-snow floods illustrate how isotopes can be useful to estimate the role of preferential flow during heavy spring rains. All these examples point to the complexity of snow hydrologic processes and demonstrate that an isotopic approach is useful to quantify snow contributions throughout the water cycle, especially in high elevation and high latitude catchments, where such processes are most pronounced. This synthesis concludes by tracing a snow particle along its entire hydrologic life cycle, highlights the major practical challenges remaining in snow hydrology and discusses future research directions.

Keywords: throughfall, stemflow, wind redistribution, ablation, isotopic lapse rate

1.1. Introduction

Seasonal snow covers 47 Mkm^2 or 30 % of the Earth's land surface, with 98 % of this cover located in the Northern Hemisphere, specifically in North America and Eurasia (Brodzik and Armstrong, 2017; Robinson et al., 1993). In fact, more than 50 % of North America and Eurasia are seasonally snow-covered. Snow is thus a key element of both the Earth's hydrological cycle and its surface energy balance (Frei et al., 2012). Depending on the different meteorological conditions, the temporary accumulation of water in the form of snow shifts daily, seasonally, and annually, from the period when precipitation falls as snow to the period when water is released via sublimation and melting. In the year 2000, around one sixth of the World's population was living in places with snow-dominated water resources and with low artificial water storage capacity, i.e. using water resources heavily reliant on the natural water storage capacity of snow (Barnett et al., 2005).

The dynamics of snow accumulation, storage, and melting play a major role in hydrological, ecological and geomorphological processes (Chen et al., 2015) and for domestic, industrial and agricultural water use (Barnett et al., 2005), as well as for hydropower production (Schaefli, 2015). Additionally, snowmelt can be a key driver of hydrological hazards (Chen et al., 2015), such as spring floods (Blöschl et al., 2017), summer droughts and rain-on-snow events (Freudiger et al., 2014). Snowmelt is also a primary temperature control for snow-influenced streams, with ensuing regulations on aquatic ecosystems (Fossheim et al., 2015) and on heat inputs to lakes and oceans (Lammers et al., 2007; Yang et al., 2014).

The natural storage of water as snow is undergoing severe changes in a warming climate (Beniston et al., 2017; Brown and Mote, 2009). In a warmer world, the percent of precipitation falling as snow and the seasonal duration of that snow cover will likely decrease (Choi et al., 2010; Steger et al., 2013). Snow may start melting earlier, thus shifting the corresponding timing and magnitude of river runoff peaks (Barnett et al., 2005). Somewhat counter intuitively, rates of snowmelt are also expected to decrease (Musselman et al., 2017).

Any change in this seasonal duration – or "snow cover phenology" (Chen et al., 2015) - has potentially important effects for water storage dynamics in mountain environments with

permanent snow cover (Huss et al., 2017), in polar regions (Bokhorst et al., 2016), in low-elevation mid-latitude snow covers (Nolin and Daly, 2006), and in general for any water resources system heavily relying on the temporal storage of water in the form of snow (Barnett et al., 2005).

Snow is certainly among the most dynamic hydrological water stores (Sturm, 2015). According to Frei et al., (2012) the "accumulation and rapid melt (of snow) are two of the most dramatic seasonal environmental changes of any kind on the Earth's surface." Compared to subsurface water storage, the presence and depth of a snowpack is far easier to estimate using remote-sensing (Frei et al., 2012) or ground-based techniques (Lundberg et al., 2010). Estimating the actual water content of a snow cover in terms of its snow water equivalent (SWE) (Jonas et al., 2009) remains, however, challenging (Dozier et al., 2016; Jonas et al., 2009). Detailed insights into snow accumulation and melt processes are difficult to obtain, given the generally harsh meteorological conditions prevailing in snow-dominated environments that make data collection very challenging.

Accordingly, we are still far from having a complete picture of how the temporary accumulation of water in the form of snow influences the catchment-scale water balance (Berghuijs et al., 2014) or how its melting is partitioned into water flow paths according to their associated time scales (Musselman et al., 2017).

Stable isotope compositions of oxygen and hydrogen in water (subsequently referred to as stable isotopes of water) have a long standing tradition as tracers in hydrology (Bowen and Good, 2015), which among many applications have been widely used to separate different sources of streamflow (Klaus and McDonnell, 2013), to understand hillslope-scale hydrologic processes (Tetzlaff et al., 2014) and to estimate the residence time of water at various catchment scales (Benettin et al., 2017a; Birkel and Soulsby, 2015; Tetzlaff et al., 2015). For snow hydrology, such measurements are particularly promising because winter precipitation falling as snow generally has distinct isotopic compositions compared to summer precipitation, meaning it may be used to trace the evolution and contribution of snow to hydrological pathways within catchments.

In this review, the aim is to provide a comprehensive overview of the state of knowledge concerning how stable isotope compositions of water can be applied to further understand snow hydrology. This is done by:

1) Providing an overview of the snow regions of the world, to place the snow hydrological studies into a geographic context across the globe,

2) Outlining the fundamentals of stable isotope variations, and the spatio-temporal variations in isotope compositions of precipitation, where snow represents the solid phase,

3) Providing an in-depth analysis of how snow operates in the hydrological cycle, and how stable isotope measurements have contributed to these interpretations,

4) Examining the current state of knowledge concerning changes in the isotopic composition of snow during its hydrological life cycle,

5) Highlighting the significance of these findings for interpreting snow contributions to overall hydrological partitioning and fluxes,

6) Suggesting avenues for future research using stable isotope compositions in snow hydrology.

1.2. Snow regions of the world

In this paper, the focus is on understanding snow hydrological processes related to (sub)seasonal accumulation and release of snow in mountainous and high latitude environments. This excludes the polar regions that have permanent snow and ice cover (glaciers) and also cryospheric processes related to formation of firn and ice. Globally, seasonally snow-influenced regions are located in mountainous areas, mostly at latitudes greater than 45° North and South (Figure 1.1), except in regions influenced by maritime climates in Europe, the Pacific Northwest and British Columbia, where moisture converges from warmer ocean currents (Barnett et al., 2005).

The relative amount of precipitation falling as snow in snow-influenced regions depends on the intra-annual precipitation variability and the relationship between precipitation seasonality and the annual air temperature cycle (Willmott et al., 1985; Woods, 2009). Ratios of relative snowfall vary strongly worldwide (Figure 1.1b). Similarly, the storage dynamics (i.e.

the building-up, transformation and ablation or mass reduction) of snow cover vary strongly from place to place, resulting in shallow cold snowpacks in the tundra or in relatively deep and warm snowpacks in maritime locations. Sturm et al., (1995) proposed a seasonal snow cover classification system with seven phenomenological classes, *tundra*, *taiga*, *alpine*, *maritime*, *prairie*, *ephemeral* and a special "*mountain*" class, and related these classes to cold season climate variables (e.g. temperature, precipitation, wind speed). Such a classification certainly has potential to transfer snow hydrological process understanding from one landscape to another, but as yet has found limited application in the hydrological literature (for examples, see Liston, (2004) and Fayad et al., (2017)).

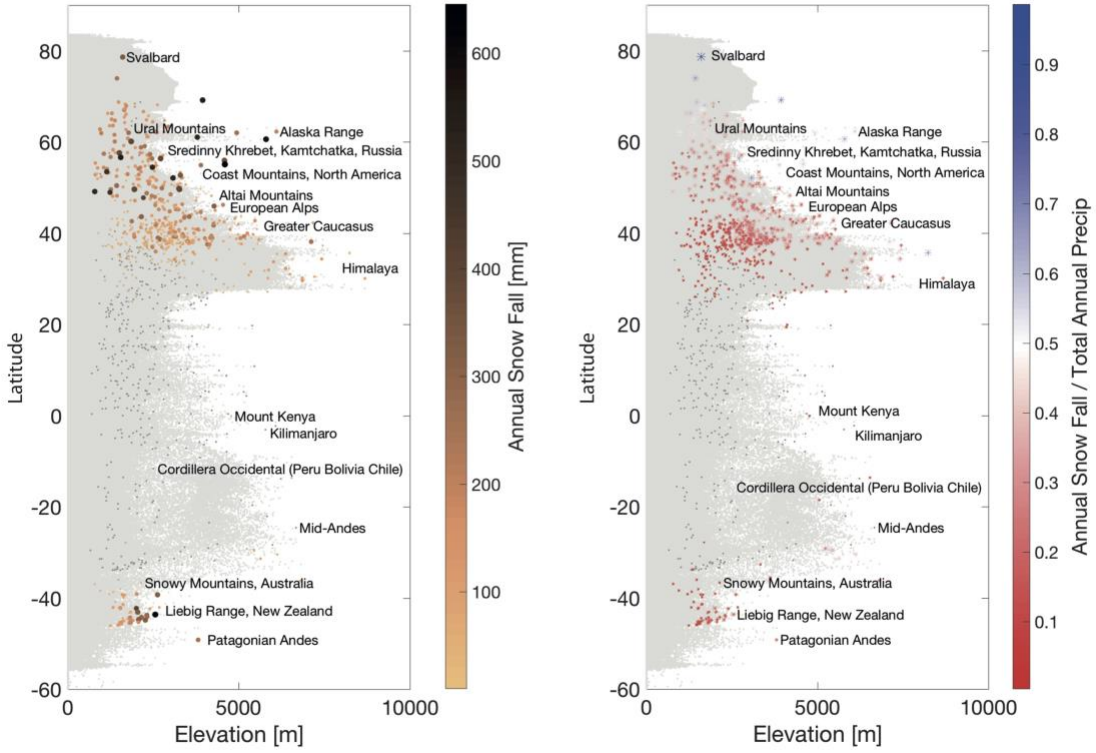

Figure 1.1. Amount of annual snowfall and ratio of snowfall to annual precipitation in world's mountain ranges; monthly snowfall computed with the equation proposed by Legates and Willmott, (1990) from monthly precipitation and monthly temperature of the WorldClim data base (Hijmans et al., 2005); mountain ranges extracted with the mountain shape files provided by Körner et al., (2017), shown are the latitude of mid points and peak elevation; peak elevation obtained from the elevation data set (called "alt" file) from the WorldClim data

set. Dark grey dots correspond to mountain ranges without snowfall, light grey shading indicates all pixels in the WorldClim data set. Colored dots on the left and colored asterisks on the right figure represent mountains with snow, with the marker size proportional to annual snowfall in the left figure and proportional to ratio of annual snowfall to annual precipitation in the right figure. The readers are referred to the electronic version for an enlarged version of the figure.

For this review, it is useful to consider fundamental regional differences in incoming and outgoing snow-water fluxes, in particular: (1) the seasonality of the snowfall period with respect to the melting period (occurring simultaneously or shifted in time), and (2) the main driver of snow ablation, either melt or sublimation or both. While only examples are given and not an extensive classification of the world's snow-influenced regions and mountain ranges, these two factors should be kept in mind as we explore isotopes in snow hydrology research. This is particularly important given that fundamental climatic differences might occur within relatively small areas, e.g. at different elevations within a given mountain range.

Most snow-influenced regions and mountain ranges have a distinct snowfall (cold) and snowmelt (warm) season. This applies especially to all northern hemisphere high latitude regions, the North American and Canadian mountain ranges, the European and the Japanese Alps and to almost all seasonally snow-influenced mountain ranges in the Southern hemisphere. An exception is the temperate Cordillera in Peru and Bolivia that has a dry cold season (see the map of Peel et al., (2007)) and, accordingly, snow accumulation and melt both occur during summer on high mountain peaks (Wagnon et al., 1999). The Himalaya is the most prominent example of a mountain range where there is a major overlap between the snowfall and snowmelt seasons (during the monsoon season (Kaser et al., 2010)) because the cold season is too dry for snow to accumulate. However, some areas of the Hindu-Kush Karakoram Himalayan region can receive a higher fraction of cold precipitation (Palazzi et al., 2013), and some areas can have an alpine-like snow season (e.g. the Himachal Pradesh). In general, any region with a distinct dry cold season will be both accumulating and melting snow within the warmer season. A special case is that of dry mountains with sporadic snowfall that is retained due to generally cold temperatures, such as in the very high elevation but largely arid Andes (MacDonell et al., 2013). Sublimation plays a key role in snow ablation,

occurring year-round under the influence of solar radiation and wind (Ayala et al., 2017; Gascoin et al., 2013). In general, sublimation is a potentially important driver of snow ablation in drier climates (see, e.g. the review on Mediterranean snow hydrology by Fayad et al., (2017a)), and in cold and windy climates (due to the stronger sublimation of blowing snow (Law and Vandijk, 1994)), e.g. in many high elevation and high latitude regions such as the Canadian Rocky Mountains (MacDonald et al., 2010). Sublimation is typically also high in cold climate forests due to the easier sublimation of canopy intercepted snowfall (Pomeroy et al., 2002).

1.3. Background of isotope hydrology

The basic concepts of how H and O isotopes are used in hydrology are summarized following Galewsky et al., (2016). In nature, hydrogen exists as two stable isotopes (^{1}H, ^{2}H or D) and oxygen as three stable isotopes (^{16}O, ^{17}O, ^{18}O) with the isotopologue (same molecule but with different isotopic composition) $H_2{}^{16}O$ being the most abundant, followed by $H_2{}^{18}O$, $H_2{}^{17}O$, $H_1D^{16}O$. $H_2{}^{18}O$ (or ^{18}O) and $HD^{16}O$ (or ^{2}H) are the most commonly used natural tracers in isotope hydrology. Accordingly, in this review, we only include studies using $^{2}H/^{1}H$ and/or $^{18}O/^{16}O$.

Isotopic values are expressed as a ratio (R) of concentration of heavier to lighter isotopes ($^{2}H/^{1}H$ or $^{18}O/^{16}O$) and standardized relative to the Vienna Standard Mean Ocean Water (VSMOW2) by the International Atomic Energy Agency (IAEA). The hydrogen or oxygen isotope composition of a sample, R_{sample}, ($^{2}H_{sample}/^{1}H_{sample}$ or $^{18}O_{sample}/^{16}O_{sample}$), is expressed using the so-called δ notation in units of per mil (‰), as

$$\delta^{18}O \text{ or } \delta^{2}H = \frac{R_{sample}-R_{VSMOW}}{R_{VSMOW}} \text{x } 1000. \quad (1.1)$$

The majority of precipitation originates from ocean evaporation, a process that preferentially samples the lighter isotopologues of water. Accordingly, the ratio of the Vienna standard, $R_{VSMOW,}$ is generally higher than the ratio of any meteoric water sample and reported δ-values of such waters are mostly negative. Samples with higher (or less negative) $\delta^{2}H$ or $\delta^{18}O$ values

have a greater proportion of heavier isotopes and are referred to as *more enriched in heavier isotopes*. Similarly, samples with lower (or more negative) δ^2H or δ^{18}O values compared to seawater have a smaller proportion of heavier isotopes and are referred to as *more depleted in heavier isotopes*.

During a phase change process (such as condensation, evaporation, etc.), fractionation changes the relative abundance of heavier and lighter isotopes in the two phases. Depending on the process, fractionation can take place under equilibrium conditions (equilibrium fractionation) or in non-equilibrium conditions (kinetic fractionation). At equilibrium, the forward and backward reaction rates of the phase change are identical. A typical example of equilibrium fractionation is condensation, where heavier isotopes are preferentially incorporated in the condensate, leaving the remaining vapor more depleted in heavier isotopes (Clark and Fritz, 1997, p.Environmental Isotopes; Kendall and McDonnell, 1998, p.Fundamentals of Isotope Geochemistry). However, during kinetic fractionation, the forward and backward reaction rates of the phase change are different. A typical example of kinetic fractionation is evaporation. During evaporation, both δ^2H and δ^{18}O values of the vapor phase decrease whereas the remaining liquid becomes proportionately more enriched in the heavier isotopes of H and O, hence increasing the δ^2H and δ^{18}O values. In contrast to condensation, which is generally an equilibrium process, the kinetic effect is stronger for changes in δ^2H compared to δ^{18}O of the vapor phase as the $HD^{16}O$ molecule is lighter than the $H_2{}^{18}O$ molecule.

Given δ^2H and δ^{18}O are both modified by mass dependent fractionation processes and are part of the same water molecule undergoing transformation, global precipitation follows a linear relationship $\delta^2 H = 8\delta^{18}O + 10$, which is called the global meteoric water line (GMWL) (Craig, 1961). The intercept of the GMWL is referred to as *d-excess* (deuterium-excess factor) and is useful in distinguishing equilibrium and non-equilibrium processes (see hereafter) (Dansgaard, 1964; Galewsky et al., 2016). However, the slope and the intercept of precipitation samples at a given location might vary from the values of the GMWL, depending on the source of precipitation water (ocean water or local moisture recycling by terrestrial evaporation or plant transpiration). Hence, local meteoric water lines (LMWL or MWL) are

used to describe the relationship between δ^2H and $\delta^{18}O$ at a given location. Any deviation from the MWL gives insights into non-equilibrium processes such as evaporation, sublimation, etc. at the given site.

During an equilibrium process (e.g. condensation), the isotopic values of δ^2H and $\delta^{18}O$ vary along the MWL (Figure 1.2). During a non-equilibrium process (e.g. evaporation), the isotopic values of δ^2H and $\delta^{18}O$ no longer vary along the MWL because of differential enrichment in ^2H and ^{18}O in the liquid phase. This results in evaporation processes having a different slope in their δ^2H-$\delta^{18}O$ relationship compared to equilibrium or condensation processes that typify atmospheric precipitation. During evaporation, the $^1H^2H^{16}O$ isotopologue of water, which is lighter than the $^1H^1H^{18}O$ isotopologue, is preferentially vaporized leaving the remaining liquid more enriched in heavier isotopologues of water (i.e. $^1H^1H^{18}O$, variants with ^{17}O are not considered here). This leads to the local evaporation line (LEL), which reflects the isotopic ratio of the remaining liquid (and not the evaporated vapor). The LEL has a slope (typically between 3 to 6) and a *d-excess* value lower than that of the MWL (Rose, 2003), meaning higher proportion of heavier isotopes of oxygen than hydrogen in the remaining liquid (Figure 1.2). Projecting the isotope values of evaporated water on the MWL by retracing its path along the LEL provides an estimate of the initial isotopic composition of water, provided there is no subsequent mixing (Rose, 2003). During summer, rain samples can also fall off the MWL and follow the LEL due to evaporation of the water droplets during their transit from the cloud to the ground (Winograd et al., 1998).

The temperature at which an air mass condenses (cloud condensation temperature) influences the fractionation that occurs when precipitation forms, which determines its original stable water isotope ratio. Fractionation factors between vapor and liquid or vapor and solid (ice) decrease with increasing temperature (Akers et al., 2017; Friedman et al., 1964). Accordingly, higher air temperatures (positively correlated with cloud condensation temperature) lead to lower fractionation factors, i.e. lower enrichment in heavier isotopes of the forming water droplets. As a result, precipitation forming at higher air temperatures is more depleted in heavier isotopes than precipitation forming at lower air temperatures.

At the beginning of a precipitation event, heavier isotopes are preferentially sampled out of the cloud as rain/snow. During the course of the event, precipitation becomes more depleted in heavier isotopes. This is also called the *rain-out effect* and it generally follows the Rayleigh distillation law during continued condensation (Good et al., 2015; Schürch et al., 2003). Controls on the isotopic composition of precipitation due to elevation gradients (isotopic lapse rates) and air temperature (due to seasonality) are described in the section below.

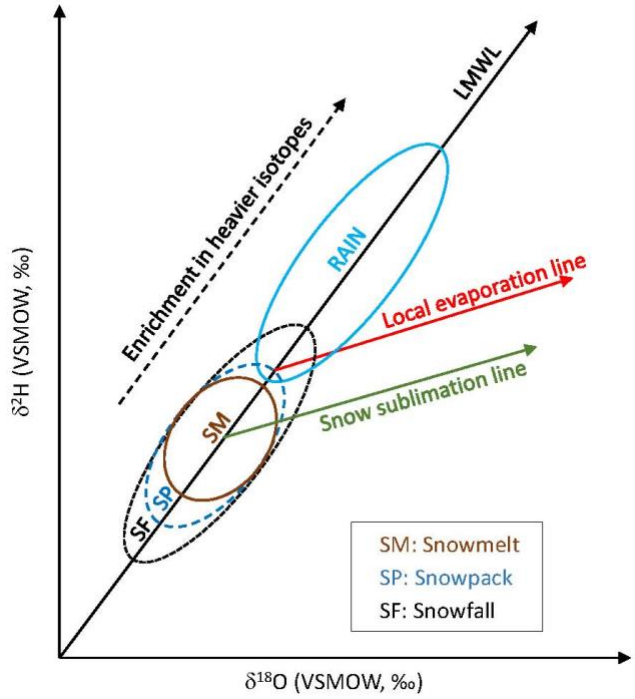

Figure 1.2. Conceptual representation of possible sample positions in the dual isotope space (formed by δ^2H and $\delta^{18}O$) for snow and rainfall samples from an entire hydrological year.

1.3.1. Elevation gradients and isotopic composition of precipitation

As moist air masses uplift (adiabatically) along a mountain range, condensation occurs at lower temperatures, which is also known as the *lapse rate* (Friedman et al., 1992; Galewsky et al., 2016; Winograd et al., 1998). The isotopic composition of precipitation varies systematically with elevation, becoming in general more depleted in heavier isotopes as rain-out increases with elevation. Accordingly, this effect is called the *isotopic lapse rate*. Lower cloud condensation temperatures with increasing elevation also increase the isotopic

fractionation between vapor and liquid, further increasing heavy isotopes in the residual air mass (Friedman et al., 1964). As condensation is an equilibrium process, the isotopic fractionation follows the MWL. An example of this effect is shown in the change of the δ^2H and $\delta^{18}O$ values measured as part of the GNIP (Global Network of Isotopes in Precipitation) network of stations across an elevation gradient in Switzerland (Figure 1.3). Here, the average isotope composition of precipitation shifts by 1.9 ‰/100/m for δ^2H and 0.27 ‰100m^{-1} for $\delta^{18}O$, noting that in winter, above around 800m asl. the precipitation is dominated by snow (Marty, 2008). Some version of this isotopic lapse rate is seen in almost all mountainous environments except on the leeward or "rain-shadow" side of mountains, which receive precipitation from clouds that have already passed over the highest elevation of the ridge and are no longer continuing to rise, keeping the cloud condensation temperature relatively stable (Bershaw et al., 2012; Dietermann and Weiler, 2013; Koeniger et al., 2008; Moran et al., 2007; Wen et al., 2012; Winograd et al., 1998). Moran et al., (2007) reported positive isotopic lapse rates (enrichment in heavier isotopes with increasing elevation) in snow samples on the leeward side of a glacierized valley in the Canadian Rockies (refer to Figure 4 in Moran et al., (2007)), which may occur only if the warmer temperatures and hence smaller vapor-liquid or vapor-ice isotopic fractionation factors offset the "rain-out" effect.

A number of studies around the world have reported on the effect of isotopic lapse rates of precipitation in streamwater (Jeelani et al., 2013; Wen et al., 2012), groundwater (Lambán et al., 2015; O'Driscoll et al., 2005) and soil water (O'Driscoll et al., 2005). However, this effect can be masked by other fractionating processes as well as elevation dependent recharge processes. In the case of snow, ablation processes like sublimation and melting change the isotopic compositions of existing snowpacks. This is especially apparent when isotopic lapse rates are calculated by sampling snow cores along an elevation gradient.

In the Ötztal Alps in Austria, Moser and Stichler, (1974) proposed reversed isotopic lapse rates due to the enrichment of surface snow with heavier isotopes due to sublimation and melting processes. Zongxing et al., (2015) also showed reversed isotopic lapse rates in snowfall in the lower elevation (3400-4000 m) region of Shiyi Glacier (Tibetan Plateau). However, regular isotopic lapse rates were again seen at higher elevations (4000-4680 m). In this case,

enrichment in heavier isotopes in the snowpack due to evaporation and sublimation along with snow drift from higher to lower elevations explained the reverse isotopic lapse rates. Additionally, the air mass trajectory can also mask the role of isotopic lapse rate as was shown in the Southeastern desert in California (USA) (Friedman et al., 1992).

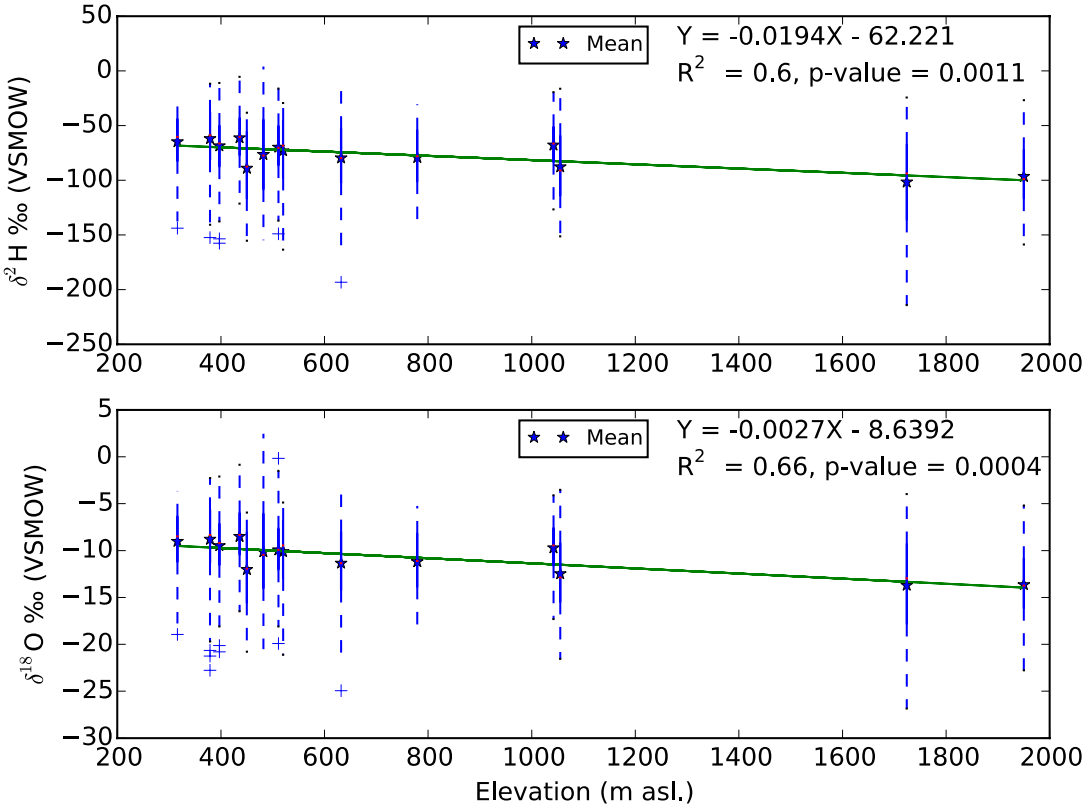

Figure 1.3. Variation of δ^2H and $\delta^{18}O$ in precipitation samples as a function of elevation, as collected by the GNIP (Global Network of Isotopes in Precipitation) network of gauging stations in Switzerland (data from 1966 to 2014). Snowfall is widespread during winter at elevations > 800 m a.s.l. (Marty, 2008).

1.3.2. Seasonality in isotopic composition of precipitation

Precipitation isotopic composition depends on cloud condensation temperature (Friedman et al., 1964), which is intrinsically linked to the ambient air temperature. Owing to the seasonality in air temperature, isotopic compositions also globally show strong seasonality (Friedman et al., 1992; Lambán et al., 2015) (see an example in Figure 1.4). This seasonality in

the isotopic composition is strongly linked to the afore-mentioned rain-out effect. In colder air masses, more water condensates than in warmer air masses, which leads to stronger depletion in heavy isotopes. Accordingly, precipitation forming in cold air masses is also more depleted in heavy isotopes than precipitation forming in warmer air masses. This explains the general tendency of rainfall being more enriched in heavier isotopes than snowfall at a given location.

The isotope lapse rates can also show seasonality with different lapse rate values at different times of the year. O'Driscoll et al., (2005) found in three catchments in Pennsylvania (USA) (elevations ranging from 225 to 740m) a strong seasonality in isotopic lapse rates, with some months even showing positive slopes (enrichment in heavier isotopes with increasing elevation). They attributed this to different sources of cloud vapor at different times of the year, and to different synoptic drivers. However, it is rare to obtain positive isotopic lapse rates. It is important to note that Pennsylvania is very flat with the highest elevation less than 750m, so the same physical processes might not be applicable in the other high elevation regions in the world like the European and Chilean Alps, the Himalayas, etc.

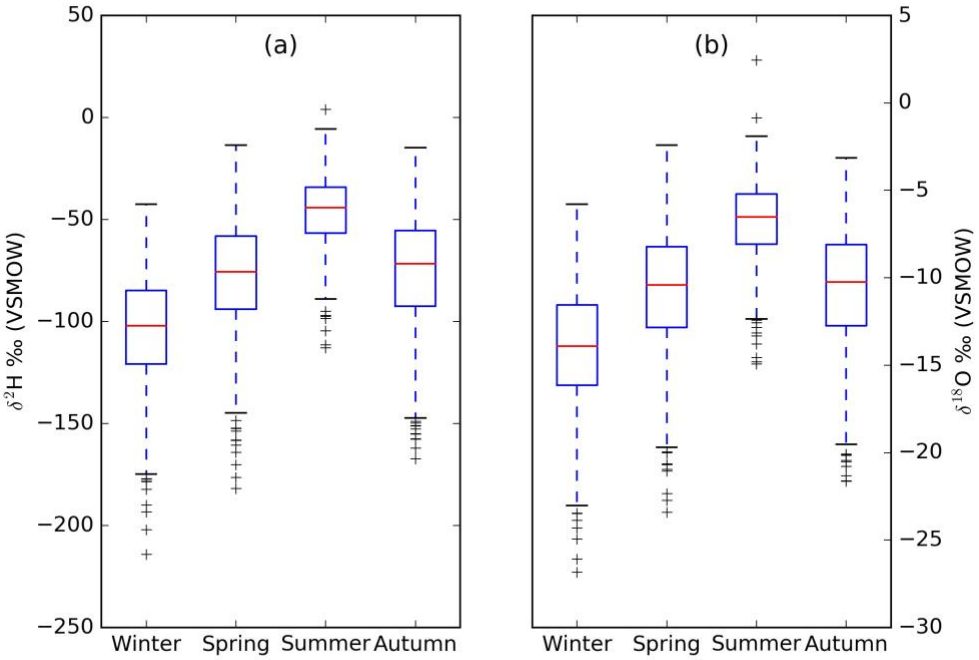

Figure 1.4. Seasonal variation of δ^2H and δ^{18}O in precipitation samples collected by the GNIP (Global Network of Isotopes in Precipitation) network of gauging stations in Switzerland (data from 1966 to 2014). The red line in the middle of each box shows median value, the box corresponds to the difference between third and first quartile values, whisker length is 1.5 times of the interquartile range and the points beyond the whiskers represent outliers.

1.4. General overview of snow in the hydrological cycle

When precipitation falls as snow, it enters a cycle of snow accumulation, redistribution and ablation (mass reduction) via sublimation and melt (see Figure 1.5 and the textbook of Dingman, (2002) for an overview of snow hydrological processes). Snow that accumulates on the ground under freezing conditions undergoes permanent snow metamorphism (change of snow grain size and shape due to vapor exchange, heat flow and pressure) (Colbeck, 1982) and vapor exchange with the atmosphere. Accordingly, most snowpacks are distinctly layered, including the formation of structurally weaker layers (e.g. depth hoar layers), which are particularly relevant for avalanche formation (Gaume et al., 2013). Snowmelt water then either refreezes or leaves the snowpack if the local water retention capacity is reached, forming preferential meltwater flow paths (Katsushima et al., 2013; Schneebeli, 1995).

Substantial amounts of meltwater leave the snowpack only once the snowpack becomes *isothermal* (Dingman, 2002), which is when all the snowpack layers are at the same temperature (i.e. at the freezing point). Runoff generation from the melting snowpack occurs via direct surface runoff or via infiltration into the subsurface, resulting in groundwater recharge or in other flow processes in the subsurface (Wever et al., 2017). Similar to purely rainfall driven infiltration, the rate of melt infiltration into the soil depends on the soil properties and in particular on its saturation state and hydraulic conductivity; frozen soil has an extremely small infiltration capacity but it is noteworthy that soil beneath a snowpack is not necessarily frozen (Wever et al., 2017) and that continuous (but low rate) snowmelt at the snow-soil interface is common in many places (Unnikrishna et al., 2002).

Redistribution of snow previously accumulated on the ground can occur via wind transport (Mott et al., 2010) or avalanching, both of which can lead to considerable displacement of snow masses. Transport by wind typically leads to snow fragmentation (Comola et al., 2017), which favors snow sublimation from blowing snow (Essery et al., 1999). Spatial precipitation patterns (orographic effects (Houze, 2012), seeder-feeder mechanisms (Choularton and Perry, 1986)) together with preferential snow deposition (Lehning et al., 2008) and wind redistribution leads to strongly heterogeneous snow accumulation patterns. Spatially variable snow ablation due to complex interactions with topography and vegetation further enhances the spatial heterogeneity of snow packs (Marks et al., 2002).

The presence of vegetation also affects snow processes through its modification of the surface energy budget (via the screening of solar radiation, emission of longwave radiation, thermal inertia, etc.). In forested areas, substantial amounts of snow can be intercepted by trees (Hedstrom and Pomeroy, 1998). Intercepted snow either returns as vapor to the atmosphere via sublimation or reaches the ground (soil or snowpack) via snow throughfall or snowmelt stemflow. These fundamental snow hydrological processes and pathways are illustrated in Figure 1.5 and are discussed in the following sections, including a detailed discussion of whether these processes are likely to change the isotopic composition of the snow.

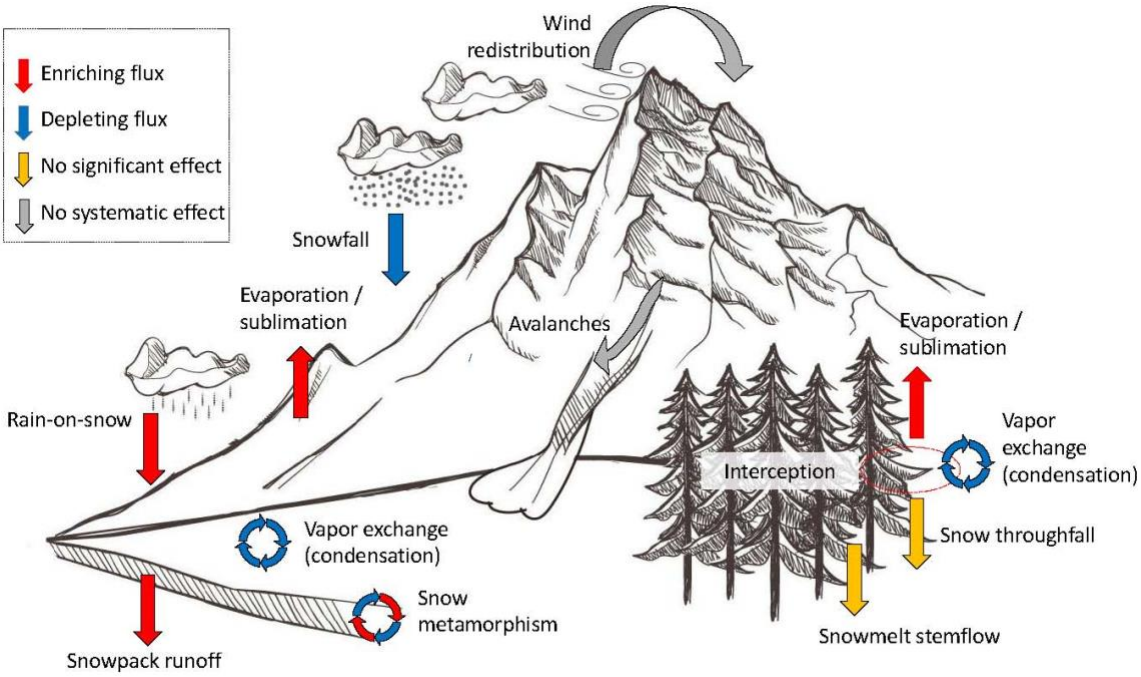

Figure 1.5. Life cycle of snow seen through the eyes of a hydrologist highlighting fluxes that lead to an enrichment or depletion in stable water isotopes of the snowpack (on the ground or intercepted by canopy); fluxes for which there is no systematic effect or no significant effect are also identified. (Graphic based on original work from www.freepik.com)

1.5. Effects of snow hydrologic processes on the isotopic composition of water

The state-of-knowledge of the dominant processes that affect the isotopic composition of snow during its life cycle are further discussed below, starting with processes occurring at the canopy (interception and throughfall), at the snowpack-atmosphere interface (sublimation, vapor exchange) and within the snowpack itself (metamorphism, melt). A short discussion on the effect of snow redistribution on snowpack isotopic composition and an overview of dominant drivers of spatial heterogeneity of snow isotopes conclude this section.

1.5.1. Interception and throughfall

Little work has been done to understand changes in the stable isotopic compositions of snow that is intercepted by the canopy (Allen et al., 2016; Claassen and Downey, 1995; Koeniger et al., 2008) or the subsequent transport to the ground via throughfall (TF) and stemflow (STF).

However, a number of studies have tried to model changes in TF on isotopic compositions by intercepted rain (Dewalle and Swistock, 1994; Gat and Tzur, 1967; Pearce et al., 1986; Saxena, 1986; Uehara and Kume, 2012). A recent review by Allen et al., (2016) summarized rainfall interception processes and their effect on the stable isotopic composition of intercepted rain. Some of this discussion is useful to further understand potential effects on snow.

The canopy affects the isotopic composition of intercepted rain falling onto the ground via TF in three major ways: (1) Canopy evaporation enriches intercepted rain in heavier isotopes, where the degree of enrichment is a function of relative humidity. The majority of evaporation occurs from micro-droplets created by rainfall splashes and the evaporation rate is accelerated by shear stress between the falling droplets and air (Murakami, 2006). (2) Isotopic exchange between canopy intercepted rain and surrounding vapor reduces variance, either by enriching or depleting the rain in heavier isotopes. In most instances, exchange leads to the progressive depletion of intercepted rain in heavier isotopes as the surrounding vapor is generally more depleted in heavier isotopes (Friedman et al., 1991). Unlike evaporation which is a kinetic process, exchange is an equilibrium process (Friedman et al., 1991) and the isotopic composition of intercepted rain remains on the MWL. (3) Selective canopy storage and transmission of rain to the ground as TF changes the isotopic composition of TF from bulk rain. For instance, if the canopy retains water at the end of a rain event which is more depleted in heavier isotopes (rainout effect, refer to Section 1.3), TF water will be more enriched than bulk rain. The residual intercepted water may also modify the isotopic composition of TF induced by the next storm, which may itself have a different isotopic composition depending on the vapor sources and its specific rain-out history. Canopy interception effects on the isotopic compositions (enrichment or depletion) are enhanced during smaller rain events (Soulsby et al., 2017) and in denser canopy stands (Allen et al., 2016).

To our knowledge, only Claassen and Downey, (1995) and Koeniger et al., (2008) have explored changes in snow isotope composition via canopy interception, in Colorado (USA) and Idaho (USA) respectively. In the evergreen forests of Showsnow Mountain in Colorado (USA), snow accounts for more than 50% of annual precipitation, and interception of snow accounts for about half of the total snowfall. Claassen and Downey, (1995) showed a high

degree of enrichment in heavier isotopes of hydrogen (13 ‰) and oxygen (2.1 ‰) in the winter TF samples of intercepted snow, relative to the isotopic composition of fresh snow. The degree of enrichment depends on: (1) the residence time of intercepted snow (Claassen and Downey, 1995) (2) the size of the snowfall (Claassen and Downey, 1995) and (3) the density of forest canopy (Koeniger et al., 2008). (1) Longer residence time leads to more enriched TF and STF, as sublimation enriches the intercepted snow in heavier isotopes (Claassen and Downey, 1995). Clear sky conditions favor longer residence time of the intercepted snow, and hence more enrichment due to snow sublimation. However, air temperature might reduce the residence time of intercepted snow. When air temperature at the surface of intercepted snow approaches melting point, interception stops and a small amount of melt leads to a lubrication effect at the snow leaf interface, causing a large fraction of the intercepted snow to slide off. (2) The size of falling snow particles also characterizes the degree of isotopic enrichment, with smaller snow particles exhibiting greater enrichment in heavier isotopes (Claassen and Downey, 1995). (3) Higher degrees of enrichment are seen in denser forest canopies due to longer exposure of the intercepted snow to atmospheric drying (Koeniger et al., 2008).

1.5.2. Snow sublimation

Sublimation is a kinetic (or non-equilibrium) fractionating process causing differential enrichment in the heavier isotopes of H and O (Earman et al., 2006; Moser and Stichler, 1974; N'da et al., 2016; Ren et al., 2013). Sublimation-induced changes on the isotopic composition of a snowpack are similar to the changes induced by evaporation on the isotopic composition of residual water (Earman et al., 2006). If a snowpack undergoes sublimation, the residual snowpack isotopic composition follows the local evaporation line (LEL) with a reduced *d-excess* value (Figure 1.2) (Ren et al., 2013; Stichler et al., 2001). It is interesting to note that snow sublimation during the trajectory of snowflakes from the cloud to the ground may not lead to substantial fractionation, presumably as it is an irreversible reaction (Friedman et al., 1992).

Snow sublimation is influenced by (1) vapor pressure deficit that is the difference in vapor pressure between surface snowpack layer and the surrounding air, (2) turbulent diffusion in

air, (3) wind speed and (4) solar radiation (Earman et al., 2006; N'da et al., 2016). Higher vapor deficit and solar radiation increase the rate of snow sublimation. Turbulent diffusion scales with wind speed, leading to an increase in the rate of snow sublimation. It is noteworthy that in Southwest USA, during periods of high solar radiation, melting is dominant and the snowpack isotope composition is governed by snowmelt (Earman et al., 2006). During periods of low solar radiation, evaporation and sublimation are the dominant controls on snowpack isotopic composition in Southwest USA (Earman et al., 2006).

Over the course of a day, if solar radiation and vapor pressure deficit are high, as they usually are in sunny and snowy conditions, sublimation from the top layer enriches the snowpack in heavier isotopes (Earman et al., 2006; Gustafson et al., 2010; Stichler et al., 2001). This is observable through snowpack *d-excess* values that decline faster over the course of the day (Moser and Stichler, 1974; Stichler et al., 2001) but remain constant during the night. At night, condensation of surrounding air moisture, which is more depleted in heavier isotopes, may compensate for the effects of daytime sublimation by increasing *d-excess* values (Moser and Stichler, 1974; Schlaepfer et al., 2014; Stichler et al., 2001). In the snowpacks in Rocky Mountains (USA), Schlaepfer et al., (2014) found no significant change in *d*-excess values over time and implied that sublimation may not always cause fractionation sufficient to influence the snowpack. However, in this case it is also possible that the diurnal changes in the isotopic composition in the snowpack may mask the net isotopic effect of sublimation on the residual snowpack.

The isotopic effect of snow sublimation is restricted to the top layer of a snowpack (Moser and Stichler, 1974; Stichler et al., 2001). However, a sharp temperature gradient within a snowpack can initiate movement of water vapor from lower to upper layers, leading to mixing within different layers of the snowpack. Sublimation from the top layer can then sample water from the deeper layers. This was observed at the Fuji Dome station in Antarctica where during one period of the year, vapor from the lower snowpack layer moved to the surface and condensed (Motoyama et al., 2005). This was initiated by a sharp temperature gradient (about 3 °C) between the firn layer of the snowpack and surface air. Moser and Stichler, (1974) in a laboratory experiment saw similar behavior. When a steep temperature gradient was induced, mass transfer took place from deeper snowpack layers to the surface.

Snow sublimation has also been shown to increase the *d-excess* of groundwater recharged via vapor condensation at higher elevations, from the vapor produced by sublimated snowpacks at lower elevation (Lambán et al., 2015). In a recent study of isotopic composition of 25 springs spanning elevations from 690 m to 2400 m in Ordesa and Monte Perdido National parks in Spain (karstic system) (Lambán et al., 2015), spring water had *d-excess* values higher than that of precipitation. Snow sublimation at low elevation had produced water vapor with a high *d-excess* that was lifted to higher elevations where it mixed with moisture from local sources and finally condensed. The majority of the springs were recharged from precipitation at higher elevations. Thus, the higher *d-excess* values in the condensed vapor propagated into the springs. The effect was more variable at higher elevations, observed by larger amplitude in $\delta^{2}H$ and in $\delta^{18}O$ values, than at lower elevations.

1.5.3. Snow metamorphism and snowmelt

A snowpack is composed of solid, liquid and vapor phases of water. Any exchange between the three phases can change the isotopic composition of the snowpack. Back in 1974, Moser and Stichler, (1974) proposed that isotopic changes due to different snow processes (snowmelt, sublimation, metamorphism, etc.) are limited to the top layer of a snowpack and that the isotopic compositions of deeper layers remain, by and large, unaltered. However, subsequent studies (Friedman et al., 1991; Taylor et al., 2001; Unnikrishna et al., 2002; Winograd et al., 1998) found that snow metamorphism can also homogenize the whole snowpack. Taylor et al., (2001) noticed in snow samples collected in California that the variability in isotopic composition reduced, following the transitions from snowfall to snowpack and finally to snowmelt. Fresh snowfall had the highest variability in isotopic composition, which then reduced with deposition time as snow accumulated within the snowpack. Subsequent snowmelt from this snowpack had the lowest variability in isotopic composition (Cooper, 1998). Similar results were also reported in Alaska (Friedman et al., 1991) and in the Spring mountains in Nevada (USA) (Winograd et al., 1998).

A number of processes can affect the isotopic composition of different layers within a snowpack. They have been summarized in a recent work on seasonal snowpacks in Idaho (USA) (Evans et al., 2016). Water percolation within the snowpack (so-called pervasive flow), from snowmelt at the surface, induces a downward translation of the isotopic composition of the snowpack along the direction of the moving water particles. In contrast, mass loss due to snow sublimation from the snowpack surface shifts the isotopic composition of the snowpack upwards towards the snowpack surface. Diffusion and dispersion of water homogenizes the isotopic variance within the snowpack. A combination of diffusion and dispersion with either pervasive flow or with sublimation shifts the isotopic composition downwards (towards the ground) or upwards (towards the snowpack surface), with some degree of homogenization within the snowpack. However, preferential flow of surface meltwater, either through macropores or through a sloped snowpack (commonly seen in mountainous regions), can release meltwater without affecting deeper snowpack layers (Eiriksson et al., 2013; Evans et al., 2016).

When the surface meltwater percolates through the snowpack, meltwater goes through cycles of crystallization and subsequent melt. Any meltwater that refreezes (crystallizes) enriches the solid phase of the snowpack in heavier isotopes, thereby depleting the residual meltwater in heavier isotopes. The heat released during crystallization can induce melting in adjacent layers of the snowpack. A number of models (Ala-aho et al., 2017; Feng et al., 2002; Lee, 2014; Lee et al., 2009, 2010b, 2010a; Taylor et al., 2001) have tried to characterize changes in the isotopic composition of snowpacks and of associated meltwater induced by snow metamorphism. It is important to note that redistribution within a snowpack but without mass loss does not change the bulk snowpack isotopic composition.

The isotopic composition within a snowpack is also affected by moisture exchange with the underlying soil. Friedman et al., (1991) noticed that the bottom of snow cores was enriched in heavier isotopes compared to the bulk snowpack before the beginning of the melt season. This could not be explained by the stratigraphy resulting from different snowfall events during the accumulation period. The enrichment was due to (1) moisture exchange with the underlying soil layer caused by diffusive water transport from the more enriched soil into the snowpack and (2) fractionation due to crystallization (or condensation) of soil water into the

snowpack. It is noteworthy that molecular diffusion of water vapor through a snowpack (either through advection up or down depending on the vapor pressure gradient) is a fractionating process.

Snowmelt that leaves the snowpack preferentially discharges isotopically light water, thereby enriching the residual snowpack in heavier isotopes (Ala-aho et al., 2017; Feng et al., 2002; Laudon et al., 2002; Shanley et al., 1995; Soulsby et al., 2000; Taylor et al., 2001, 2002). It has been widely observed that early meltwater is more depleted in heavier isotopes and that, as the melt season progresses, both the residual snowpack and the generated meltwater become more enriched in heavier isotopes (Dietermann and Weiler, 2013; Taylor et al., 2001), which is also referred to as the *melt-out effect* (Ala-aho et al., 2017). To the best of our knowledge, the physical mechanisms of this melt-out effect are not well understood but likely involve the partial melting of snowpack which results in preferential loss of lighter isotopes in the early season meltwater.

Both meltwater rates and their isotopic composition show a strong diurnal variation, with higher snowmelt in the middle of the day due to stronger solar radiation. These higher melting rates provide less time for meltwater to remain in contact with solid phase water within the snowpack, which minimizes re-crystallization and thus midday meltwater is more enriched in heavier isotopes (Taylor et al., 2001).

1.5.4. Snow redistribution

Redistribution of snow either by wind transport (Mott et al., 2010) or avalanching (Schweizer et al., 2003) typically takes place over spatial scales from a few tens (wind) to hundreds of meters (Comola, 2017) (avalanching) and can involve significant amounts of snow mass redistribution. It does not have a systematic effect on the composition of snowpack isotopes. When an avalanche redistributes a large fraction of a snowpack from higher to lower elevations, the isotopic composition of the higher elevation snowpack is mixed, to some (and highly variable) extent, with the snowpack at lower elevations. Similarly, when wind blows snow from one place to another, the drifting snow carries the original isotopic composition with it, leading to mixing between snowpacks from distinct places. While this wind-induced

mixing might have a significant effect around mountain ridges, the dominant wind effect on the isotopic composition is the enhanced sublimation of drifting snow, due to i) snow fragmentation (Comola et al., 2017) and ii) enhanced evaporative demand of the atmosphere in presence of wind. Sublimation enriches the underlying snowpack in heavier isotopes (refer to Section 1.5.2) (Essery et al., 1999).

Thus, it is difficult to clearly state the net effect of wind and avalanche on the isotopic composition of snow, especially in complex terrains. In contrast, in flatter areas a more continuous snow drift from the surface layer can occur, and the corresponding enhancement of sublimation might result in a clear pattern in the isotopic composition of the snowpack, but this phenomenon has, to our knowledge not yet been studied.

1.5.5. From the point to the catchment scale

The spatial variability of a snow cover and its isotopic ratios are driven by the temporal sequence of snow accumulation, redistribution, transformation and ablation processes that vary strongly in space and whose dominance varies according to climate and topography. Understanding their joint effect on a catchment scale snowpack requires necessarily detailed local studies, including a characterization of the initial isotopic heterogeneity of snowfall and its subsequent evolution through time in the snowpack. Understanding isotopic heterogeneity at the catchment scale, and its impact on the isotopic signature of snowpack and snowmelt, necessarily begins with identifying the locally dominant processes that drive the isotopic ratios of a snowpack away from its initial snowfall ratios. The key processes that affect the isotopic spatial heterogeneity after initial snowfall are wind redistribution, vapor exchange, snow sublimation and snowmelt. Their importance can be categorized for different snowpack types at different spatial scales. As an example, we propose in Figure 1.6 a classification of the dominant drivers of heterogeneity for the six global snowpack types proposed by Sturm et al., (1995) (Tundra, Taiga, Alpine, Maritime, Prairie and Ephemeral). Such a classification of snowpack types and the associated driving processes at finer spatial scales can help in the identification of corresponding hydrological snowpack units (in analogy to hydrological response units (Gassman et al., 2007)), which might provide a way forward to characterize the isotopic composition of snow at the catchment scale. It is important to

emphasize that these processes occur at a hierarchy of spatial scales (Clark et al., 2011), meaning it can be difficult to isolate the effects of individual processes on the isotopic ratios of snowpack and snowmelt. In addition, slope and aspect will play a role in the spatial heterogeneity of snowpack isotope evolution at hillslope to catchment scales, e.g. through their influence on solar radiation, wind and tree cover. This means a detailed analysis of individual processes at a point scale cannot necessarily account for all the complex spatial dynamics that may occur at the catchment scale. Ideally then, detailed point scale snowpack and snowmelt information should be considered in the context of how spatially representative such conditions are expected to be within a given catchment.

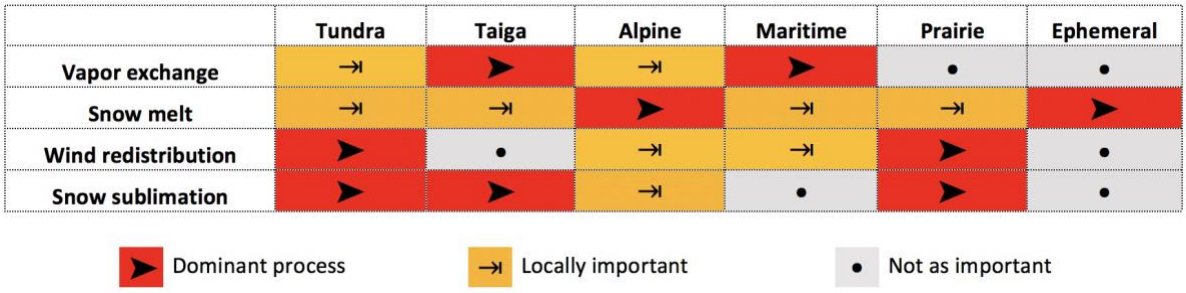

Figure 1.6. Dominant drivers of spatial isotopic heterogeneity according to the different snowpack types as defined by Sturm et al., (1995). Highlighted here is the relative importance of vapour exchange, snowmelt, wind redistribution and snow sublimation in enhancing the isotopic heterogeneity of the final snowmelt beyond what was initially introduced by snowfall.

Sidebar 1: Modelling snowpack isotope fractionation and isotope ratios in snowmelt
Stable isotope compositions of water have a great potential to constrain catchment-scale hydrological models that predict river streamflow as a function of incoming precipitation (see Birkel and Soulsby, (2015) for a review). In the presence of snow, the use of stable water isotopes to improve a hydrological process model hinges on the ability to characterize snowmelt isotopic composition based on observed precipitation isotopes through the entire life cycle of snow. Only few studies have attempted to build such a complete model from precipitation to streamflow isotopes for snow-influenced catchments. One such example is the work of Ala-aho et al., (2017) who incorporated changes incurred in the isotopic composition of snow during its hydrologic life cycle, and coupled it with a snow process model. The key advancements were the fully distributed (spatially) and parsimonious nature of the model. This is a major step forward in tracer-aided hydrologic modeling (Birkel and Soulsby, 2015; Capell et al., 2012; Delavau et al., 2017; van Huijgevoort et al., 2016b, 2016a; McMillan et al., 2012; Regan et al., 2017; Stadnyk et al., 2013; Tetzlaff et al., 2015; Tunaley et al., 2017).

1.6. Focus on selected snow hydrological processes

Below we present examples of how stable isotope composition can be used to unravel snow processes within the hydrological cycle. We focus on three topics that have received particular research focus in the recent past, 1) the effects of canopy on snowpacks, 2) rain-on-snow events and 3) ground water recharge from snow.

1.6.1. Canopy effects on underlying snowpack

Canopy cover affects the underlying snowpack by altering the snow water equivalent (SWE) along with its isotopic composition (Biederman et al., 2014b, 2014a; Gustafson et al., 2010; Koeniger et al., 2008). Koeniger et al., (2008) found that the snowpack in a forested watershed in Idaho (USA) was enriched in heavier isotopes due to enriched throughfall, caused by sublimation of the canopy intercepted snow and associated evaporation. Longer exposure time of the intercepted snow led to greater enrichment in heavier isotopes. Gustafson et al.,

(2010) investigated the effect of canopy shading on the isotopic composition of a snowpack in Jemez Mountain in New Mexico (USA). During the maximum snow accumulation period with similar winter precipitation, the snowpack in a non-shaded area showed greater enrichment in heavier isotopes than that under shade.

Another interesting use of isotopic variation to understand canopy interception processes was seen in the Central Rocky Mountains (USA) (Biederman et al., 2014b, 2014a). A mountain pine beetle (MPB) infestation destroyed most of the tree canopy in the Central Rocky Mountains. The canopy formerly intercepted a large amount of snow, much of which sublimated before reaching the forest floor. After the infestation, less snow was intercepted due to reduced canopy, and the SWE of the underlying snowpack was expected to increase. However, Biederman et al., (2014b, 2014a) found SWE during maximum snow accumulation phase to be unchanged, despite small changes in winter precipitation. To answer this anomaly, Biederman et al., (2014b, 2014a) carried out a study in two headwater catchments in the region over the winters of 2011 and 2012. One of the catchments was MPB affected, while the other one was used as a control. In the MPB affected catchment, the underlying snowpack was enriched in heavier isotopes, supporting kinetic fractionation due to sublimation and accompanying evaporative loss. However, there was no change in the isotopic composition in snowpack of the unaffected catchment. Newly exposed forest floor due to MPB experienced more direct solar radiation, which increased direct sublimation and evaporative loss from the underlying snowpack. This enhanced sublimation from the snowpack was equivalent in quantity with sublimation from the snow intercepted by the canopy, hence keeping the total SWE constant. The variation in isotopes provided insight on the "invisible snow" processes that went undetected by simply monitoring snow volume.

1.6.2. Rain-on-snow

Rain-on-snow (ROS) events can release amounts of water that are substantially higher than the actual rainfall amounts onto the pre-existing snowpack. Such events can be associated with large flood events and are known to trigger landslides, change channel morphology by enhancing erosion processes and influence water quality (Brunengo, 1990; Guan et al., 2016; McCabe et al., 2007, 2016; Rössler et al., 2014; Singh et al., 1997; Surfleet and Tullos, 2013).

The frequency of ROS peak flow events is projected to increase at number of places under a warming climate (Surfleet and Tullos, 2013). Given that rainfall has a different isotopic composition than the pre-existing snowpack, stable water isotopes can be used to investigate two key characteristics of ROS events: 1) the origin of the water that is released during the event (rainfall versus melted water that was stored in the snowpack); 2) the flow paths and associated transmission times of the released water.

The amount of runoff induced by ROS events depends on the spatial extent and cold content of the snowpack prior to the onset of rain. Cold content represents the amount of energy needed to raise the entire snowpack to the 0 °C melting point. An isothermal snowpack is associated with higher temperature, higher density, and with larger crystal sizes. Such snowpacks are known to produce higher proportional runoff than snowpacks that are not isothermal. This comes from the fact that less additional energy from the incoming rainfall is required to heat the isothermal snowpack to 0 °C (Colbeck, 1975; Gerdel, 1945; Juras et al., 2016; Maclean et al., 1995). During a ROS event, radiation (Mazurkiewicz et al., 2008) rain and turbulent exchanges with the atmosphere transport heat into the snowpack. As incoming rain percolates through the snowpack, refreezing occurs, which releases heat and increases the temperature of the snowpack. As a result, large amounts of water can be released from the snowpack, either infiltrating into the ground or running off directly into the stream. In contrast, in a non-isothermal snowpack, incoming heat is not as efficient at producing snowmelt and the snowpack can retain more liquid water on crystal surfaces and in the voids (Gerdel, 1945).

Stable water isotopes have been used to analyze these snowpack processes and ensuing water flow paths at the plot scale during artificially induced ROS experiments (a review is given in (Juras et al., 2016)). Juras et al., (2016) showed for example with the help of δ^2H measurements that such an artificial ROS event in the Krkonoše mountains (Czech Republic) led to percolation of rain water through the snowpack, pushing old water out of the snowpack via a piston flow mechanism.

Several studies observing the evolution of the isotopic content of snowpacks during natural rainfall events noted that ROS-induced snowmelt leads to higher ratios of surface flow to total

runoff, than subsurface flow. These results have been reported in the Sierra Nevada forests (USA) (Kattelmann, 1987), in the Central Adirondack Mountains (USA) (Burns and McDonnell, 1998), in headwater and suburban catchments in Ontario (Canada) (Buttle et al., 1995; Maclean et al., 1995; Wels et al., 1991b) and in the Krkonoše mountains (Czech Republic) (Juras et al., 2016). Interestingly, in two forested catchments in Ontario (Canada), Casson et al., (2014) found using streamflow isotopes that ROS-induced events were dominated by baseflow and not by surface runoff.

Overall, stable water isotopes have a high potential to provide insights into ROS events across a range of spatial and temporal scales. Given that ROS events typically result in a rapid hydrologic response, progress in terms of high temporal resolution of isotopic observations will certainly yield new insights into snow hydrological processes across scales.

1.6.3. Estimating the contribution of rain versus snow to streamflow and groundwater recharge using mixing models

In a warming climate, more precipitation is expected to fall as rain than as snow (Choi et al., 2010; Steger et al., 2013). This is likely to change the proportion of rain versus snow contributing to the outgoing fluxes, and potentially the magnitude of the fluxes, from catchments such as evapotranspiration, groundwater recharge, and runoff. Stable isotopes of water are commonly used as tracers to identify the proportion of rain versus snow contributions to these fluxes, especially runoff and groundwater recharge (Earman et al., 2006). This is because snow is generally more depleted in the heavier isotopes than rain (Figure 1.2), which allows samples of runoff or groundwater falling within the isotopic range between rain and snow 'end members' to be assigned proportional contributions using a linear mixing model (Obradovic and Sklash, 1986).

An impressive number of studies (Cervi et al., 2015; Earman et al., 2006; Herrera et al., 2016; Jasechko et al., 2014, 2017; Jasechko and Taylor, 2015; Jeelani et al., 2010; Kohfahl et al., 2008; Lechler and Niemi, 2012; Maule et al., 1994; Mountain et al., 2015; O'Driscoll et al., 2005; Penna et al., 2014b, 2017; Rose, 2003; Simpson et al., 1970; Winograd et al., 1998; Zappa et al., 2015) have used a stable isotope approach to attribute percentages of snow and

rain as sources for annual groundwater recharge (see a summary in Table 1.1). In general, they found that the snowmelt yield to groundwater recharge per unit of precipitation is higher than that of rain-induced recharge. The dominance of snowmelt induced groundwater recharge has been shown in the USA (Earman et al., 2006; O'Driscoll et al., 2005; Rose, 2003; Simpson et al., 1970; Winograd et al., 1998), in Canada (Jasechko et al., 2017; Maule et al., 1994; Mountain et al., 2015), in the Himalayas (Jeelani et al., 2010), in Switzerland (Halder et al., 2013), in Spain (Kohfahl et al., 2008), in Georgia (Zappa et al., 2015), in Italy (Cervi et al., 2015; Penna et al., 2014b, 2017) and in Chile(Herrera et al., 2016). A recent analyses (Jasechko et al., 2014; Jasechko and Taylor, 2015) of published stable isotope data with the help of a global hydrologic model, suggest that spring snowmelt due to winter precipitation dominates recharge in temperate and arid climates. In tropical regions of the world, where snowfall generally does not contribute to the overall water balance, the isotope approach revealed that majority of groundwater recharge occurred during heavy storm events (Jasechko and Taylor, 2015).

Earman et al., (2006), using δ^2H and $\delta^{18}O$ values in the Southwestern U.S., suggested two mechanisms behind snowmelt-dominated groundwater recharge: (1) During the snowmelt season in the Southwest U.S., vegetation is still mostly dormant which leads to smaller losses by evapotranspiration than during the summer, allowing more time for meltwater to infiltrate, and recharge groundwater; (2) The summer storms in Southwest U.S. are high intensity, and short duration causing a higher proportion of overland flow. On the other hand, snowmelt in the Southwest U.S. is typically low intensity but long in duration, which gives more opportunity for infiltration and groundwater recharge.

This enhanced snow proportion in groundwater is a good explanation for the proportionally higher snow contributions to streamflow as noted in several studies (Li et al., 2017). This might especially be the case in higher elevation areas where shallow groundwater is critical for streamflow generation.

It is important to note that using stable isotope compositions of snowfall or from snowpack as a proxy for the meltwater recharging groundwater and supplying streamflow might result in a considerable bias of actual snow contributions (Earman et al., 2006; Lechler and Niemi,

2012; Pavlovskii et al., 2018). This can be understood within the dual isotope space, where groundwater and streamflow samples are usually located somewhere between rain and snow. Snowmelt samples are on average closer to groundwater and streamflow samples than snowpack or snowfall samples. Accordingly, a mixing model may underestimate the contribution of snowmelt to streamflow and groundwater recharge when computed with (uncorrected) snowfall or snowpack samples, instead of actual snowmelt samples. An overview of the processes that can bias snow end member estimates in mixing models is given in Table 1.2. In general, it is recommended to either use the stable isotope composition of snowmelt, or where this is not practical, to examine correcting for potential snowpack enrichment after snowfall, resulting from evaporative losses through sublimation and melt-out effects.

Table 1.1. Summary of studies estimating groundwater recharge from summer (rain) and winter precipitation (snow), along with the used snow end member, i.e. snowfall or snowmelt or a combination of the two.

Authorship	**Year (isotopes used)**	**Location**	**Summary**	**Snow end member**
(Simpson et al., 1970)	1968-69 (δ^2H, δ^{18}O)	Arizona (USA)	Winter runoff dominant in groundwater recharge (numerical estimates not provided)	Snowmelt
(Maule et al., 1994)	1986-87 (δ^2H,δ^{18}O)	Alberta (Canada)	~44% groundwater recharge due to winter precipitation (~21% of annual precipitation) (fractionation corrected estimates)	Snowfall
(Winograd et al., 1998)	1966-88 (δ^2H, δ^{18}O)	Spring mountains, Nevada (USA)	~90% groundwater recharge due to snow (~66% of annual precipitation)	Snowfall & Snowmelt
(Rose, 2003)	1999-02 (δ^2H, δ^{18}O)	4 sites in Sierra Nevada (USA)	>90% groundwater recharge due to winter precipitation (75-80% of annual precipitation)	Snowfall & Snowmelt
(O'Driscoll et al., 2005)	1999-00 (δ^{18}O)	3 catchments in Pennsylvania (USA)	~90% groundwater recharge due to snow (~66% of annual precipitation)	Snowmelt
(Earman et al., 2006)	2002-04 (δ^2H,δ^{18}O)	4 sites in South Western U.S. (USA)	40-70% groundwater recharge due to snow (25-50% of annual precipitation	Snowfall & Snowmelt
(Kohfahl et al., 2008)	2004-05 (δ^2H, δ^{18}O)	Granada basin (Spain)	Recharge predominantly due to winter rain and melting snow	Snowfall & Snowmelt
(Penna et al., 2014b)	2011-13 (δ^2H, δ^{18}O)	Saldura catchment, Eastern Italian Alps (Italy)	Seasonal variation in groundwater recharge due to snowmelt with annual contribution varying from (58 ± 24% to 72 ± 19%)	Snowfall & Snowmelt
(Jasechko et al., 2014)	Metadata study		Isotopes and global hydrologic model suggest dominant winter precipitation recharge in temperate and arid climates and suggest wet season bias in tropical regions	Snowfall
(Jasechko and Taylor, 2015)	Metadata study		Preferential recharge of groundwater from heavy storm in the tropics	Rainfall
(Zappa et al., 2015)	2010-13(δ^2H, δ^{18}O)	Gudjareti (Georgia)	Winter precipitation is very important source of groundwater recharge	Snowfall & Snowmelt

(Cervi et al., 2015)	2004-08($\delta^{18}O$)	Mt. Modino area, northern Apennines (Italy)	Predominant recharge from winter and spring precipitation	Snowmelt
(Herrera et al., 2016)	2004-05 ($\delta^{2}H$, $\delta^{18}O$)	Andean alps (Chile)	Predominant groundwater recharge from winter precipitation	Snowfall
(Jasechko et al., 2017)	1991-12 ($\delta^{2}H$,$\delta^{18}O$)	Nelson river watershed (Canada)	Fraction of groundwater recharge by winter precipitation ~ 1.3-5 times that of precipitation during warm months	Snowfall
(Penna et al., 2017)	2011-15 ($\delta^{2}H$,$\delta^{18}O$)	Rio Vauz Catchment, Eastern Italian Alps (Italy)	Recharge predominantly due to snowmelt (64 ± 8%)	Snowfall & Snowmelt

Sidebar 2: Snowmelt isotope sampling methods

Snowmelt samples are critical as water from snowmelt contributes significantly to groundwater recharge via infiltration and to streamflow via both surface and subsurface flow paths. However, obtaining representative snowmelt samples is difficult because of the spatial and temporal variability across snowpacks, requiring snowmelt measurements at a number of remote locations, typically at high elevations, which becomes a major technical challenge. This is why snowpack samples are often used as a substitute for snowmelt samples. The problem with this substitution is that stable water isotope measurements obtained from conventional snow coring methods do not necessarily yield a representative sample of the isotopic ratio of snowmelt that will leave the snowpack (Earman et al., 2006; N'da et al., 2016). Snow lysimeters are most commonly used to obtain snowmelt samples beneath the snowpack. Recently, a number of studies (Frisbee et al., 2010b, 2010a; Holko et al., 2013; N'da et al., 2016; Penna et al., 2014a) have also recommended the use of passive capillary sampling procedures to sample meltwater at the base of a snowpack. The advantage of this method is obtaining a snowmelt sample without the potential water ponding that can occur with lysimeters, and thereby avoiding evaporative fractionation.

Table 1.2. Overview of the processes that can bias snow end member estimates in mixing models: Potential biases introduced when a linear mixing model is used to estimate snow proportions in streamflow or groundwater recharge derived from snow samples taken at different stages of the hydrologic cycle of snow; *scale* refers to the spatial scale at which the discussed bias is relevant, *places* refers to locations where the bias might be relevant.

Sample type	**Omitted process**	**Type of estimation bias**	**Scale**	**Places**
Snowmelt	Spatial snowmelt heterogeneity	*Unbiased* if samples from all dominant flow generation locations *Biased* otherwise	Hillslope to catchment	Areas with spatially heterogeneous snow recharge or runoff generation (hotspots)
Snowpack	Time-variable isotope signal of snowmelt water	*Underestimated* if many early season snowpack samples *Overestimated* if samples from ripe snowpack only	Point to catchment	Areas with significant snow accumulation period
Snowfall	Snowpack evolution and melt	*Underestimated*	Point to catchment	Areas with significant snow accumulation period
Snowfall	Snowpack sublimation	*Underestimated*	Point to catchment	Areas with significant sublimation
Snowfall	Snow interception and related sublimation	*Underestimated*	Point to catchment	Areas with significant snow interception and sublimation
Snowfall/Snowpack	Snow lapse rate	*Overestimated* if majority of samples from low elevation *Underestimated* if majority of samples from high elevation	Catchment	Area with large elevation range

1.7. The hydrological life cycle of seasonal snow – a synthesis

We can summarize the key steps in the isotopic evolution of snowfall, snowpack, and snowmelt as representative shifts in the dual isotope space over the course of a typical snow season (Figure 1.7). Fresh snowfall may fall directly on bare ground or pre-existing snow, or be intercepted by the canopy. The intercepted snow, and the top layer of fresh snow on the ground, will be subject to varying degrees of sublimative enrichment. The developing snowpack will therefore represent some mixture of unmodified, and isotopically enriched snow.

Over the course of a snow season, both the snowpack and snowmelt undergo three key phases of isotopic evolution. The first is during the longer period of snowpack accumulation, within which melting phases can still occur. These melt events flush the lighter isotopes, resulting in depleted meltwater and a proportionately enriched snowpack, which in combination is commonly referred to as the '*melt-out effect*'. However, the majority of snowmelt release typically occurs in a relatively shorter period of time at the end of the snow season; and this is the most significant phase in terms of snow meltwater contributions to the catchment hydrological cycle. The rapid reduction in snowpack volume produces a well-mixed snowmelt that homogenizes the isotopic signal, and therefore reduces isotopic variance relative to the snowpack. Finally, the melting of minor amounts of residual snow patches at the very end of the season can produce highly variable isotopic compositions of snowmelt, albeit with a considerably lower total flux. This end-of-season variability results from isotopic enrichment of the residual snowpack due to sublimation, and limited mixing at low snowpack depths and volumes.

Given that snowfall is strongly depleted in heavier isotopes with respect to summer rainfall, the average isotopic composition of a snowpack will generally remain more depleted than summer rainfall throughout the accumulation and ablation season despite the enriching effect of snowmelt and sublimation (Figure 1.2). Accordingly, snowmelt runoff from seasonal snowpacks can be assumed to show a narrow range of isotopic compositions (compared to snowfall) especially during the main phase of snowpack melting. The average isotopic ratios

of snowfall, snowpack and snowmelt are statistically similar, which is also reflected in Figure 1.2. All this can be used in the context of mixing models to estimate source contributions, e.g. for streamflow or groundwater.

In environments where sublimation is low, the snowmelt composition lies on the local meteoric water line; and conversely, any departure of snow samples from the meteoric water line can provide some insights into the importance of sublimation in a given environment.

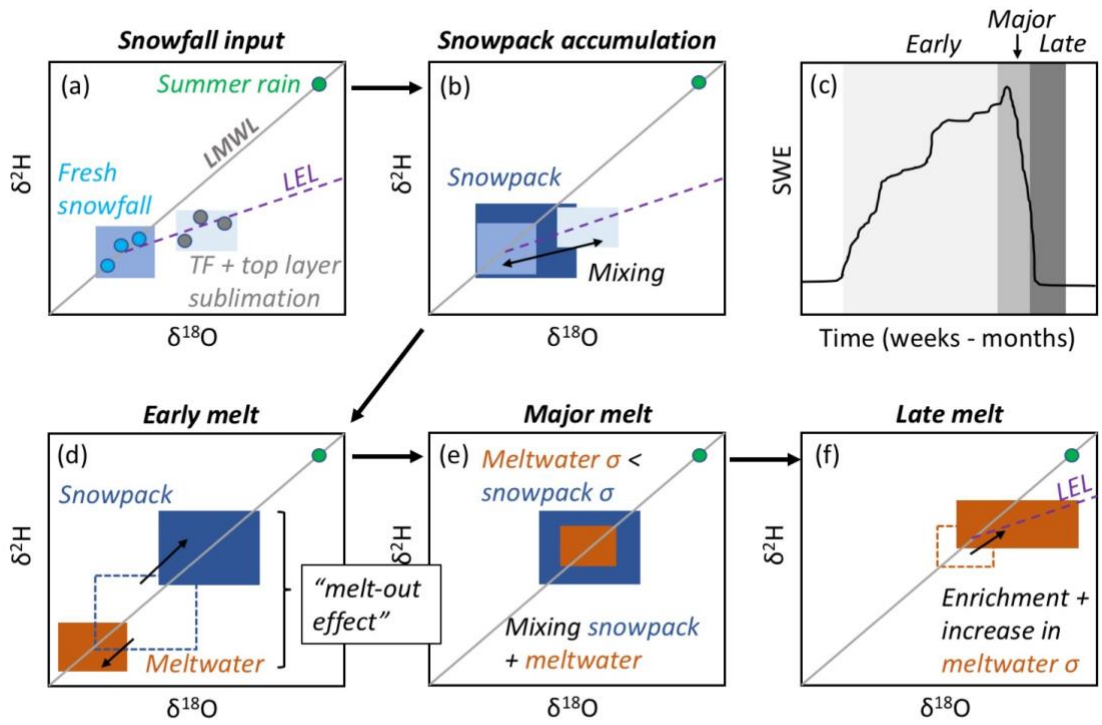

Figure 1.7. Tracking the evolution of snow isotopes from inputs of snowfall (a) to snowpack (b), and throughout the melting process (d – f). A representative temporal evolution of snowpack (represented as SWE) is provided in (c), highlighting the ranges over which early, major, and late melting phases and isotope changes are likely to occur. Plots b,d,e,f synthesize the isotopic evolution of snowpack and snowmelt from a 'control volume' perspective, while (a) is from the perspective of a 'pulse' of snowfall that could fall directly to the ground or be intercepted by the canopy and undergo isotopic modification due to sublimation (along the LEL) and subsequent transport to the ground as snow throughfall (TF). The evolution of hypothetical samples (circles) and their ranges in dual isotope space (colored boxes) are

shown in (a), with subsequent plots only showing the range as colored boxes. In subplot (e), σ represents the standard deviation of the meltwater or the snowpack sample.

1.8. Directions for future research

In 1998, Kendall and McDonnell, (1998) proposed the use of alternative tracers, other than the stable water isotopes of water (^{2}H and ^{18}O), to better understand snowmelt processes. These include using alternative tracers such as electrical conductivity, water temperature, anions and cations. In the last decade, ^{17}O has been suggested as an additional tracer to better constrain the hydrologic cycle (Berman et al., 2013; Birkel and Soulsby, 2015; Galewsky et al., 2016). However, very little work has been done using ^{17}O in snow hydrology, largely related to the difficulty of routinely measuring the ^{17}O concentrations in water. It is now well known that ^{17}O is relatively insensitive to temperature, but sensitive to humidity (Angert et al., 2004; Berman et al., 2013). Due to differences in rates of molecular diffusivity between ^{17}O and ^{18}O, using *O17-excess* in addition to *d-excess* may help to better constrain kinetic processes like evaporation and sublimation (from both intercepted snow and from the snowpack). To our knowledge however, there are no studies using ^{17}O to better quantify snow sublimation or snowpack processes in general. Future research using all the three stable water isotopes (^{2}H, ^{17}O and ^{18}O) will certainly provide insights into the potential use of ^{17}O in snow hydrology.

Most of the work in snow isotope hydrology has focused on either estimating the proportion of snow and rain in streamflow and groundwater, or on the isotopic changes in snowmelt induced by snowmelt and sublimation. Much remains to be known on how canopy alters the isotopic composition of snow via interception, which is a substantial part of the water budget, especially in forested regions. The spatial variability in canopy interception is also understudied. Future research should focus on improving the spatial representation of stable water isotopes in intercepted snow and accumulated snowpack, and on understanding how this spatial heterogeneity translates into changes in the isotopic composition of the final meltwater.

Despite advancements in understanding isotopic evolution within seasonal snowpacks, there are very few studies that use them in predictive modeling to draw insights into the overall water budget. Examples on how to draw on isotope-based process understanding for snow hydrological modeling at the catchment scale are still rare. We hope that our synthesis encourages hydrologists to find new ways of constraining models with insights gained from stable isotope compositions of water.

1.9. Conclusions

Snow undergoes significant changes from the time of its formation as precipitation to when it leaves the snowpack via sublimation or melt. These changes might not completely "overwrite" the stable water isotopic composition of the initial snowfall and, accordingly, research has been focused on understanding the isotopic composition of snow and its usefulness to track hydrological fluxes. We reviewed in detail the current knowledge of changes in the isotopic composition of snow across its entire hydrological life cycle. The effects on the isotopic composition of the different snow processes can be summarized as follows:

1. Variability in the isotopic composition of snow reduces from the onset of snowfall to the date of final snowmelt. Reduction in variance is caused by isotopic redistribution within the snowpack during the snow accumulation phase, in combination with other snow metamorphism processes.
2. Snowmelt during the early melt season is more depleted in the heavier isotopes which in due course of the melt season, becomes more enriched. Snowmelt isotopic compositions are correlated with melt rates, being more enriched in the heavier isotopes when melt rates are higher (typically during the day).
3. Snow interception can alter the isotopic composition of snow, from the time when snow first falls on the canopy to when it leaves the canopy and builds up on the ground. Longer snow residence times on the canopy are typically associated with higher degree of enrichment, especially when snow sublimation is significant.
4. The degree of canopy shading can substantially alter the isotopic composition of the underlying snowpacks. Snowpacks are more depleted in heavier isotopes in a well-

shaded area, as their direct exposure to the solar radiation is small, leading to a smaller sublimation effect.

5. Snow sublimation enriches the isotopic composition of the residual snowpack in heavier isotopes. After enrichment, the remaining snowpack isotopes plot along the local evaporation (sublimation) line in the dual isotope space.
6. The fact that snow is isotopically lighter than rain can be leveraged to examine seasonal dependence of stream runoff or groundwater recharge.

Author contributions: The paper was written by HB with contributions from all coauthors. HB and BS formulated the conceptual underpinnings of the article. NCC led the section on *Snow Regions of the World*. TV reviewed the theoretical foundations of isotope chemistry. All coauthors provided critical feedback during different phases of writing the article.

2. HydroMix v1.0: a new Bayesian mixing framework for attributing uncertain hydrological sources

Harsh Beria, Joshua R. Larsen, Anthony Michelon, Natalie C. Ceperley, Bettina Schaefli

Published[2] in *Geoscientific Model Development.*

[2] Beria, H., Larsen, J. R., Michelon, A., Ceperley, N. C. and Schaefli, B.: HydroMix v1.0: a new Bayesian mixing framework for attributing uncertain hydrological sources, Geosci. Model Dev., 13(5), 2433–2450, doi:10.5194/gmd-13-2433-2020, 2020.

Abstract

Tracers have been used for over half a century in hydrology to quantify water sources with the help of mixing models. In this paper, we build on classic Bayesian methods to quantify uncertainty in mixing ratios. Such methods infer the probability density function (pdf) of the mixing ratios by formulating pdfs for the source and target concentrations and inferring the underlying mixing ratios via Monte Carlo sampling. However, collected hydrological samples are rarely abundant enough to robustly fit a pdf to the source concentrations. Our approach, called HydroMix, solves the linear mixing problem in a Bayesian inference framework where the likelihood is formulated for the error between observed and modelled target variables, which corresponds to the parameter inference set-up commonly used in hydrological models. To address small sample sizes, every combination of source samples is mixed with every target tracer concentration. Using a series of synthetic case studies, we evaluate the performance of HydroMix using a Markov Chain Monte Carlo sampler. We then use HydroMix to show that snowmelt accounts for around 61% of groundwater recharge in a Swiss Alpine catchment (Vallon de Nant), despite snowfall only accounting for 40-45% of the annual precipitation. Using this example, we then demonstrate the flexibility of this approach to account for uncertainties in source characterization due to different hydrological processes. We also address an important bias in mixing models that arises when there is a large divergence between the number of collected source samples and their flux magnitudes. HydroMix can account for this bias by using composite likelihood functions that effectively weight the relative magnitude of source fluxes. The primary application target of this framework is hydrology, but it is by no means limited to this field.

Keywords: Markov Chain Monte Carlo; stable water isotopes; hydrograph separation; isotopic lapse rate; rain; snow;

2.1. Introduction

Most water resources are a mixture of different water sources that have travelled via distinct flow paths in the landscape (e.g. streams, lakes, groundwater). A key challenge in hydrology is to infer source contributions to understand the flow paths to a given water body using a source attribution technique. A classic example is the two-component hydrograph separation model to quantify the proportion of groundwater and rainfall in streamflow, often referred to as "pre-event" water vs "event" water (Burns et al., 2001; Klaus and McDonnell, 2013; Schmieder et al., 2016). Other examples include estimating the proportional contribution of rainfall and snowmelt to groundwater recharge (Beria et al., 2018; Jasechko et al., 2017; Jeelani et al., 2010), fog to the amount of throughfall (Scholl et al., 2011, 2002; Uehara and Kume, 2012), and soil moisture (at varying depths) and groundwater to vegetation water use (Ehleringer and Dawson, 1992; Evaristo et al., 2017; Rothfuss and Javaux, 2017).

The primary goal of such attribution in hydrology is to infer the contribution of different sources to a target water body, where the tracer can be an observable compound like a dye, or a conservative solute, or even a proxy for chemical composition such as electrical conductivity. The key requirement is that the concentration of the tracer is distinguishable between different sources. The stable isotope composition of hydrogen and oxygen in water (subsequently referred to as 'stable isotopes of water') are used as tracers in hydrology. Other commonly used tracers include electrical conductivity (Hoeg et al., 2000; Laudon and Slaymaker, 1997; Lopes et al., 2018; Pellerin et al., 2007; Weijs et al., 2013) and conservative geochemical solutes such as chloride (Rice and Hornberger, 1998; Wels et al., 1991a).

Classically, attribution analysis is done by assigning an average tracer concentration to each source, estimated typically from time or space-averages of observed field data (Maule et al., 1994; Winograd et al., 1998), and then solving a series of linear equations. In order to express uncertainty in the attribution analysis, a tracer-based hydrograph separation approach was first proposed in the work of Genereux, (1998) and has subsequently been used in many studies (Genereux et al., 2002; Koutsouris and Lyon, 2018; Zhu et al., 2019). Bayesian mixing approaches offer a useful alternative to classic hydrograph separation, as Bayesian approaches explicitly acknowledge the temporal variability of source tracer concentrations

estimated from observed samples (Barbeta and Peñuelas, 2017; Blake et al., 2018). Rather than a single estimate of source contributions, Bayesian approaches yield full probability density functions (pdfs) of the fraction of different sources in the target mixture (Parnell et al., 2010; Stock et al., 2018), hereafter referred to as 'mixing ratios'.

Bayesian mixing was first developed in ecology to estimate the proportion of different food sources to animal diets (Parnell et al., 2010; Stock et al., 2018). Hydrological applications of such models are still rare (Blake et al., 2018; Evaristo et al., 2016, 2017; Oerter et al., 2019). In a Bayesian mixing model, a statistical distribution is fitted to both the measured source tracer concentrations, and to the measured tracer concentrations from the target (e.g. river, groundwater, vegetation). The distribution of the mixing ratios is then inferred via Bayesian inference. With recent advances in probabilistic programming languages like Stan (Carpenter et al., 2017), Bayesian inference has become a relatively simple task.

However, the key limitation with the above approach is that the source compositions are assumed to come from standard statistical distributions. Typically, the sources are assumed to be drawn from Gaussian distributions, which can be fully characterized by the mean and variance of the data available for each source (Stock et al., 2018). This limits both the potential applicability and the insights that can be gained from tracer information in hydrology because the sample mean and variance may not accurately reflect the statistical properties of the actual source composition and the Gaussian approach represents an unnecessary simplification in cases where a large amount of information on source composition is available.

An additional complication in hydrology comes from the fact that observed point-scale samples do not necessarily capture the tracer concentrations in the actual sources, which are distributed heterogeneously in space and whose contribution can be temporally variable depending on the state of the catchment (Harman, 2015). For instance, if we were to characterize the contribution of snowmelt to groundwater, we would need to capture (1) the temporal evolution of the isotopic ratio of snowmelt, which strongly varies in space (Beria et al., 2018; Earman et al., 2006), and (2) the temporal evolution of the area actually covered by

snow. This spatially and temporally distributed nature of the sources can be hard to account for in both the analytical and the Bayesian mixing approaches.

To overcome the limitations of source heterogeneity and the previously discussed restriction to Gaussian distributions, we present a new mixing approach for hydrological applications, called HydroMix. This approach does not require a parametric description of observed source or target tracer concentrations. Instead, HydroMix formulates the linear mixing problem in a Bayesian inference framework similar to hydrological rainfall-runoff models (Kavetski et al., 2006a), where the mixing ratios of the different sources are treated as model parameters. Multiple model parameters can be inferred in such a setup allowing parameterization of additional hydrologic processes that can modify source tracer concentrations (shown in Section 2.3.5). A more detailed account of the advantages and limitations of this new approach is given in Section 2.5.

In this paper, we first describe the theoretical details of HydroMix for a simple case study with two sources, one mixture and one tracer (Section 2.2). Section 2.3 presents synthetic and real-world case studies that demonstrate the accuracy, robustness and flexibility of HydroMix. In the synthetic case study, we use a conceptual hydrologic model to simulate tracer concentrations. We also introduce a composite likelihood function that accounts for the magnitude of the different sources. The real-world case study applies HydroMix in a high-elevation headwater catchment in Switzerland. The results of these applications are presented in Section 2.4 before summarizing the main outcomes, applicability, and limitations of HydroMix in Section 2.5.

2.2. Model description and implementation

A system with *n* sources mixing linearly in a target water body can be written as:

$$\rho_1 S_1^k + \rho_2 S_2^k + \cdots + \rho_n S_n^k = Y^k, \qquad 2.1$$

where Y^k is the concentration of the k^{th} tracer in the target mixture, S_i^k is the concentration of the k^{th} tracer in source *i*. ρ_i (*i=1, .., n*) are the fractions of all sources in the mixture, with

$\sum_{i=1}^{n} \rho_i = 1$, corresponding to the aggregation of different sources in the mixture. In order to solve this system of linear equations, "*n-1*" different tracers are required.

Section 2.2.1 details the general modeling approach for a simplified system with two sources and one tracer. This is followed by a detailed discussion on the choice of the parameter inference approach used.

2.2.1. Linear mixing model with non-concomitant observed data

For a system with two sources that combine linearly to form a mixture, the mixing model can be formulated as:

$$\rho S_1(t - \tau_1) + (1 - \rho) S_2(t - \tau_2) = Y(t), \quad 2.2$$

where $S_1(t - \tau_1)$ is the tracer concentration in source 1 at timestep $t - \tau_1$, $S_2(t - \tau_2)$ is the tracer concentration in source 2 at timestep $t - \tau_2$, $Y(t)$ is the concentration of the mixture (i.e. the tracer concentration in the target) at timestep t, ρ is the mixing ratio and τ_i is the time delay between the time when source *i* enters the system and the time when it is observed in the mixture. As an example, for a case where the two sources are snowmelt and rainfall and the mixture is groundwater, ρ represents the proportional groundwater recharged from snowmelt and τ represents the average time lag for rain or snowmelt to reach groundwater once they enter into the soil. In other words, the time lag (τ) stands for any delay caused by tracer transport from the source to the output; we assume that the source components are conservative in nature.

The two parameters in this system, the mixing ratio (ρ) and the time delay (τ), can be inferred via classical Bayesian parameter inference which is widely used in hydrology (Kavetski et al., 2006a, 2006b; Schaefli and Kavetski, 2017). This implies taking an observed timeseries of the target (e.g. the tracer concentration in groundwater) and building a vector of model residuals:

$$\varepsilon_t = \tilde{Y}_t - \hat{Y}_t, \quad 2.3$$

where $\tilde{Y}_t$ represents the observed mixture concentration and $\hat{Y}_t$ represents the simulated mixture concentration. However, in real environmental systems like that of groundwater recharge from rainfall and snowmelt, there are four major difficulties which can prevent the inference of ρ and τ from the observed data.

i. ρ and τ strongly vary in time depending on catchment conditions such as soil moisture (as previously discussed in the context of the 'inverse storage effect' (Benettin et al., 2017b; Harman, 2015)).
ii. Long time series of the tracer concentration in both the sources and mixture are rare.
iii. The effect of seasonality in precipitation can make the inference of τ very difficult in case the goal is to understand intra-annual recharge dynamics.
iv. The tracer concentration in the different sources are generally measured at point scales whereas the tracer concentration in the target integrates inputs over the entire source area.

Our practical solution to limitation iv) is to assume that tracer concentrations in the two sources are functions of observable point processes:

$$S_i(t) = f_i\big(P_i(t)\big), \qquad 2.4$$

where the function f_i represents the transformation from the point to the catchment scale for source *i*. Limitation iii) can be relaxed by assuming a long enough timestep (eg: long term groundwater recharge dynamics), where the observed samples are samples from the long term (>> 1 year) source and target compositions. This allows to replace the timestep 't' and '$t+\tau$' with Δt and write Eq. (2.2) as:

$$\rho S_1'(\Delta t) + (1-\rho) S_2'(\Delta t) = Y'(\Delta t), \qquad 2.5$$

where the $'$ signifies the new time-integrated variables. Now, any observed point-scale tracer concentration p_i in a given source *i* or in the output (e.g., the isotopic ratio of snowmelt) can

be assumed to represent a sample from a stationary process (from S'_1 or S'_2 or Y'). This assumption is in fact implicitly underlying most of the existing hydrological mixing models where point samples are used to characterize a spatial process and where the time reference of the samples is discarded.

By utilizing all the available measurements $\{p'_1\}_{i=1..n}$ and $\{p'_2\}_{j=1..m}$ of the two sources in the above model, with n samples of source 1 and m samples of source 2, we can build $n \times m$ predictions and compare them with the q observed samples of the target as:

$$\varepsilon_{ij}^k = \tilde{Y}_{obs}^k - \hat{Y}_{ij}, \qquad 2.6$$

where $\tilde{Y}_{obs}^k$ is the *k*-th observed target concentration out of a total number of q target concentrations. Assuming that the residuals can be described with a Gaussian error model with a mean of zero and constant variance σ^2,

$$\varepsilon \sim N(0, \sigma^2), \qquad 2.7$$

we can compute the likelihood function of the residuals as the joint probability of all the residuals:

$$L_j(\tilde{Y}_{obs}|P_1, P_2, \boldsymbol{\theta}) = \prod_{k=1}^{q} \prod_{j=1}^{m} \prod_{i=1}^{n} (2\pi\sigma^2)^{-0.5} \exp\left(-\frac{1}{2} \frac{(\tilde{Y}_{obs}^k - \hat{Y}_{ij})^2}{\sigma^2}\right), \qquad 2.8$$

where $\boldsymbol{\theta}$ represents all the model parameters and P_i (i=1,2) is the observed point process (see Eq. 2.4). The above Gaussian error model could in principle be replaced with any other stochastic process. However, the Gaussian error model has been shown to be relatively robust in this kind of an application (Lyon, 2013; Schaefli and Kavetski, 2017).

In the case of linear mixing between two sources, the two model parameters considered at this stage are the mixing ratio ρ and the error variance σ^2. The error variance can either be computed from the observed residuals or be treated as a model parameter (Kuczera and Parent, 1998; Schaefli et al., 2007). For the examples shown in this paper, the error variance

is computed from the residuals. In order to avoid numerical problems, we use the log-likelihood form of Eq. (2.8):

$$\log L_j(\tilde{Y}_{obs}|P_1, P_2, \theta) = \sum_{k=1}^{q}\sum_{j=1}^{m}\sum_{i=1}^{n} -0.5\left[\log(2\pi\sigma^2) + \frac{\left(\tilde{Y}_{obs}^{k} - \hat{Y}_{ij}\right)^2}{\sigma^2}\right]. \quad 2.9$$

2.2.2. Parameter inference in a Bayesian framework

Following the general Bayes' equation, the posterior distribution of the model parameters can be written as:

$$p\left(\boldsymbol{\theta}\middle|P_1, P_2, \tilde{Y}\right) = \frac{p(\tilde{Y}|\theta, P_1, P_2)p(\theta)}{p\left(\tilde{Y}\middle|P_1, P_2\right)}, \quad 2.10$$

where $p(\boldsymbol{\theta})$ is the prior distribution of the model parameters and $p\left(\tilde{Y}|\boldsymbol{\theta}, P_1, P_2\right)$ is the likelihood function. The denominator of Eq. (2.10) can generally not be computed as that would require integration over the whole parameter space which is computationally expensive, which is why Eq. (2.10) is reduced to:

$$p\left(\boldsymbol{\theta}\middle|P_1, P_2, \tilde{Y}\right) \propto p\left(\tilde{Y}|\boldsymbol{\theta}, P_1, P_2\right)p(\boldsymbol{\theta}). \quad 2.11$$

Two methods are traditionally used in hydrology to sample from the posterior distribution from Eq. (2.11), Markov Chain Monte Carlo (MCMC) sampling (Hastings, 1970; Metropolis and Ulam, 1949) and importance sampling (Glynn and Iglehart, 1989; Neal, 2001). In the case of MCMC sampling, a common approach is the Metropolis algorithm (Kuczera and Parent, 1998; Schaefli et al., 2007; Vrugt et al., 2003). In importance sampling, the posterior distribution is obtained from weighted samples drawn from the so-called importance distribution. For typical multivariate hydrological problems, the only possible choices for the importance distribution are either uniform sampling over a hypercube or sampling from an over-dispersed multi-normal distribution (Kuczera and Parent, 1998). A stochastic process is defined as over-dispersed when the variance of the underlying distribution is greater than its

mean (Inouye et al., 2017). The sampling distributions in such cases have large variance, allowing sufficient sampling over the entire parameter range.

We implement a MCMC sampling algorithm using a Metropolis-Hastings (Hastings, 1970) criterion to infer the posterior distribution of the mixing ratio. For the synthetic case study (Section 2.3.1), we setup 10 parallel MCMC chains to monitor convergence according to the classical Gelman-Rubin convergence criterion (Gelman and Rubin, 1992). Each chain is initiated by assigning a uniform prior distribution for the mixing ratio, where the mixing ratio varies between 0 and 1. For the subsequent case studies, we use importance sampling for the sake of simplicity. The prior distribution of additional model parameters (if applicable) are discussed in the corresponding case study section. Apart from the prior distribution of the model parameters, HydroMix requires tracer concentration of the different sources and of the mixture. The error model variance is not jointly inferred with other model parameters but calculated for each sample parameter set from the residuals according to Eq. (2.6).

2.3. Case studies

We provide a comprehensive overview of the performance of HydroMix based on a set of synthetic case studies (case studies 2.3.1 and 2.3.2) and a real-world application to demonstrate the practical relevance for hydrologic applications (case studies 2.3.4 and 2.3.5). The first case study demonstrates the ability of HydroMix to converge on the correct posterior distribution for synthetically generated data. The second case study uses a synthetic dataset of rain, snow and groundwater isotopic ratios using a conceptual hydrologic model, and compares the results of HydroMix to the actual mixing ratios assumed to generate the data set. It then weights the sources samples and evaluates the effect of weighting on the mixing ratio (case study 2.3.3). In the last two case studies, HydroMix is applied to observed tracer data from an Alpine catchment in the Swiss Alps to infer source mixing ratios and an additional parameter (isotopic lapse rate).

2.3.1. Mixing using Gaussian distributions

In this example, source concentrations S_1 and S_2 are drawn from two Gaussian distributions with different means (μ_1, μ_2) and standard deviations (σ_1, σ_2) and combined to form the mixture *Y* with a constant mixing ratio ρ:

$$\rho S_1 + (1-\rho)S_2 = Y. \quad 2.12$$

Assuming the two distributions are independent, the resultant mixture is normally distributed with mean (μ_y) and variance (σ_y^2) defined as:

$$\mu_y = \rho\mu_1 + (1-\rho)\mu_2;\ \sigma_y^2 = \rho^2\sigma_1^2 + (1-\rho)^2\sigma_2^2. \quad 2.13$$

A given number of samples are drawn from the distributions of S_1 and S_2 and of the mixture Y. The posterior distribution of the mixing ratio, $p(\boldsymbol{\rho}|\tilde{S_1}, \tilde{S_2}, \tilde{Y})$, is then inferred using HydroMix for i) a case where the two source distributions are well identifiable, and ii) a case where the distributions have a large overlap. Different values of mixing ratios are tested, with ratios varying from 0.05 to 0.95 in steps of 0.05.

The sensitivity of HydroMix to the number of samples drawn from S_1, S_2 and Y, along with the time to convergence is assessed based on the sum of the absolute error between the estimated mixing ratio $\hat{\rho}$ and its true value ρ.

2.3.2. Mixing with a time series generated using a hydrologic model

In this case study, we build a conceptual hydrologic model where groundwater is assumed to be recharged directly from rainfall and snowmelt. Stable isotopes of deuterium (δ^2H) is used to see how the isotopic ratio in groundwater evolves under different assumptions of rain and snow recharge efficiencies.

Synthetic time series are generated for precipitation, isotopic ratio in precipitation and air temperature at a daily timestep. For generating the precipitation time series, the time between two successive precipitation events is assumed to be a Poisson process with the precipitation intensity following an exponential distribution (Botter et al., 2007; Rodriguez-Iturbe et al., 1999). Time series of air temperature and of isotopic ratios in precipitation are obtained by generating an uncorrelated Gaussian process with the mean following a sine function (to emulate a seasonal signal) and with constant variance (Allen et al., 2018; Parton and Logan, 1981). The separation of precipitation into rainfall (P_r) and snowfall (P_s) is done based on a temperature threshold approach (Harpold et al., 2017a), where the fraction of rainfall $f_r(t)$ at time step t is computed as a function of air temperature $T(t)$:

$$f_r(t) = \begin{cases} 0 & \text{if } T(t) < T_L \\ \frac{T(t)-T_L}{T_H-T_L} & \text{if } T_L \leq T(t) \leq T_H \\ 1 & T(t) > T_H, \end{cases} \quad 2.14$$

where T_L and T_H are the lower and upper threshold bounds. A double air temperature threshold approach has been shown to be more accurate than a single temperature threshold (Harder and Pomeroy, 2014; Harpold et al., 2017a, 2017b). In this case study, T_L and T_H are set to -1 °C and +1 °C. The evolution of the snow water equivalent (SWE) in the snowpack (h_s) is computed as:

$$\frac{dh_s(t)}{dt} = P_s(t) - M_s(t), \quad 2.15$$

where M_s is the magnitude of snowmelt, computed using a degree-day approach as proposed by Schaefli et al., (2014):

$$M_s = \begin{cases} a_s(T(t) - T_m), & \text{if } T(t) > T_m \\ 0 & \text{otherwise} \end{cases}, \quad 12.16$$

where a_s is the degree-day factor (set here to 2.5 mm/°C/day) and T_m is the threshold temperature at which snow starts to melt (set to 0 °C). Enhanced heat exchange processes happening during rain-on-snow events are not explicitly considered as this lies beyond the

scope of this paper. The snowpack is assumed to be fully mixed, and the isotopic ratio of snowpack is computed as:

$$\frac{d(h_s(t)C_s(t))}{dt} = C_p(t)P_s(t) - C_s(t)M_s(t), \quad 2.17$$

where C_s is the isotopic ratio of snowpack and C_p is the isotopic ratio of precipitation. The amount of groundwater recharge (R) is the sum of groundwater recharged from rainfall and snowmelt:

$$R(t) = R_r P_r(t) + R_s M_s(t), \quad 2.18$$

where R_r and R_s are the rainfall and snowmelt recharge efficiencies. Recharge efficiency is defined as the fraction of rainfall or snowmelt that reaches groundwater and is assumed to be a constant value. The groundwater storage is assumed to be fully mixed, and the isotopic ratio of groundwater is computed as:

$$\frac{d(G(t)C_g(t))}{dt} = R_r C_p(t)P_r(t) + R_s C_s(t)M_s(t) - C_g(t)Q(t), \quad 2.19$$

where C_g is the isotopic ratio in groundwater, G is the volume of groundwater and Q is the amount of groundwater outflow to the stream defined as:

$$Q(t) = k(G(t) - G_C), \quad 2.20$$

where k is the recession coefficient and G_C is a constant groundwater storage that does not interact with the stream (added here to avoid zero storage and thus very small outflow). This formulation follows the linear groundwater reservoir assumption used in numerous hydrological modeling frameworks (Beven, 2011). The volume of the groundwater storage is computed as:

$$\frac{dG(t)}{dt} = R(t) - Q(t). \quad 2.21$$

The model is run for a period of 100 years, allowing the system to reach a long term steady state. The parameters used to generate daily precipitation, air temperature and precipitation isotopic ratios are shown in Table 2.4. The number of yearly precipitation events is set to 30. The snow accumulation and the degree-day snowmelt models are then used to compute the number of snowfall days and of snowmelt events. The static volume of groundwater that does not interact directly with the stream, G_C, is set to 1000 mm.

Only the last 2 years of the model runs are used to obtain the time series of isotopic ratios in rainfall, snowmelt and groundwater. These years are then used to estimate the mixing ratio of snowmelt in groundwater, which is the fraction of groundwater recharged from snowmelt. Rainfall and snowmelt samples are the two sources and groundwater samples represent the mixture. For the HydroMix application, all the modeled rainfall and snowmelt samples generated using the hydrologic model are used, whereas for groundwater, only one isotopic ratio per month is used (randomly sampled). The mixing ratios inferred using HydroMix are compared to the actual recharge ratio obtained from the hydrologic model as:

$$R_S^a = \frac{\sum_t R_S M_S(t)}{\sum_t R(t)}, \qquad 2.22$$

where R_S^a represents the proportion of groundwater recharge derived from snowmelt, summed over all the time steps. The numerical implementation of the evolution of isotopic ratio in snowpack and groundwater are given in the Appendix.

2.3.3. Weighting mixing ratios in the hydrologic model

In Section 2.3.2, rainfall and snowmelt samples are not weighted by the magnitude of their fluxes while computing the mixing ratios with HydroMix. As all rainfall and snowmelt samples are used, the weights are implicitly determined by the number of rainfall and snowmelt events, instead of their magnitudes. This is a general problem in all mixing approaches and has not been adequately acknowledged in the literature. Ignoring the weights may lead to biased mixing estimates if the proportional contribution of one of the components (e.g.: rainfall or snowmelt) is low, but the number of samples obtained to represent that

component is proportionally much higher (Varin et al., 2011). For example, in a given catchment, the amount of total snowfall maybe a small proportion of the annual precipitation, but the number of days when snowmelt occurs maybe comparable to the total number of rainfall days in a year. If this is not specified *a priori*, HydroMix may overestimate the proportion of groundwater being recharged from snowmelt. To account for this, we introduce a weighting factor in the likelihood function originally formulated in Eq. (2.8), to make a new composite likelihood (Varin et al., 2011):

$$L_j(\tilde{Y}_{obs}|P_1, P_2, \boldsymbol{\theta}) = \prod_{k=1}^{q}\prod_{j=1}^{m}\prod_{i=1}^{n}\left[(2\pi\sigma^2)^{-0.5}\exp\left(-\frac{1}{2}\frac{(\tilde{Y}_{obs}^{k}-\hat{Y}_{ij})^2}{\sigma^2}\right)\right]^{w_i w_j}, \qquad 2.23$$

where *i* and *j* correspond to snowmelt and rainfall samples, and the weights w_i and w_j reflect the proportion of snowmelt and rainfall contributing to groundwater recharge (Vasdekis et al., 2014), where w_i is expressed as:

$$w_i = \frac{R_i S_i}{\sum_{i=1}^{n} R_i S_i}, \qquad 2.24$$

where R_i is the snowmelt magnitude and S_i *i*s the isotopic ratio of the i^{th} snowmelt event. Rain weights (w_j) are also expressed similarly to Eq. (2.24). The obtained mixing ratio estimates are then compared with the unweighted estimates (in Section 2.3.2) to see if weighting by magnitude makes a significant difference.

2.3.4. Real case study: Snow ratio in groundwater in Vallon de Nant

The objective of this case study is to infer the proportional contributions of snow versus rainfall to the groundwater of an Alpine headwater catchment, Vallon de Nant (Switzerland), using stable water isotopes.

2.3.4.1. Catchment description

Vallon de Nant is a 13.4km^2 catchment located in the Vaud Alps in South-West of Switzerland (Figure 2.1), with elevation ranging from 1253 m to 3051 m asl. Steep slopes form a major part of the catchment with a mean catchment slope of around 36° (Thornton et al., 2018). At lower elevations, a dense forest dominated by *Picea abies* covers 14% of the catchment area. At around 1500 m asl., there is an active pasture area with scattered trees and an open forest dominated by *Larix decidua*. Additional species scattered throughout the catchment include *Pinus sp., Alnus sp.* and *Acer pseudoplatanus*. Alpine meadows cover most of the higher elevation land surfaces. Despite the relatively low elevation, there is a small glacier on its South-western tip, which covers around 4.4% of the catchment area, below which an extended moraine occupies 10.1% of the catchment area. A large part (28% of catchment area) of the hillslopes are composed of steep rock walls. At lower to mid-elevations, talus slopes account for about 6% of the catchment area.

Vallon de Nant has a typical Alpine climate, with around 1900 mm of annual precipitation and a mean air temperature of 1.8 °C (Michelon, 2017). For this paper, long term climate statistics are computed using MeteoSwiss gridded precipitation and air temperature dataset from 1961-2015 (Isotta et al., 2013; MeteoSwiss, 2016, 2017). Applying a simple temperature threshold (0 and 1 °C) to observed precipitation indicates that on average, 40-45% of the total precipitation falls as snow in the catchment. There is a small degree of seasonality in precipitation, with higher precipitation between June to August, and lower precipitation in the months of September and October.

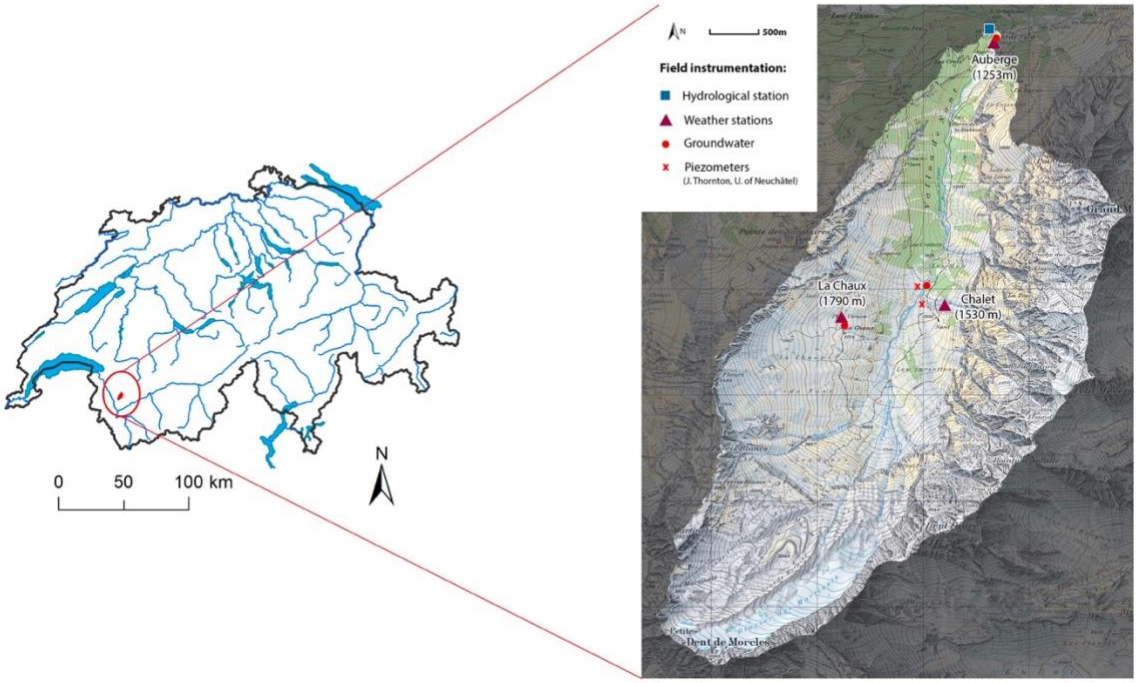

Figure 2.1. Map showing Vallon de Nant along with the locations of meteorologic and hydrologic observations and the frequent sampling sites. Composite samples of precipitation were collected at the weather stations. Groundwater samples were collected at the groundwater monitoring points and the installed piezometers. The groundwater piezometers were installed by James Thornton from University of Neuchâtel (Thornton et al., 2018).

2.3.4.2. Data collection

Vallon de Nant has been extensively monitored since February 2016. Water samples are collected from streamflow, rain, snowpacks and groundwater at different elevations, which are then analyzed for the isotopic ratios in deuterium (δ^2H) and oxygen-18 ($\delta^{18}O$). Vallon de Nant is remotely located with very limited winter access, frequently experiencing winter avalanches. Due to these logistical constraints, snowmelt lysimeters or passive capillary samplers could not be setup to sample snowmelt water; accordingly, grab snowpack samples are used here as a proxy for snowmelt. A summary of the isotopic data is shown in Table 2.1.

Table 2.1. Summary of the isotopic data (δ^2H and $\delta^{18}O$) collected in Vallon de Nant between February 2016 to July 2017

Sample name	Number of samples	Lowest elevation	Highest elevation
Rainfall	32	1253	1773
Top snowpack layer	80	1241	2455
Groundwater	22	1253	1779

2.3.4.3. Model implementation

HydroMix is used to estimate the proportion of snow recharging groundwater (subsequently referred to as 'snow recharge coefficient'). In order to obtain a pdf of the snow recharge coefficient, isotopic ratios in all the water samples from rain, snowpack and groundwater are used. A uniform prior distribution is assigned to the snow recharge coefficient, which varies between 0 and 1, representing the entire range of possible values.

2.3.5. Introduction of an additional model parameter

In any mixing analysis, it may be useful or desirable for users to specify an additional model parameter that is able to modify the tracer concentrations based on their process understanding of the system. In the case of Alpine catchments with large elevation gradients, stable isotopes in precipitation often exhibit a systematic trend with elevation, becoming more depleted in heavier isotopes with increasing elevation. This is also known as the 'isotopic lapse rate' (Dansgaard, 1964; Friedman et al., 1964). In typical field campaigns, because of logistical challenges, precipitation samples are collected only at a few points in a catchment, with often fewer precipitation samples at high elevations. This leads to oversampling at lower elevations, and under sampling at higher elevations, which can bias mixing estimates. This has been found specially relevant for hydrograph separation in forested catchments (Cayuela et al., 2019). To allow a process compensation for this, an additional lapse rate factor is introduced in which each observed point scale sample (observed at a given elevation) is corrected to a reference elevation as follows:

$$\bar{r} = \frac{\sum_{j=1}^{k}[\alpha(e_j - e) + r]a_j}{\sum_{j=1}^{k} a_j}, \qquad 2.25$$

where r is the isotopic ratio in precipitation collected at elevation e, $\bar{r}$ is the catchment averaged isotopic ratio in precipitation, α is the isotopic lapse rate factor, e_j is the elevation of the *j*-th elevation band, and a_j is the catchment area under the *j*-th elevation band, where the catchment is divided into *k* elevation bands. These bands are obtained by constructing a hypsometric curve of the catchment (Strahler, 1952).

The lapse rate factor is allowed to modify both rainfall and snowpack isotopic ratios to obtain a catchment averaged isotopic ratio, which is then used in the mixing model. Using this formulation of an isotopic lapse rate makes the following implicit assumptions: (1) precipitation storms on aggregate move from the lower part of the catchment to the upper part of the catchment thus creating a lapse rate effect, and (2) precipitation falls uniformly over the catchment. It is important to note that the isotopic lapse rate is different from the precipitation lapse rate, i.e., the rate of change of precipitation with elevation is different from the rate of change of precipitation isotopic ratio with elevation.

It is important to note that precipitation isotopic ratio is not only a function of elevation, but also depends on other factors such as the source of moisture origin, cloud condensation temperature, secondary evaporation, etc. Similarly, a strong spatial variability exists in the isotopic ratio of snowmelt water, depending on catchment aspect, snow metamorphism, wind distribution, etc. This case study is a mere demonstration that HydroMix allows inference of additional parameters that can account for various physical processes that may modify isotopic ratios.

The prior distribution of the isotopic lapse rate is specified based on isotopic data collected across Switzerland under the Global Network of Isotopes in Precipitation (GNIP) program (IAEA/WMO, 2018). Using the monthly isotopic values collected in between 1966 and 2014, average lapse rate values are obtained for both δ^2H and $\delta^{18}O$. These were (-)1.94 ‰/100m for δ^2H, and (-)0.27 ‰/100m for $\delta^{18}O$ (Beria et al., 2018).

A uniform prior distribution is assigned to the isotopic lapse rate parameter, with the lower bound specified as three times the Swiss lapse rate for both δ^2H and $\delta^{18}O$. The observed isotopic lapse rate data from Switzerland suggests average lapse rates are weakly negative; however, positive lapse rates can *a priori* not be excluded for the case study catchment. Accordingly, we do not specify an upper lapse rate bound of zero but set it as three times the Swiss lapse rate (Table 2.2). In the case of Vallon de Nant, the elevation ranges from 1253 m to 3051 m asl. For computing the Swiss lapse rate, the elevation range over which the monthly precipitation samples were collected was 300 m to 2000 m asl. This difference in elevation ranges between Vallon de Nant and the GNIP network should be kept in mind during interpretation of results.

Table 2.2. Prior distribution of the different model parameters as specified to HydroMix

Variable	**Prior distribution**	**Lower bound**	**Upper bound**
Snow recharge coefficient	Uniform	0	1
Isotopic lapse rate in δ^2H	Uniform	(-)5.82 ‰/100m	(+)5.82 ‰/100m
Isotopic lapse rate in $\delta^{18}O$	Uniform	(-)0.81 ‰/100m	(+)0.81 ‰/100m

2.4. Results

The results for the different case studies are discussed in the sections below.

2.4.1. Mixing with normal distributions

The mean and standard deviations used to generate the low and high variance source distributions for the synthetic case studies are summarized in Table 2.3. We randomly generated 100 samples from each of the two source distributions and from the target distribution, and varied the mixing ratios between 0.05 and 0.95 in 0.05 increments. It should be noted that HydroMix permits using different number of samples for the sources and for the mixture.

For the low variance case, the mixing ratio inferred with HydroMix with 1000 MCMC simulations reproduce closely the theoretical mean of the mixing ratios used to generate the synthetic data (Figure 2.2a). However, for the high variance case, the inferred mixing ratios do not match the true underlying mixing ratios, especially for low and high mixing ratios. This is partly due to the poor identifiability of the sources (given that their distributions are highly overlapping), and partly due to the relatively small sample size of 100. The inferred mean should reproduce the theoretical mean with increasing sample size and we clearly see this for the low variance case in Figure 2.2b, where the model performance markedly improves with increasing number of samples. The performance is measured here in terms of the absolute error between the posterior mixing ratio mean and the true mean, summed and averaged over all tested ratios from 0.05 to 0.95. We did not perform inferences for sample sizes larger than 100 as the computational requirement increases exponentially with increasing sample sizes.

The model converges fairly quickly for the low variance case after ~100 runs as shown in Figure 2.3a. The obtained model residuals have zero mean and are approximatively normally distributed as revealed by quantile-quantile plots (not shown), in line with the assumption of an unbiased normally distributed error model, as stated in Eq. 2.7.

Table 2.3. Mean and variance of the two sources S_1 and S_2 drawn from Normal distributions

Dataset	$\mu_{S_1}(\sigma_{S_1})$	$\mu_{S_2}(\sigma_{S_2})$
Low variance	10 (0.5)	20 (0.5)
High variance	10 (5.0)	20 (5.0)

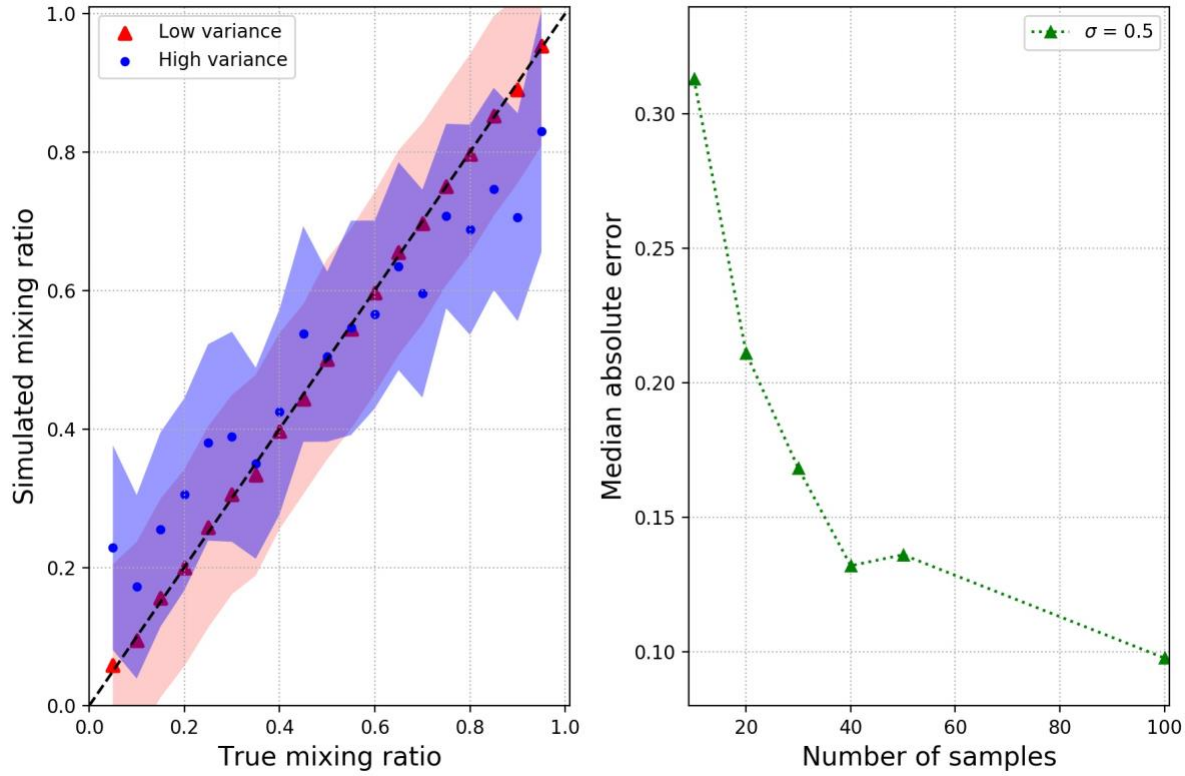

Figure 2.2. (a) Scatterplot showing the mixing ratio ($\boldsymbol{\rho}$) values inferred using HydroMix for the low and high variance synthetic case of Table 2.3. The uncertainty band represents the inferred mixing ratio ± error standard deviation obtained from Eq. 2.13. The number of source and target samples are 100. (b) Performance of HydroMix in terms of the absolute error between the posterior mixing ratio mean and the true mean for the low variance dataset, over all tested ratios plotted as a function of the number of samples drawn for the two sources.

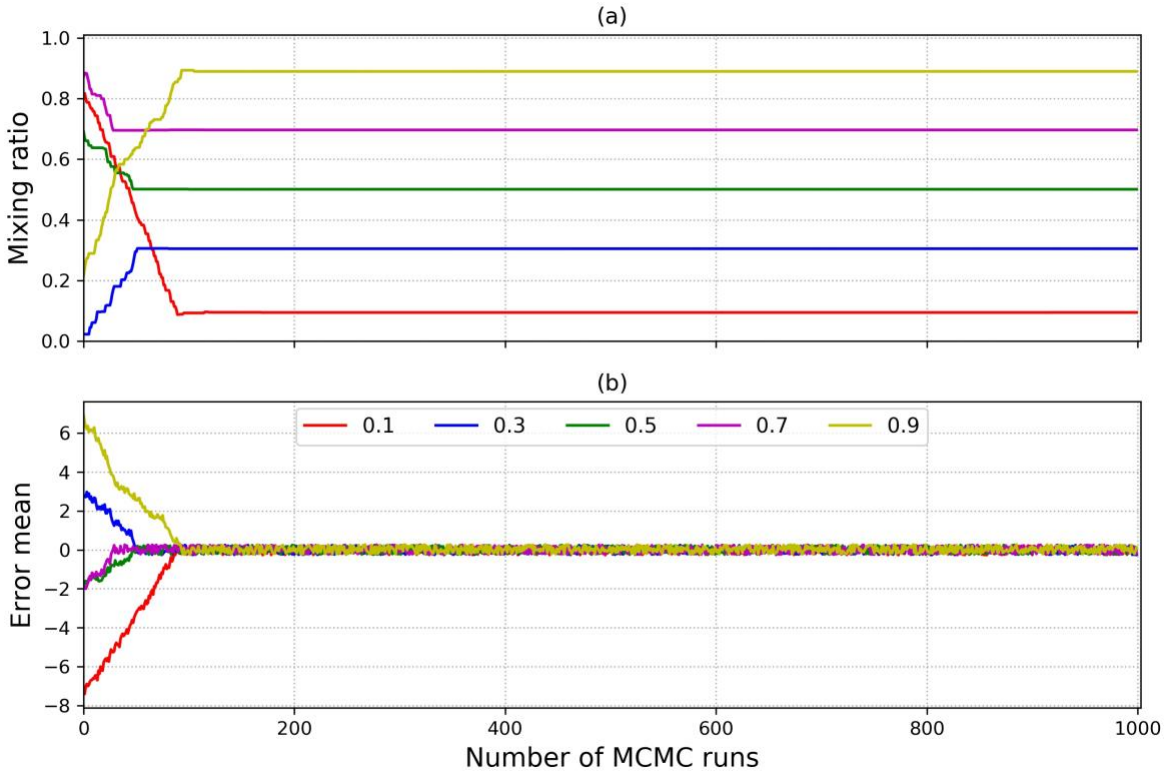

Figure 2.3. Diagnostic plots showing the convergence characteristics of MCMC chains for five different mixing ratios for the low variance dataset (shown in Table 2.3). Subplots (a) and (b) show variations in the inferred mixing ratio and the error mean with increasing MCMC runs.

2.4.2. Contribution of rain and snow to groundwater recharge using a hydrologic model

Figure 2.4 shows the variation in the isotopic ratio of groundwater over the entire 100 year period, showing the system achieves a steady state condition after ~15 years of simulation. The mixing ratio is estimated with HydroMix using: (1) samples of the isotopic ratio in snowfall, and (2) samples of the isotopic ratio in snowmelt. The two sample distributions differ, as shown in Figure 2.5, where the variability of the isotopic ratio is lower in snowmelt when compared to snowfall. In the model at hand, this reduction is obtained because of mixing occurring within the snowpack, leading to homogenization, thus reducing the variability in the isotopic ratio of snowmelt. In field data, such a reduction in variability is also generally observed (Beria et al., 2018), as a result of the homogenization as modelled here and from more complex snow physical processes, which lie beyond the scope of this study.

Table 2.4. Parameters used to generate time series of precipitation, air temperature and isotopic ratios in precipitation. μ represents the mean, *A* is the amplitude and ϕ the time lag of the underlying sine function. For the precipitation process, μ is the mean intensity on days with precipitation. The resulting mean winter length (air temp. below 0°C) is 119.5 days.

Variable	**Parameter values**
Precipitation	# events/year = 30, μ = 33.45 mm/day
Air temperature	μ = 4 °C, *A* = 8 °C, ϕ = -π/2
Precipitation isotopic ratio	μ = (-80) ‰, *A* = 40 ‰, ϕ = -π/2

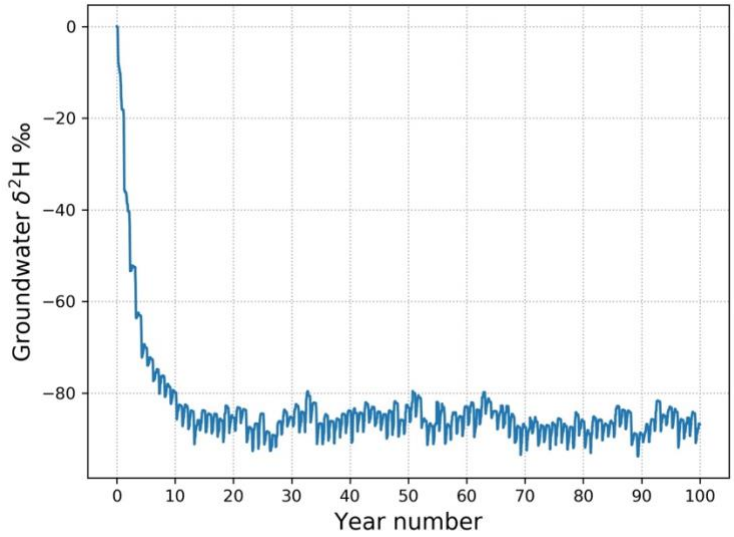

Figure 2.4. Evolution of the modeled isotopic ratio in groundwater over a 100-year period with $\boldsymbol{R_r}$= 0.3 and $\boldsymbol{R_s}$=0.6.

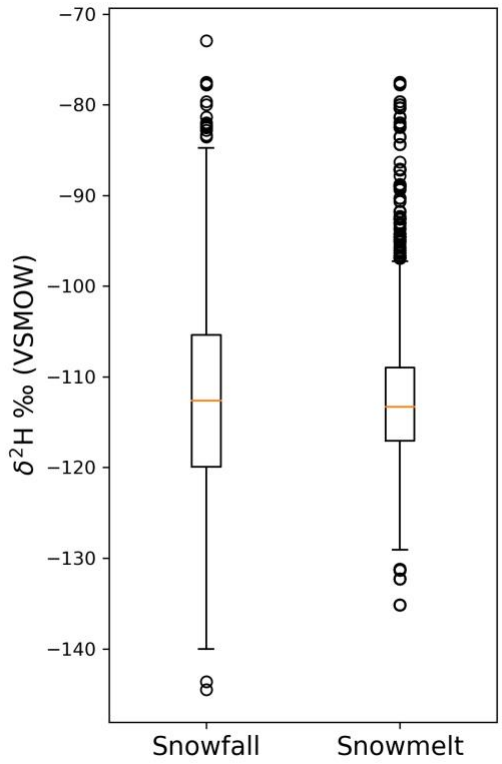

Figure 2.5. Boxplot showing the variability in the isotopic ratio of snowfall and snowmelt as simulated by the hydrologic model. The boxplot extends from 25th to 75th percentile value, with the median value depicted by the orange line. The whiskers extend up to 1.5 times of the interquartile range. The black circles are the outliers.

The mixing ratios inferred with HydroMix are very similar regardless of whether snowfall or snowmelt is used across the entire range of recharge efficiencies (Figure 2.6). This provides confidence in the use of snowfall samples as a proxy for snowmelt when estimating mixing ratios. However, it is clear from Figure 2.6 that an important bias emerges between the estimated mixing ratio from HydroMix and the actual mixing ratio known from the hydrologic model, especially for low mixing ratios.

This bias can be expected to emerge where the source contributions are not weighted according to their fluxes, which to our knowledge has not been explicitly addressed in the hydrological literature. As already discussed in Section 2.3.3, the absence of sample weighting typically induces a bias when there is a large divergence between the number of samples taken over a certain period (e.g. one year) to characterize a source, and the magnitude of source flux over that period (e.g. 40 snow and 10 rain samples taken to characterize the two

sources, where snow only accounts for a very small portion (e.g. 10%) of the annual precipitation).

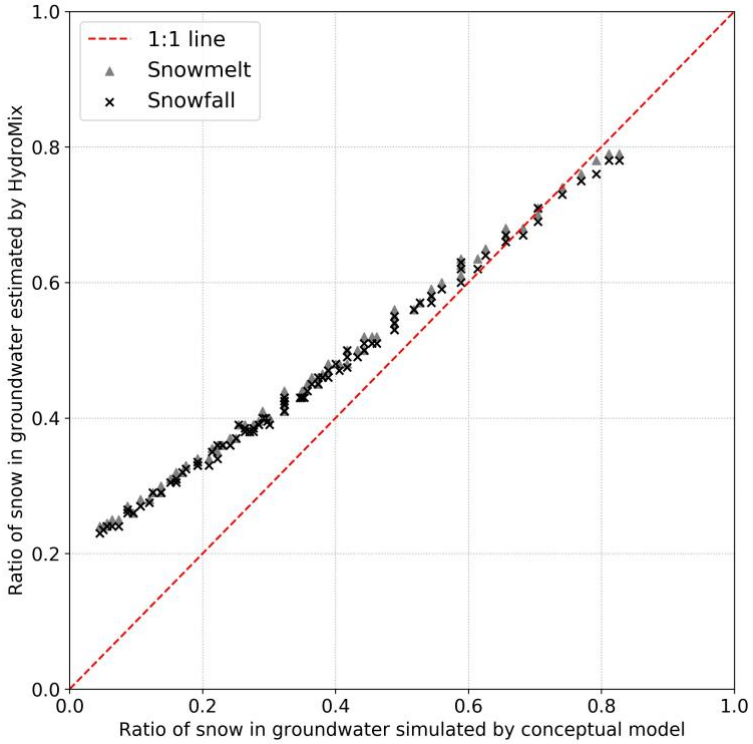

Figure 2.6. Ratios of snow in groundwater estimated with HydroMix plotted against ratios obtained from the hydrologic model for the last two years of simulation. Also shown are the separate results obtained by using samples of either snowmelt or snowfall. The full range of ratios is obtained by varying rainfall and snowmelt recharge efficiencies from 0.05 to 0.95. The number of rainfall, snowfall and snowmelt days are 39, 24 and 107 in the last two years of simulation.

2.4.3. Effect of weights on estimates of mixing ratios using a hydrologic model

After taking into account the magnitude of rainfall and snowmelt events in the composite likelihood function of Eq. (2.23), it is clear that much of the un-weighted biases can be removed (Figure 2.7). The most significant improvement is seen at very low mixing ratios where the divergence between the conceptual model and the mixing model estimates error reduces by almost 50%. In this study, we have used a relatively simple normalization based

weighting function (Eq. (2.25)). Testing other weighting functions which have been proposed in the past (Vasdekis et al., 2014) is left for future research.

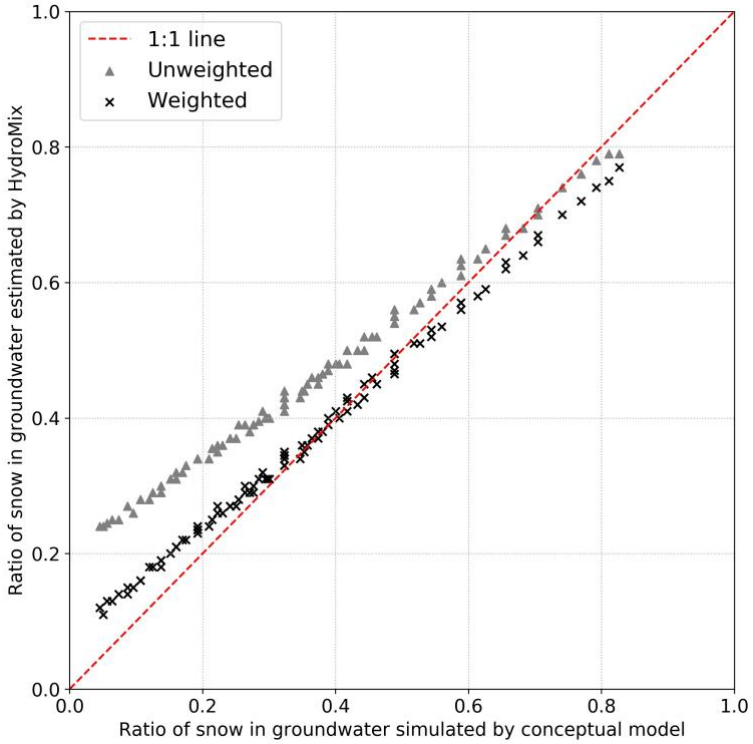

Figure 2.7. Ratios of snow in groundwater estimated using HydroMix plotted against ratios obtained from the hydrologic model, for both weighted and unweighted mixing scenarios. The full range of ratios is obtained by varying rainfall and snowmelt recharge efficiencies from 0.05 to 0.95. The number of rainfall, snowfall and snowmelt days are 39, 24 and 107 in the last two years of simulation.

2.4.4. Inferring fraction of snow recharging groundwater in a small Alpine catchment along with an additional model parameter

Using the dataset from an Alpine catchment (Vallon de Nant, Switzerland), HydroMix estimates that 60-62% of the groundwater is recharged from snowmelt (using unweighted approach), with the full posterior distributions shown in Figure 2.8a. This estimate is consistent for both the isotopic tracers (δ^2H and $\delta^{18}O$), which are often used interchangeably in the hydrologic literature (Gat, 1996). Comparing this recharge estimate to the proportion

of total precipitation that falls as snow (around 40-45%, see Section 2.3.4.1), suggests that snowmelt is more effective at reaching the aquifer than an equivalent amount of rainfall falling at a different period of the year. Similar results have been obtained in a number of previous studies across the temperate and mountainous regions of the world (see Table 1.1 for a summary).

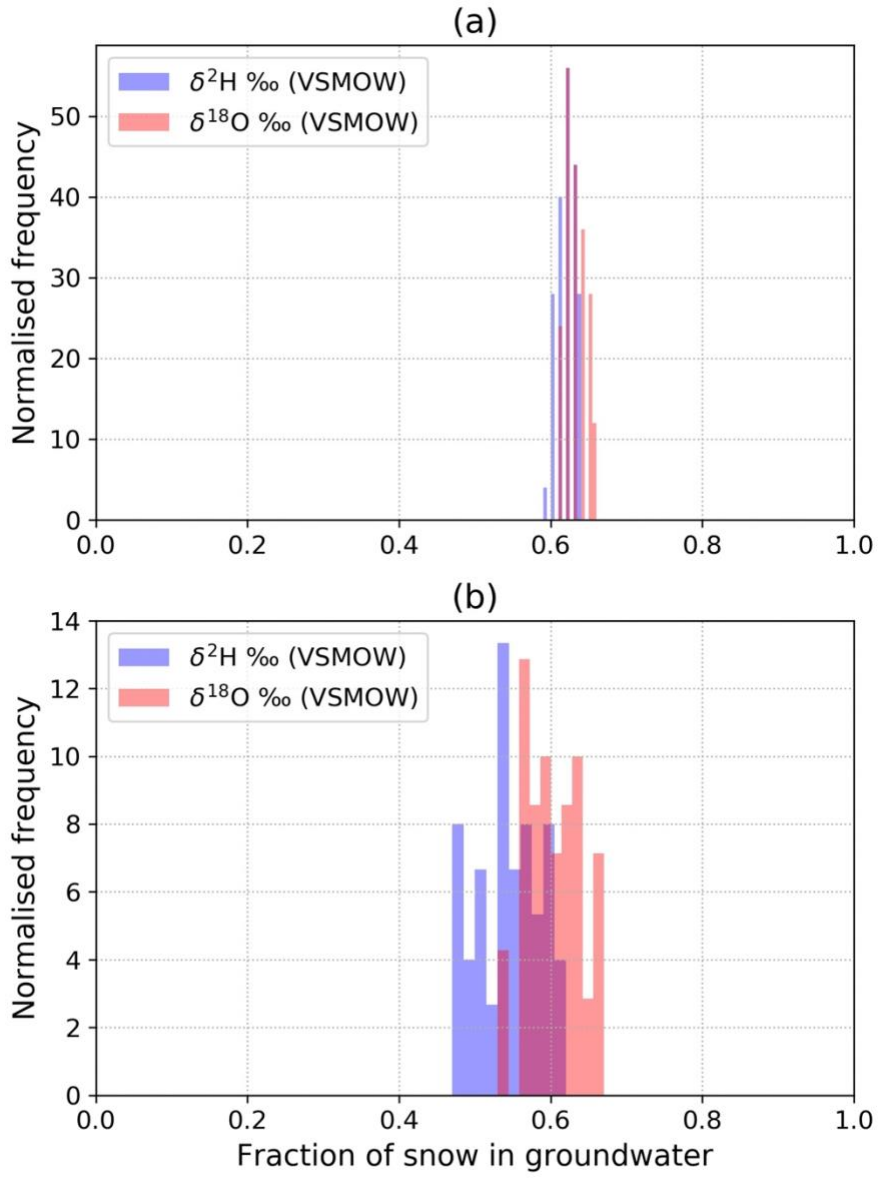

Figure 2.8. Histogram showing the fraction of snow recharging groundwater in Vallon de Nant using the isotopic ratios in δ^2H and $\delta^{18}O$ (a) without correcting for lapse rate and (b) after correcting for lapse rate.

As can be seen from Figure 2.8a, the estimated distribution of snow ratio in groundwater is very narrow. This can be explained by the fact that we assume that the collected precipitation samples represent the variability actually occurring in the catchment. To overcome this limitation, we infer an additional parameter called the isotopic lapse rate that accounts for the spatial heterogeneity in terms of catchment elevation. As shown in Figure 2.9, the posterior distributions of the isotopic lapse rate (for both δ^2H and $\delta^{18}O$) largely overlap with the spatially averaged isotopic lapse rate as estimated from precipitation isotopes across Switzerland. The overlap with the average Swiss isotope lapse rate suggests our inferred lapse rates are reasonable, with the spread in the estimates likely reflecting the temporal variation in the catchment specific isotope lapse rate that can develop from a wide range of moderating factors (e.g. air masses contributing precipitation without traversing the full elevation range of the catchment due to varying trajectories). The Swiss lapse rate is constructed as a long term spatial average, whereas the inferred isotopic lapse rate in Vallon de Nant is constructed from the temporal variations in the isotopic ratios. These results demonstrate that it is relatively straightforward to jointly infer multiple parameters within the HydroMix modeling framework.

However, an important consequence of additional parameter inference without providing additional data or constraints is an increase in the degree of freedom, which can then increase the uncertainty on source contributions. This effect is seen in Figure 2.8b, especially in contrast with the previous result in Figure 2.8a, where the median mixing ratios of the posterior distributions remain similar (~0.6), but the spread increase drastically, from 0.005 to 0.2.

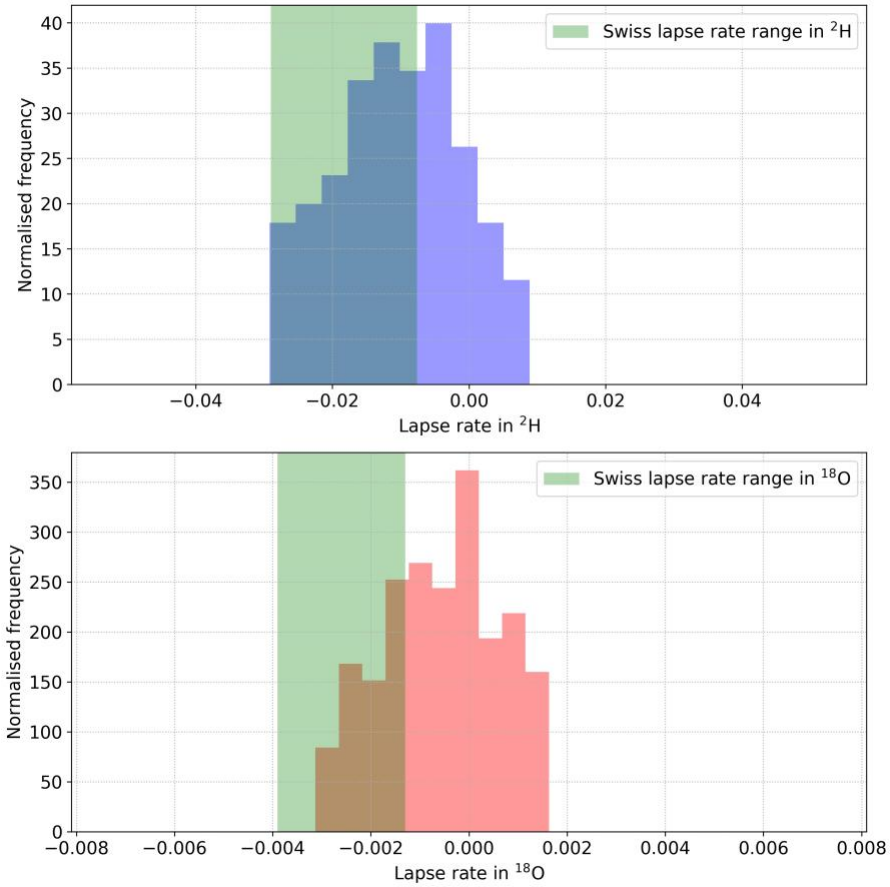

Figure 2.9. Histogram showing the posterior distribution of the isotope lapse rate parameter in $\delta^{2}H$ and $\delta^{18}O$. The green region shows the confidence bounds (significant at α =0.01) of lapse rate computed over Switzerland by using inverse variance weighted regression. Limits of the prior distribution of the isotopic lapse rates correspond to limits of the x-axis. The slope of the isotopic ratio when plotted against elevation for the Swiss-wide data is shown in Figure 1.3.

2.5. Limitations and opportunities

As with all linear mixing models, the quality of the underlying data determines the accuracy and utility of the results. If the tracer compositions of the different sources are not sufficiently distinct, the uncertainty in the estimated mixing ratios will become very large. This means that if either the underlying data quality is poor, or the source contribution dynamics are not well conceptualized, then the uncertainty in the mixing ratios will be too high to be useful.

In cases where a large number of source samples are available, the computational requirements of HydroMix outweigh the benefit from using it. These are likely cases where the statistical distribution of the source tracer composition is well understood, therefore fitting a probability density curve to the source and target samples, and then inferring the distribution of the mixing ratio using a probabilistic programming approach is more appropriate (Carpenter et al., 2017; Parnell et al., 2010; Stock et al., 2018). Also HydroMix might not be an appropriate method in instances where fitting statistical distributions to source and target compositions reflect *a priori* knowledge of the system.

A key difference between HydroMix and other Bayesian mixing approaches is that HydroMix parameterizes the error function whereas other Bayesian approaches parameterize the statistical distribution of source and mixture compositions. Parameterizing source compositions require large sample sizes, which is seldom the case in tracer hydrology. Error parameterization offers a useful alternative and can be also verified against the posterior error distribution. In the case studies demonstrated in this paper, a normally-distributed error model was found to be appropriate. However, error models other than Gaussian can be used by formulating the respective likelihood function.

HydroMix builds the model residuals by comparing all the observed source samples with all the observed samples of the target mixture, assuming that all available source and target samples are independent. Interestingly, the assumption of independence holds even if the source and target samples are taken at the same time, since the target samples result from water that has travelled for a certain amount of time in the catchment, and hence is not related to the water entering the catchment. However, if a system has instantaneous mixing, then the source and target samples taken at the same moment of time will necessarily be strongly correlated. In such cases, the assumption of independent samples would not make sense and the method might give spurious results.

Finally, it is noteworthy that adding additional parameters to characterize the source tracer composition increases the degree of freedom of the model, which implies that adding such parameters leads to an increase in the uncertainty of the source contribution estimates unless new information, i.e. new observed data, is added to the model. This means that users who

are interested in incorporating additional modification processes by adding parameters should ideally provide additional tracer data able to constrain this process, subject to tracer data being available.

For consistency and simplicity, the case studies and synthetic hydrological examples provided here focused on the contribution of rain and snow in recharging groundwater. However, it is important to emphasize that the opportunities to implement HydroMix extend to all cases where mixing contributions are of interest, and where it is difficult to build extensive databases of source tracer compositions. Such examples include quantifying the amount of "pre-event" vs. "event water" in streamflow, where "pre-event water" refers to groundwater and "event water" refers to rainfall or snowmelt. Another interesting use case might be to quantify the proportion of streamflow coming from the different source areas in a catchment, to capture the spatial dynamics of streamflow. Other uses include quantifying the amount of fog contributing to throughfall, the proportion of glacial melt vs. snowmelt flowing into a stream, the amount of vegetation water use from soil moisture at different depths vs groundwater, the interaction between surface water and groundwater at the hyporheic zone (Leslie et al., 2017), sediment fingerprinting to quantify the spatial origin of river sediments , etc. In all of these cases, understanding source water contributions, both spatially and temporally, will improve the physical understanding of the system.

2.6. Conclusions

We develop a new Bayesian modeling framework for the application of tracers in mixing models. The primary application target of this framework is hydrology, but it is by no means limited to this field. HydroMix formulates the linear mixing problem in a Bayesian inference framework that infers the model parameters using a Metropolis-Hastings based MCMC sampling algorithm, based on differences between observed and modelled tracer concentrations in the target mixture, using all possible combinations between all source and target concentration samples. This is especially useful in data scarce environments where fitting probability distribution functions is not feasible. HydroMix also makes the inclusion of additional model parameters to account for source modification processes straightforward.

Examples include known spatial or temporal tracer variations (e.g. isotopic lapse rates or evaporative enrichment).

An evaluation of HydroMix with data from different synthetic and field case studies leads to the following conclusions:

1. HydroMix gives reliable results for mixing applications with small sample sizes (< 20-30 samples). As expected, the variance in source tracer composition and the ensuing composition overlap determines the bias in the mixing ratio estimates. The bias in mixing ratio estimates increases with increasing variance in source tracer compositions. Mixing ratio estimates improve (in terms of lower error) with increasing number of source samples.
2. As revealed by our synthetic case study with a conceptual hydrological model, at low source contributions (i.e. < 20%), a strong divergence between the actual and estimated mixing ratios emerges. This arises if HydroMix assigns equal weights to all source samples proportionally oversampling the less abundant source, which then leads to significant biases in mixing estimates. This problem is inherent to all mixing approaches, and to our knowledge has not been adequately addressed in the literature.
3. The use of composite likelihoods to weight samples by their amounts can significantly reduce the bias in the mixing estimates. At low source proportions, the estimated mixing ratio improves by more than 50% after accounting for the amount of all the sources. We show this using a simple normalization based weighting function. Future studies should explore the usage of different weighting functions that have been proposed in the past (Vasdekis et al., 2014).
4. A synthetic application of HydroMix to understand the amount of snowmelt induced groundwater recharge, revealed that using snowfall isotopic ratio instead of snowmelt isotopic ratio leads to similar mixing ratio estimates. This is particularly useful in high mountainous catchments, where sampling snowmelt is logistically difficult.
5. A real case application of HydroMix in a Swiss Alpine catchment (Vallon de Nant) showed a clear winter bias in groundwater recharge. About 60-62% of the groundwater is recharged from snowmelt (unweighted mixing approach), when

snowfall only accounts for 40-45% of the total annual precipitation. This has also been previously suggested elsewhere in the European Alps (Cervi et al., 2015; Penna et al., 2014b, 2017; Zappa et al., 2015).

To conclude, HydroMix provides a Bayesian approach to mixing model problems in hydrology that takes full advantage of small sample sizes. Future work will show the full potential of this approach in hydrology as well as other environmental modelling applications.

2.7. Code and data availability

The model code is implemented in python 2.7 and can be downloaded along with the dataset from Zenodo at http://doi.org/10.5281/zenodo.3475429. The most recent version of the model code is available on GitHub at https://github.com/harshberia93/HydroMix/tree/20191007_GMD.

2.8. Appendix

The equations below show the numerical implementation of the evolution of isotopic ratios in snowpack, isotopic ratios in groundwater, and groundwater storage at a daily timestep.

$$C_s(t) = \frac{C_s(t-1)h_s(t-1)+C_p(t)P_s(t)-C_s(t-1)M_s(t)}{h_s(t-1)+P_s(t)-M_s(t)} \quad 2.26$$

$$C_g(t) = \frac{C_g(t-1)G(t-1)+C_p(t)R_rP_r(t)+C_s(t)R_sM_s(t)-C_g(t-1)Q(t)}{G(t-1)+R_rP_r(t)+R_sM_s(t)-Q(t)} \quad 2.27$$

$$G(t) = G(t-1) + R_rP_r(t) + R_sM_s(t) - k(G(t) - G_C) \quad 2.28$$

Author contributions: The paper was written by HB with contributions from all coauthors. HB and BS formulated the conceptual underpinnings of HydroMix. JRL helped in framing the statistical and hydrological tests to evaluate HydroMix. AM and NCC helped in compiling data used for model evaluation and provided critical feedback during model validation.

3. Improving hydrologic modeling with stable water isotopes

Harsh Beria, Lionel Benoit, Gregoire Mariethoz, Bettina Schaefli

In preparation

Abstract

The last century of hydrological research has led to significant improvements in representing different hydrological processes in rainfall-runoff models. Despite this progress, most rainfall-runoff models are still calibrated only against streamflow, which informs the celerity i.e. the fast response behavior of a catchment. Using environmental tracers such as stable water isotopes can help constrain the velocity aspect of the catchment. However, stable water isotopes have either been used qualitatively to learn more about the dominant hydrological processes or to calibrate a much more complex solute transport model, where the added benefit of using stable water isotope data is not entirely clear.

In this study, we use stable water isotopes to design a semi-distributed conceptual rainfall-runoff model for an Alpine catchment (Vallon de Nant), and incorporate information about pre-event water fraction in the stream within the rainfall-runoff model. Pre-event water fraction during summer rains is estimated using stable water isotope data and a Bayesian mixing model, and is used to calibrate the rainfall-runoff model. This kind of a calibration scheme increases the pre-event water fraction within the stream making the model simulations more realistic. We discuss the advantages and limitations of such a modeling approach and how it can be extended to other experimental catchments.

3.1. Introduction

The last century of hydrological research has led to significant improvements in our understanding of different hydrological processes, and how these processes are represented in rainfall-runoff models (Peters-Lidard et al., 2019). Such models allow us to make predictions about water resources, helping us gauge the impact of climate change on the different facets of the water cycle. This is becoming increasingly relevant as climatic extremes such as floods and droughts become more frequent (Stott, 2016), and changes in atmospheric dynamics and precipitation patterns impact the health and functioning of the biosphere (Malhi et al., 2020).

Traditionally, most rainfall-runoff models are calibrated against streamflow, as streamflow data are widely available (Hrachowitz et al., 2016). However, this often limits the predictive power of such models, often leading to the right answers (i.e. matching streamflow hydrographs) but for the wrong reasons (Kirchner, 2006) (e.g. underestimation in evaporation compensated by higher soil moisture in the model domain (Sutanudjaja et al., 2014)). This problem mainly arises because the model fails to correctly simulate the internal system dynamics such as flux partitioning, while doing a good job at curve fitting (Hrachowitz and Clark, 2017). This has been often referred to as equifinality in the hydrologic literature, where multiple model parameter states lead to similar model performance (Beven and Freer, 2001; Khatami et al., 2019), making it difficult to identify the most reliable parameter set. Ideas such as including auxiliary datasets such as remote sensing based estimates of evapotranspiration (Odusanya et al., 2019; Rajib et al., 2018), snow cover (Nijzink et al., 2018; Parajka and Blöschl, 2008; Salvatore et al., 2018), groundwater (Bai et al., 2018; Dembélé et al., 2020), and soil moisture (Kunnath-Poovakka et al., 2016; Sutanudjaja et al., 2014) have been proposed to improve the parameter identifiability. More recently, calibration based on hydrologic signatures such as flow duration curves have also been proposed to get around the problem of overfitting, while aptly constraining the hydrologic model (Addor et al., 2018; Branger and McMillan, 2020; Jayathilake and Smith, 2019; Kelleher et al., 2017; Shafii and Tolson, 2015). A detailed review linking hydrologic signatures to hydrologic processes is given in McMillan, (2020).

Most conceptual rainfall-runoff models do not adequately differentiate celerity and velocity in a catchment (Mcdonnell and Beven, 2014). Celerity represents the speed of propagation of a large rainfall or snowmelt event through a catchment whereas velocity represents the speed at which a water particle traverses through the catchment. A rainfall-runoff model which is only calibrated with streamflow captures the celerity or the fast response behavior of a catchment which is mainly controlled by storage deficit. However, such a model fails to resolve the velocity aspect, which is largely controlled by the geomorphological characteristics of subsurface storage (Mcdonnell and Beven, 2014). Accounting for both celerity and velocity is especially relevant in mountainous catchments, where large convective summer rainfall events often trigger very flashy response in the stream (Brunner et al., 2018; Stoffel et al., 2016; Weingartner et al., 2003). However during such flood events, most of the streamwater still comes from pre-event water (Kirchner, 2003; Klaus and McDonnell, 2013; Obradovic and Sklash, 1986; Pearce et al., 1986), i.e. the rainfall event only helps mobilize older water that was stored within the catchment. This distinction is often not made in conceptual rainfall-runoff models.

Environmental tracers such as stable water isotopes, conservative solutes, etc. capture the velocity response of a catchment, which if used with streamflow data, can help in constraining both celerity and velocity responses of the catchment. However, stable water isotopes have mostly been used to learn about the dominant hydrologic processes occurring within a catchment (Birkel and Soulsby, 2015; Son and Sivapalan, 2007; Vaché and McDonnell, 2006), thereby helping inform the hydrologic model structure. More recently, stable water isotopes have been used in more quantitative ways. Their usage can be categorized into two groups:

1) *Transport modeling*: Of late, tracer-aided rainfall-runoff modeling has garnered a lot of attention (Birkel et al., 2020; Birkel and Soulsby, 2015; Capell et al., 2012; Delavau et al., 2017; Hrachowitz et al., 2013; van Huijgevoort et al., 2016b, 2016a; Kuppel et al., 2018; Lessels et al., 2016; McDonnell et al., 2010; McMillan et al., 2012; Mosquera et al., 2018; Soulsby et al., 2010, 2015; Stadnyk et al., 2013; Tetzlaff et al., 2015; Tunaley et al., 2017). The idea here is to solve the full solute transport equation in addition to the water balance, and use the isotopic ratio to calibrate the parameters of the transport model. This kind of an approach is very useful in solute modeling, as

isotopic ratios provide an additional measurement against which the transport model can be calibrated or validated. However, the number of parameters in such a transport model is much higher than in regular rainfall-runoff models, due to the additional parameters of the advection diffusion equations. Hence, due to the enhanced model complexity, it is unclear if information gained by using additional isotope data compensates for the subsequent increase in model complexity (Kelleher et al., 2019). In the absence of sufficient data to constrain the model, issues related to equifinality might occur, where the observed dataset is insufficient to constrain the most likely model parameter state (Beven and Freer, 2001; Shafii et al., 2019), reducing confidence in the predictive power of such a model.

2) *Transit time modeling*: Transit time of water is the time taken by a water particle to exit a catchment after being first introduced into the catchment, it represents the velocity aspect of a catchment (Benettin et al., 2015). By solving a Master equation for the average residence time of water within a catchment (Botter et al., 2011), the expected (or the mean) transit time (Kirchner, 2016) of a catchment can be estimated. Stable water isotope ratios are used to infer the model parameters of the master equation (Harman, 2015). Transit time distributions provide a stochastic alternative to modeling solute transport and hence can be used in water quality modeling (Hrachowitz et al., 2016). Also, such transit time modeling approaches have been used to estimate catchment storage (Soulsby et al., 2009), and the degree of mixing within the different catchment storage compartments (Hrachowitz et al., 2016).

Few conceptual rainfall-runoff models parameterize celerity and velocity, which if ignored can result in spurious results because of conflicts in internal flux partitioning within the model (Delavau et al., 2017). Given the very fast runoff response to convective summer rainfall events in Alpine catchments (Weingartner et al., 2003), sometimes on the order of a few minutes, such models overestimate the fraction of streamflow derived from the current rainfall event i.e. incorrectly represents the velocity behavior of a catchment.

In this article, we develop a semi-distributed conceptual rainfall-runoff model that parameterizes both the velocity and celerity behavior of an Alpine catchment. The model

simulates the different hydrologic fluxes at very high temporal resolution, along with the amount of pre-event vs event water flowing into the stream. This fraction of pre-event water in the stream is simultaneously inferred with stable water isotopes using an independent Bayesian mixing model, and is used to calibrate the rainfall-runoff model. This novel framework allows us to use the results of the mixing model during the calibration of the rainfall-runoff model, ensuring similar levels of model complexity. The model is extensively tested in an experimental catchment called Vallon de Nant, located in the Southwestern Swiss Alps, during summers of 2017 and 2018. In the article, we discuss the advantages and limitations of such a modeling approach and how it can be extended to other catchments.

In this study, we use stable water isotopes to design a semi-distributed conceptual rainfall-runoff model for an Alpine catchment (Vallon de Nant), and incorporate information about pre-event water fraction in the stream within the rainfall-runoff model. Pre-event water fraction during summer rains is estimated using stable water isotope data and a Bayesian mixing model, and is used to calibrate the rainfall-runoff model. This kind of a calibration scheme increases the pre-event water fraction within the stream making the model simulations more realistic. We discuss the advantages and limitations of such a modeling approach and how it can be extended to other experimental catchments.

3.2. Study area and measurements

Vallon de Nant is a snow-dominated headwater catchment located in the Vaud Alps in South-west of Switzerland (Figure 3.1). Stretching across an area of 13.4 km^2, catchment elevation ranges from 1253 m to 3051 m a.s.l. Vallon de Nant has a protected status (Natural Reserve of the Muveran) since 1969, and is one of the few relatively unperturbed Alpine catchments in Switzerland. Steep slopes form a large part of the catchment, with mean catchment slope of around 36 ° (Thornton et al., 2018). At lower elevations, there is a dense forest dominated by *Picea abies* (Norway spruce) occupying about 14% of the catchment area. There is an active pasture area along with an open forest dominated by *Larix decidua* (Larch) in the middle part of the catchment. Floodplains and talus span from lower to mid-elevation levels and form 12.3% and 6% of the catchment area. In the South-western tip of the catchment, there is a

small glacier occupying around 4.4% of the catchment area. The detailed catchment geology is summarized in Thornton et al., (2018).

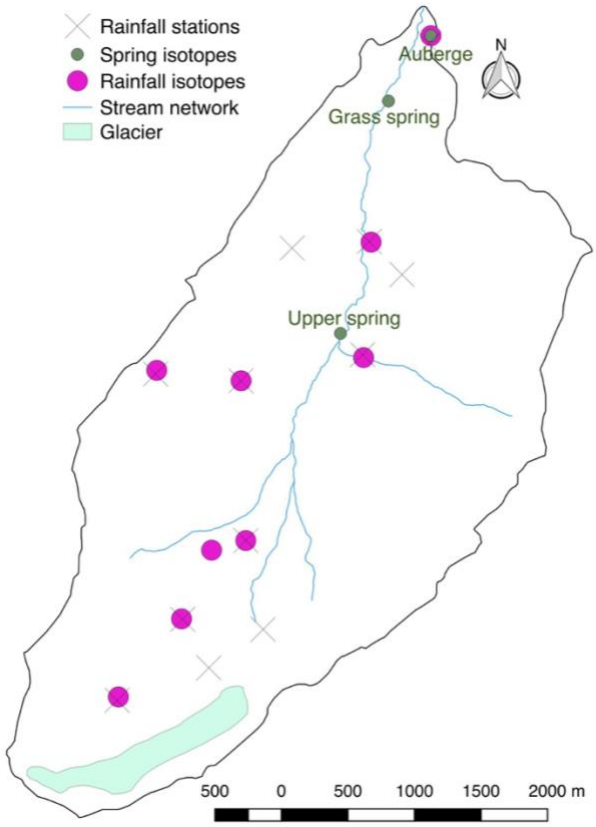

Figure 3.1. Map showing Vallon de Nant along with various monitoring sites for rain, spring and stream waters and their isotopic compositions.

Vallon de Nant experiences a typical Alpine climate, with most of the precipitation originating from the North Atlantic Ocean, followed by the Mediterranean, the European land surface and the North and Baltic sea (Sodemann and Zubler, 2010). The winter precipitation is dominated by the North Atlantic Ocean whereas summer precipitation has a more continental influence. The annual precipitation amounts to ~1900 mm with snowfall accounting for 40-45% of annual precipitation (Beria et al., 2020). The mean annual air temperature is 1.8 °C. Long term climate statistics are computed using the MeteoSwiss gridded air temperature and precipitation dataset (MeteoSwiss, 2016, 2017) and a Thiessen Polygon based interpolation approach (Schumann, 1998).

Vallon de Nant was extensively monitored for different hydrometeorological variables such as streamflow, rainfall, etc. along with stable water isotopes in rainfall, snowpack, streamflow, and springs (Beria et al., 2019). Rainfall isotopes were sampled bi-weekly at two regular locations, with one site located next to the catchment outlet and the other in the middle part of the catchment on the right tributary (Figure 3.1). A high resolution rainfall isotope network was installed in September 2018 to capture the spatial variability in rainfall isotopes. This network is shown in Figure 3.1, and was successful in capturing three major rainfall events. Grab snowpack isotope samples were collected during the winters of hydrologic years 2017 and 2018 as snowmelt lysimeters could not be installed due to the harsh weather conditions and frequent avalanches during winters, limiting access to the catchment. An automatic ISCO sampler was installed at the catchment outlet during the summers of 2017 and 2018, collecting streamwater samples at 6-12 hourly temporal frequency. Spring isotope samples were collected at three different locations.

A Cavity Ring Down Spectrometer (CRDS) system (Picarro L2140-i) was used to measure the stable water isotopes in precipitation, streamflow, and springs. The stable water isotope values were standardized against the Vienna Standard Mean Ocean Water (VSMOW) using three different water standards (ANZO, EMEB, SAAS).

During the summers of 2017 and 2018, a spatially dense network of drop-counting rain gauges called Pluvimates (www.driptych.com) were installed in 12 different locations within Vallon de Nant (Figure 3.1). Pluvimates record rainfall at a 0.01 mm resolution and were setup at a 2-minute temporal frequency (Michelon et al., 2020a). Rainfall data were aggregated at a 10-minute temporal resolution and the point measurements were interpolated to 300-m spatial resolution using a Thiessen Polygon approach (Schumann, 1998). Due to the remote catchment location, harsh winter weather and unavailability of electricity, pluvimates were not heated and could only be installed during the warmer part of the year, limiting the focus of rainfall-runoff modeling to the June-September period of 2017 and 2018.

Stream water level was continuously measured at the catchment outlet (1-minute temporal frequency) using a sonar-based stream gauge installed on top of a weir. Streamflow is

estimated using a rating curve based on 23 salt discharge measurements (Ceperley et al., 2018). Streamflow is quality controlled and aggregated at a 10-min temporal resolution.

3.3. Methodology

3.3.1. Bayesian mixing model

A Bayesian mixing model called HydroMix, previously described in Beria et al., (2020), is used to gain insights into the fraction of pre-event water flowing into the stream from stable water isotope data. HydroMix formulates the linear mixing problem in a Bayesian inference framework and parameterizes an error function to compute the mixing ratio. For a system with two sources that linearly combine into a mixture, mixing ratio shows the contribution of source 1 in the mixture. Such a model can be used in applications such as hydrograph separation. HydroMix differs from the traditional Bayesian mixing models as it does not make assumptions about the parametric form of the probability distribution of the source compositions but is based on the formulation of an error function between the simulated target tracer concentrations and the observed concentrations. This is especially advantageous when the amount of available data is insufficient to robustly fit a probability distribution function to observed tracer concentrations.

In this article, HydroMix is used to estimate the fraction of summer vs winter precipitation recharging springs and stream. A slightly different variant of HydroMix is then used to estimate the fraction of pre-event water flowing into the stream during a given summer rainfall event. In this setting, for each storm event, only one event stream isotope measurement is available. Accordingly, HydroMix is not applied in its original set-up, which draws samples from all the available source and target measurements. Instead we assume a Gaussian distribution for pre-event and event water isotopes and assume that the mean of the distribution corresponds to the observed sample concentrations and the standard deviation is assumed to be equivalent to the analytical measurement error. Given this assumed source and target distributions, 1000 pre-event and event water isotope samples

are generated and the posterior distribution of the mixing ratio is inferred by a Monte Carlo sampler.

Pre-event water isotope samples are identified using streamflow isotope measurements just before a rainfall event. Event water isotope samples are grab samples of the stream at a given point of time during a rainfall event taken by the automatic ISCO machine setup at 6-hourly time steps. As variability in rainfall isotope compositions is much higher relative to the scale of variability in streamflow (Beria et al., 2018), all the rainfall isotope measurements are used to fit a probability distribution curve to rainfall isotopes.

3.3.2. Rainfall-runoff model

Based on the insights gained from stable water isotopes, streamflow is conceptualized as the sum of direct flow and delayed subsurface flow. Direct flow (Q_d) represents the flow generated from the shallow soil layer, and is modeled as a space-time filter of rainfall (R) with a spatially distributed runoff production function (P_F), convoluted using a travel time distribution approach (Rinaldo et al., 1991) (eq. 3.1). The travel time function is split into hillslope travel time (H_T) and open stream travel time (S_T). Hillslope travel time routes flow from a given location i in the catchment to the nearest point in the stream and is parameterized with hillslope velocity (v_H) and catchment geometry. Open stream travel time is parameterized with stream velocity (v_S).

$$Q_d = \sum_{i \, \epsilon \, \text{catchment}} P_F(R_i) * (H_T(i) + S_T(i)). \qquad (3.1)$$

The runoff production function (splitting incoming precipitation into direct flow and leakage into the fast subsurface storage) is parameterized based on the initial abstraction concept of the curve-number approach (Boughton, 1989), where direct flow response to rainfall follows an affine behavior: no response if cumulative rainfall is below a given threshold called initial abstraction (I_a), followed by a linear response:

$$PF(R(t)) = 0 \; if \; \int_{t_i}^{t} R(t)dt < I_a$$
$$PF\big(R(t)\big) = \beta R(t) \text{ otherwise,} \qquad (3.2)$$

where t_i is the initiation time of the rain event, β is the runoff production coefficient (Boughton, 1989), and Q is the streamflow at the outlet. In order to separate the pressure wave response of the catchment from actual surface runoff, Q_d is divided into two components using parameter ρ, where ρQ_d is regarded as the event water entering directly into the stream, illustrating hydrologic processes such as surface and fast lateral subsurface flow. The remainder Q_d, i.e. $(1-\rho)Q_d$ represents the pressure wave response of the catchment, i.e. it depicts the piston-flow mechanism where the water flowing into the stream is non-event water pushed out by the event water entering the catchment.

The subsurface is divided into two storages (fast and slow), similar to the conceptualization used in Schaefli et al., (2014). The reason for using two subsurface storages is given in Section on *Overview of isotope hydrology of Vallon de Nant*. The flow generated from these storages (Q_{fast} and Q_{slow}) are modeled as non-linear function of storage volumes (S_{fast} and S_{slow}) (Roques et al., 2017; Tashie et al., 2020).

$$Q_{\text{fast}} = k_{\text{fast}} \mathrm{S}_{\text{fast}}^{\gamma \text{fast}}, \qquad (3.3)$$

$$Q_{\text{slow}} = k_{\text{slow}} \mathrm{S}_{\text{slow}}^{\gamma \text{slow}}, \qquad (3.4)$$

where k_{fast}, k_{slow} are the recession coefficients and γ_{fast} and γ_{slow} are the exponents of the fast and slow subsurface storages. A γ value of unity yields a linear reservoir special case. The fast subsurface storage (S_{fast}) is fed by the part of rainfall that is not routed to direct flow (eq. 3.5) and the slow subsurface storage (S_{slow}) is fed by fast subsurface storage (S_{fast}) with a constant flux (L_{max}) limited by the water input in S_{fast} (eq. 3.6) (Schaefli et al., 2014). Both the fast and slow subsurface storages are lumped in space and assumed to be fully mixed.

$$\frac{dS_{\text{fast}}(t)}{dt} = (1-\beta)R(t) - k_{\text{fast}} S_{\text{fast}}(t)^{\gamma \text{fast}} - \min\{(1-\beta)R(t), L_{\max}\} \qquad (3.5)$$

$$\frac{dS_{\text{slow}}(t)}{dt} = \min\{(1-\beta)R(t), L_{\max}\} - k_{\text{slow}} S_{\text{slow}}(t)^{\gamma\text{slow}} \quad (3.6)$$

The full rainfall-runoff model is summarized in the Figure 3.2.

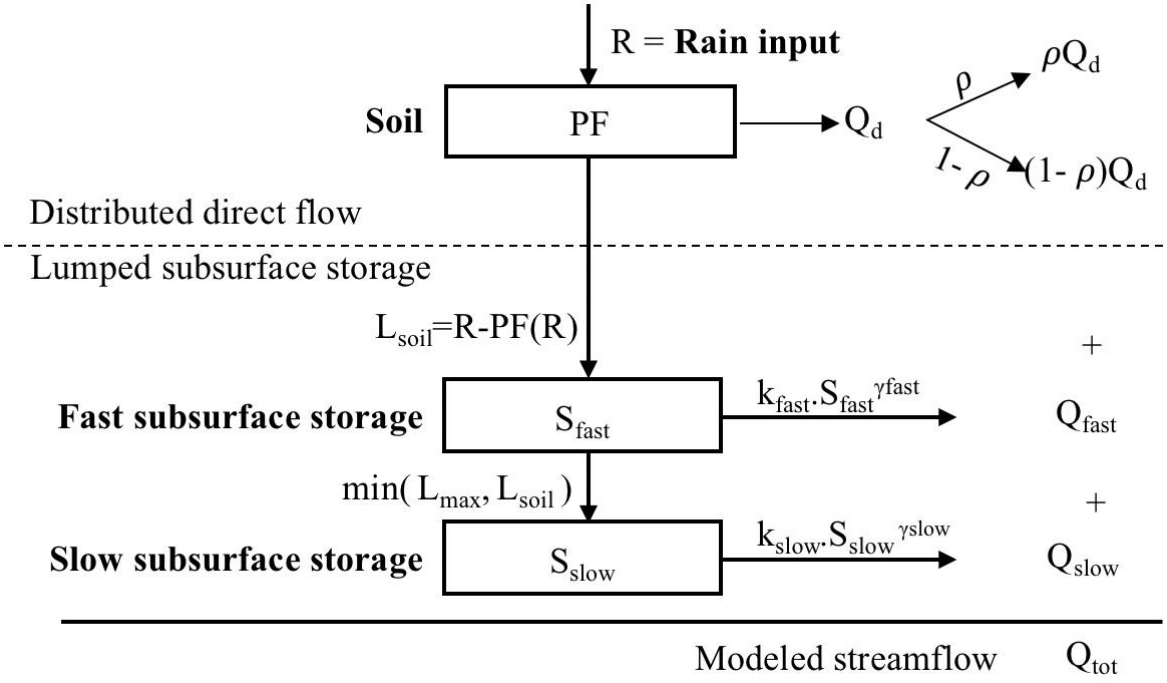

Figure 3.2. Flowchart showing the different components of the rainfall-runoff model.

3.3.3. Rainfall-runoff model calibration with streamflow data

In order to capture the very fast catchment response to convective summer rainfall events, the rainfall-runoff model is setup at a 10-minute temporal resolution. In the first step, the model is calibrated against streamflow aggregated over a 10-minute time step. A split sampling calibration strategy is used where the model is first calibrated using streamflow data for the year 2017 and then validated against 2018 streamflow data and vice versa. Multiple model diagnostics summarized in Table 3.1 are used to verify the model estimates.

The model is calibrated in a Bayesian framework, where a Metropolis-Hastings sampler is used to infer the posterior distribution of the model parameters. All the model parameters $\theta = \{I_a,\ \beta,\ \rho,\ v_H,\ v_S,\ k_{\text{fast}},\ \gamma_{\text{fast}},\ l_{\max},\ k_{\text{slow}},\ \gamma_{\text{slow}}\}$ (summarized in the appendix) and

the initial storage of the slow and fast subsurface (S_{slow}, S_{fast}) are jointly inferred. The likelihood function of the streamflow model is specified based on the model residuals Δ:

$$\Delta = Q_{\mathrm{obs}} - Q_{\mathrm{sim}}. \qquad (3.7)$$

Where Q_{obs} and Q_{sim} are observed and simulated streamflow. For the given model residual Δ, the log-likelihood function (L_s) reads as:

$$L_s = -\frac{n}{2}\log(2\pi\,{\sigma_\Delta}^2) - \frac{1}{2\,{\sigma_\Delta}^2}\sum_{i=1}^{n}(Q_{\mathrm{obs}}(i) - Q_{\mathrm{sim}}(i))^2 \qquad (3.8)$$

where the residuals are normally distributed with zero mean and standard deviation of σ_Δ.

The standard deviation σ_Δ of the residuals Δ is specified *a priori* as 0.01 mm/hr during high flow conditions, representing the theoretical uncertainty in stage height measurements (converted to streamflow using the rating curve). In practice, however, streamflow measurement errors are much larger than 0.01 mm/hr as they are impacted by additional uncertainty sources, for instance rating curve calibration or occasional sediment deposits under the sonar leading to spurious measurements. These additional uncertainties are modeled by adding an exponentially correlated noise ε to model residual Δ. The additional noise ε pools together uncertainty introduced by the imperfect measurements and simplifications in the rainfall-runoff model. ε is modeled as a zero-mean temporally correlated Gaussian process with standard deviation σ_ε and exponential autocorrelation function with range parameter ρ_ε (which is equivalent to an order 1 autocorrelated random process). The hyper-parameters of the noise ε (i.e. σ_ε and ρ_ε) are inferred by adding a Gibbs sampler step within the Metropolis routine (Diggle and Ribeiro, 2002).

During low flow conditions, σ_Δ is inflated to 0.15 mm/hr to account for the absence of ε, resulting in a simplified subsurface storage model, which neglects some important hydrologic processes such as diel fluctuations in streamflow during early summer induced by melt of residual snowpacks. This error model of low flow conditions is oversimplified since it neglects autocorrelation and heteroscedasticity in streamflow (Ammann et al., 2019; Smith et al.,

2015), but is deemed sufficient to coarsely handle low flow conditions which is not the core aspect of this article.

Table 3.1. Summary of different statistical indices used to evaluate streamflow estimates of the rainfall-runoff model (*X*: observed streamflow; *Y*: simulated streamflow; *n*: Number of data points)

Index	**Formula**	**Best value**	**Worst value**
Percentage bias (Pbias)	$\frac{\sum(X-Y)}{\sum X} * 100$	0	+∞ / - ∞
Nash Sutcliffe efficiency (NSE)	$1-\frac{\sum(X-Y)^2}{\sum(X-\bar{X})^2}$	1	- ∞ (negative value means that mean is a better estimator than the model).
Root mean squared error (RMSE)	$\sqrt{\frac{\sum(X-Y)^2}{n}}$	0	+∞

3.3.4. Rainfall-runoff model calibration with streamflow and stable water isotopes

In the above configuration, the parameter ρ that modulates the contribution of event water in direct flow is not constrained by streamflow, leading to large uncertainties on the estimated pre-event water fraction in stream water. Pre-event water is composed of the pressure wave component of direct flow and flux coming from the two subsurface storages, accounting for the fully mixed assumption. Stable water isotopes can be used to estimate the pre-event water fraction in the stream at the time of streamwater sampling, thereby helping constrain ρ. In order to incorporate stable water isotope data during model calibration, a new acceptance criterion is added to the Metropolis sampler, where the amount of pre-event water estimated from stable water isotopes is compared to the one simulated by the rainfall-runoff model. The parameter ρ is therefore calibrated conditional to the other model parameters (which influence both the partitioning between direct and subsurface water fluxes, and the balance between event and pre-event water fluxes in the subsurface), but is

informed by its own observation equation. The likelihood function for the isotopes driven part of the model is specified based on the pre-event water fraction residuals η:

$$\eta = f_{\mathrm{p,obs}} - f_{\mathrm{p,sim}} \qquad (3.9)$$

where $f_{\mathrm{p,obs}}$ and $f_{\mathrm{p,sim}}$ are observed and simulated pre-event water fraction in the stream. The observed pre-event water fraction is derived from stable water isotopes using the mixing model (described in Section 3.3.1). For the given model residual η, the log-likelihood function (L_f) reads as:

$$L_{\mathrm{f}} = -\frac{n}{2}\log\left(2\pi\,{\sigma_{\eta}}^2\right) - \frac{1}{2\,{\sigma_{\eta}}^2}\sum_{i=1}^{n}\left(f_{\mathrm{p,obs}}(i) - f_{\mathrm{p,sim}}(i)\right)^2 \qquad (3.10)$$

where the residuals are normally distributed with zero mean and standard deviation of σ_{η}. The standard deviation σ_{η} of pre-event water fraction is derived from the mixing model.

3.3.5. Model initialization and set-up

Model calibration is performed in two different settings. In the first case, all the model parameters are calibrated using all available data, i.e. rainfall, streamflow and isotope measurements over the summers of 2017 and 2018. An initial burn-in period of 5000 iterations is used and the sampling chain is initialized at parameter values leading to reasonable streamflow simulations. Vague uniform priors are used for all model parameters (including hyper-parameters of noise ε) and these priors are scanned by random walk proposals. The settings of the Metropolis algorithm are summarized in the appendix.

In the second setting, subsurface model parameters (k_{fast}, γ_{fast}, l_{max}, k_{slow}, γ_{slow}) and their associated state parameters (i.e. S_{slow}, S_{fast}) are fixed to their estimated value, equivalent to the median of their posterior distribution, and the parameters of the direct flow component (corresponding to the surface soil box) are re-calibrated at an event basis to evaluate their inter-event variability. For this re-calibration, the exact same procedure as

above is applied, except that only 5 parameters are sampled by the Metropolis algorithm (I_{a}, $\beta,\ \rho,\ v_{\mathrm{H}},\ v_{\mathrm{S}}$).

3.4. Results

3.4.1. Overview of isotope hydrology of Vallon de Nant

The slope of the local meteoric water line (LMWL) for Vallon de Nant is very close to that of the global meteoric water line (Figure 3.3). Rainfall and snowpack are isotopically distinct, with rainfall being much more enriched in heavier isotopes compared to snowpack. This is mainly because of differences in cloud condensation temperature at the time of precipitation generation, rainout of air masses as it traverses the landscape over summer and winter periods and the ambient temperature (Akers et al., 2017; Friedman et al., 1964). This large seasonal variability in isotopic composition allows us to use rain and snow as two end-members for subsequent mixing analysis.

Streamwater and groundwater are recharged by rainfall and snowmelt, with streamwater and groundwater isotopes showing much lower variability than precipitation isotopes (Figure 3.3), suggesting that Vallon de Nant acts as a low-pass filter. The isotope variability is slightly lower in groundwater than streamwater, while both stream- and groundwater tend towards a “winter precipitation” composition. Streamwater, groundwater, rainfall and snowpack isotopes lie along the LMWL suggesting no significant evaporation or sublimation within the catchment. Consequently, sublimation is not included within the rainfall-runoff model.

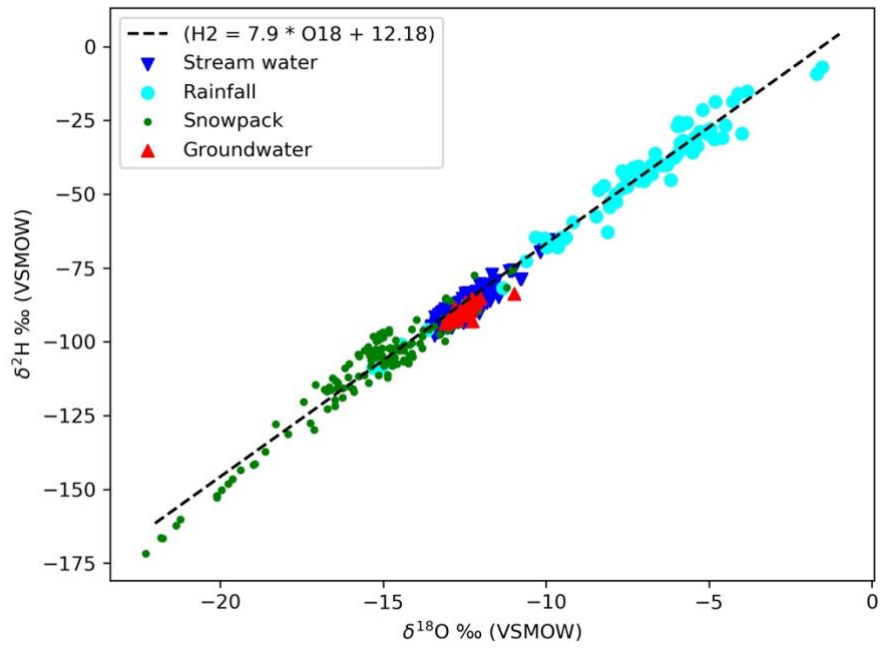

Figure 3.3. The local meteoric water line (LMWL) of Vallon de Nant showing relationship between δ^2H and δ^{18}O in rainfall, snowpack, groundwater and streamwater.

Snowfall forms a large part of the annual water budget in Vallon de Nant. The impact of snowmelt is clearly visible on stream isotopes during the melt season (in May and June), when streamflow becomes more depleted in heavier isotopes (Figure 3.4), which suggests that a large part of streamflow is generated from snowmelt. Streamflow becomes more enriched in heavier isotopes during the course of the summer season, suggesting the relative importance of summer rainfall and groundwater in recharging the stream during summer and autumn periods. Most of the catchment snowpack disappears by the end of June, having limited impact on streamflow generation during the July to September period, which is the focus period for this study. Consequently, a snowmelt model is not included in this study.

Another interesting observation from Figure 3.4 is the lack of diel variation in stream isotopes, suggesting minimal glacial melt. Glacial melt is mostly generated during the peak of summer season (in the July- August period), with water melting during the day due to higher solar radiation. As meltwater is more depleted in heavier isotopes compared to groundwater (Beria et al., 2018), streamwater is expected to be more depleted in heavier isotopes during the day than night in periods of large glacial melt. However, no such effect can be seen in Vallon de Nant during 2017 and 2018 summers, which suggest that glacial melt contributes little to

streamflow generation. Consequently, glacial melt is not included within the rainfall-runoff model.

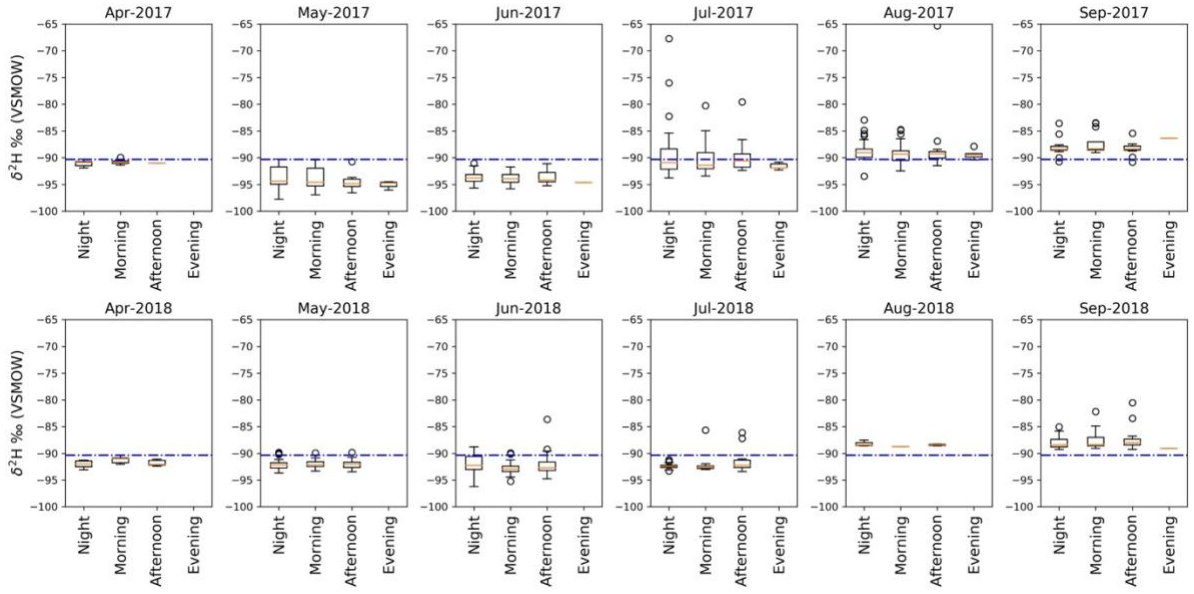

Figure 3.4. Diel variation within monthly streamflow isotopes plotted from April to September for 2017 and 2018. A given day is divided into 6-hour blocks starting from mid-night to 6:00 (called night block), followed by morning, afternoon and evening time blocks. The blue line represents the average of streamflow isotopes over the two hydrologic years.

Although snowfall accounts for only 40-45% of annual precipitation, it contributes disproportionately to stream and groundwater recharge, with >60% of streamwater and groundwater recharge coming from snow (Figure 3.5). Both stream and groundwater show distinct seasonality in recharge from snow, with higher snow contribution during the months of May and June when snowmelt peaks. Additionally, the Grass spring seems to be slightly less influenced by snow dominated recharge compared to the Upper spring and the groundwater fountain located close to the outlet (called Auberge groundwater) (Figure 3.5b). Conductivity measurements show Grass spring to have higher conductivity values than the Upper spring and groundwater fountain at Auberge (Mächler et al., 2019). Both these lines of evidence suggest the existence of two distinct groundwater pools within Vallon de Nant. In order to incorporate this information, two distinct subsurface storages are conceptualized within the rainfall-runoff model.

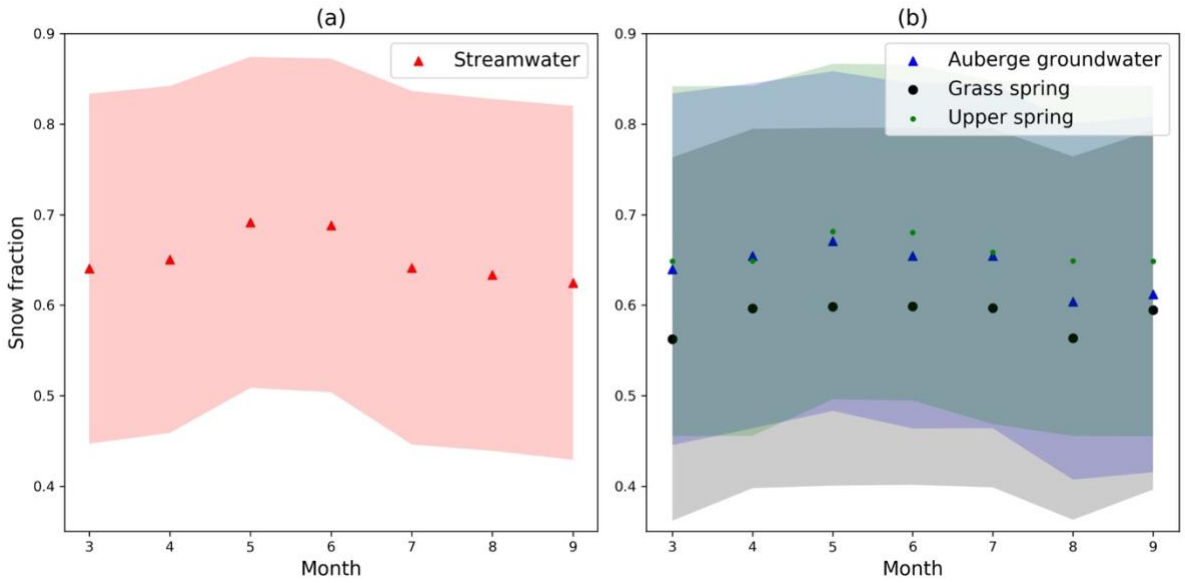

Figure 3.5. Fraction of snow recharging (a) streamwater and (b) the three springs in Vallon de Nant for the months of March to September of 2017. The uncertainty band represents the inferred snow fraction plus or minus the standard deviation.

3.4.2. Rainfall-runoff model validation with streamflow and isotopes

The rainfall-runoff model is assessed using a split sampling strategy, where 2017 data is used to calibrate and 2018 data is used to validate, and vice versa. Results in Figure 3.6 show that the model captures the high flow dynamics reasonably well, with an overall NSE value of 0.65 and 0.66 for years 2017 and 2018, and RMSE values of 0.04 mm/hr for both years. The low flow dynamics are oversimplified within the model as the main focus is to simulate streamflow response to summer rainfall events. This leads to imperfect low flow simulations, and in particular during recessions. The model is also unable to capture diel variations because it does not include a snow component, which results in inflated simulation errors in early July of 2017 (Figure 3.6a) because of an extended snowmelt season.

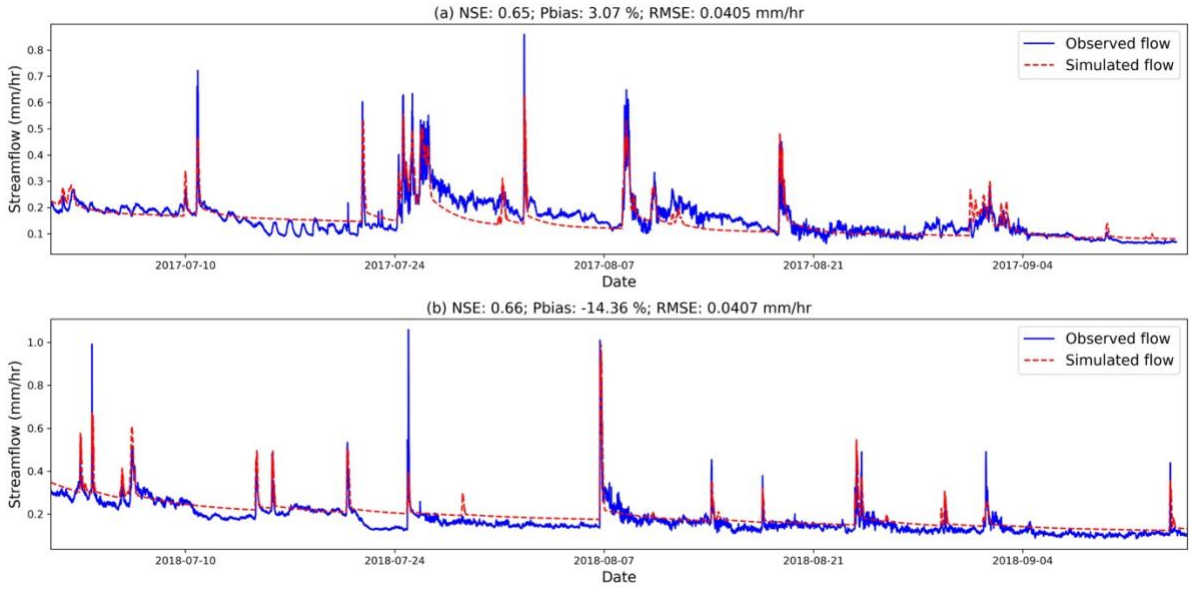

Figure 3.6. Simulated and observed hydrograph along with the model diagnostics for the summer of (a) 2017 and (b) 2018. The subplot (a) was calibrated with 2018 streamflow data whereas the subplot (b) was calibrated using 2017 streamflow data.

In addition to streamflow data, isotope derived pre-event water fraction is used to inform the parameters of the soil component of the rainfall-runoff model (see flowchart in Figure 3.2). This allows improving the estimation of the pre-event water fraction. Indeed, when calibrated with streamflow data alone, the rainfall-runoff model systematically underestimates the fraction of pre-event water within the stream during rain (Figure 3.7). This is because the ρ parameter, which represents the event water fraction of direct flow, can only be constrained using isotope data. When only streamflow measurements are available, ρ is set to 1 *a priori* (i.e. all direct flow is assigned as event water), which leads to a higher proportion of event water in simulations. Stable water isotopes allow this parameter to be constrained, thus ensuring that the simulated event and pre-event water fractions are closer to reality.

The posterior distribution of ρ (Appendix Figure 3.S1) suggests that about 40% of direct flow goes into the stream, while the rest 60% contributes to piston-flow, where the event water pushes the older water stored within the catchment into the stream. However, at the scale of a rain event, the ρ parameter varies from 10% to 90% depending on the type and magnitude of the rain storm (Figure 3.8a). This large variability in ρ shows that a large part of streamflow during rains is derived from subsurface storage, because even when all the direct

flow recharging the stream is event water, i.e. when ρ is close to 90%, the pre-event water fraction is still >50%. This unique model conceptualization allows for a better understanding of these finer aspects of the catchment behavior, which is often covered in literature.

10-minute resolution streamflow simulations (Figure 3.6) show that the Vallon de Nant catchment has a very dynamic behavior, with very quick response to a given rainfall forcing (sometimes on the order of a few minutes). Interestingly, despite such dynamic catchment characteristics, more than 50% streamwater is derived from the catchment storage even during the most severe summer downpours (Figure 3.8b). This suggests the dominance of piston-flow mechanism within Vallon de Nant, where most event water mobilizes water stored within the catchment, which then recharges the stream.

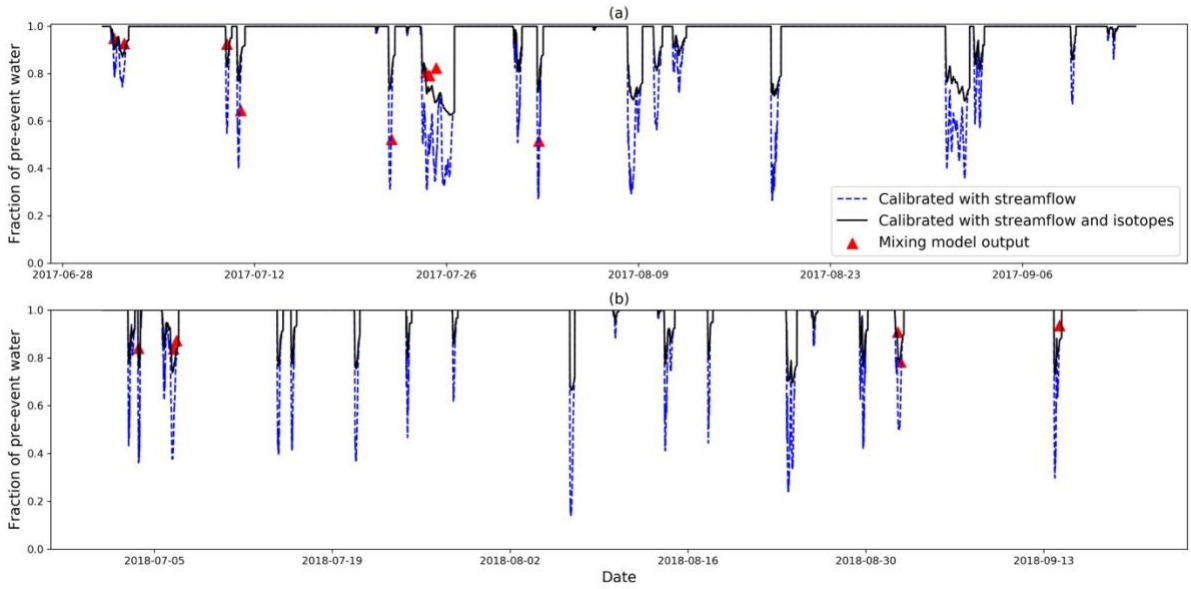

Figure 3.7. Pre-event water fraction simulated by the rainfall-runoff model calibrated using streamflow data vs streamflow and isotope data. Subplot (a) shows the model simulation for 2017 and subplot (b) shows the model simulation for 2018.

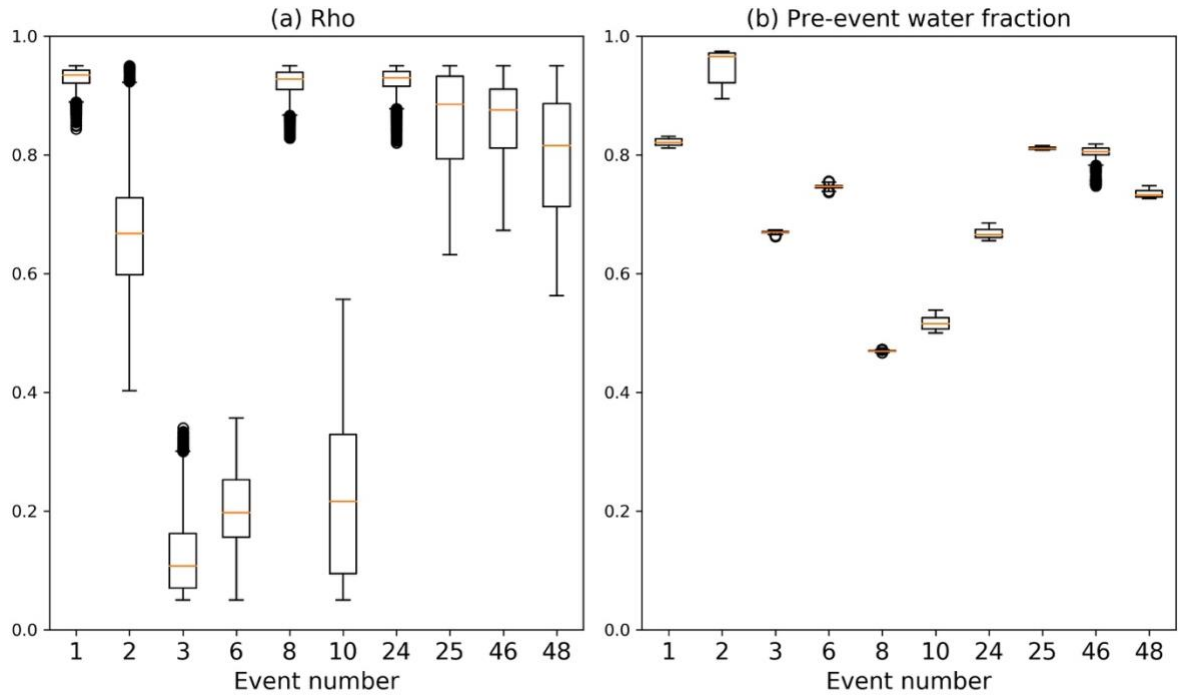

Figure 3.8. Posterior distribution of (a) ρ and (b) pre-event water fraction when calibrated on an event-by-event basis for rainfall events that are larger than 10 mm and have available isotope data.

3.5. Discussions and conclusion

In this article, we combine stable water isotopes with a classical rainfall-runoff modeling approach to learn about the dominant hydrologic processes occurring within Vallon de Nant. Stable water isotopes are first used to gain qualitative insights about the catchment hydrology, and this information is leveraged to design a rainfall-runoff model with the objective of simulating summer streamflow at 10-minute temporal resolution. In a second step, stable water isotopes are used to infer the proportion of piston-flow within direct flow. This novel way of incorporating stable water isotopes within a rainfall-runoff model leads to an improved characterization of catchment hydrologic processes, and enables the simulation of both streamflow and pre-event water fraction at very high temporal resolution.

The results of this study reveal a very rapid streamflow response to convective summer rains within Vallon de Nant (Figures 3.6, 3.7), sometimes on the order of a few minutes. Although intensive, the isotope campaigns carried out at Vallon de Nant did not sample at such a high

temporal resolution, which means that a lot of storms events were simply missed in raw isotope data. The proposed combination of isotopes and streamflow data overcomes this limitation, thus making it possible to estimate pre-event water fraction in stream water at 10-minute resolution. Results show that this parameter varies tremendously through time, which call for fostering the recent efforts in designing isotope sampling strategies in view to properly capture this parameter (Wang et al., 2017, 2019).

Past attempts to incorporate stable water isotopes into rainfall-runoff models mostly involved adding a solute transport component to the rainfall-runoff model (Birkel and Soulsby, 2015; Kuppel et al., 2018), thereby significantly increasing model complexity. In contrast, our approach introduces only one additional parameter (ρ). Adding ρ slightly increases model complexity, but allows for a proper estimation of pre-event water fraction as shown in Figure 3.9. In our model, ρ separates direct runoff into a piston-flow and an event runoff component, explicitly parameterizing the celerity and velocity responses of a catchment. This implies ρ to be a potential catchment hydrologic signature which can be related to physical catchment characteristics. To further investigate this point, the present rainfall-runoff setup could be tested over a larger number of catchments in order to verify if ρ can be linked to geomorphological attributes of a catchment.

A key limitation of this approach is the fully mixed assumption used for the two subsurface storages. However, this assumption can be relaxed using storage selection functions (Rinaldo et al., 2015) that are commonly used in transit time distributions (Hrachowitz et al., 2015, 2016). By using the transit time distribution approach, the storage selection function can be made to vary depending on the current catchment state, in terms of antecedent soil moisture content. This will make an interesting future work.

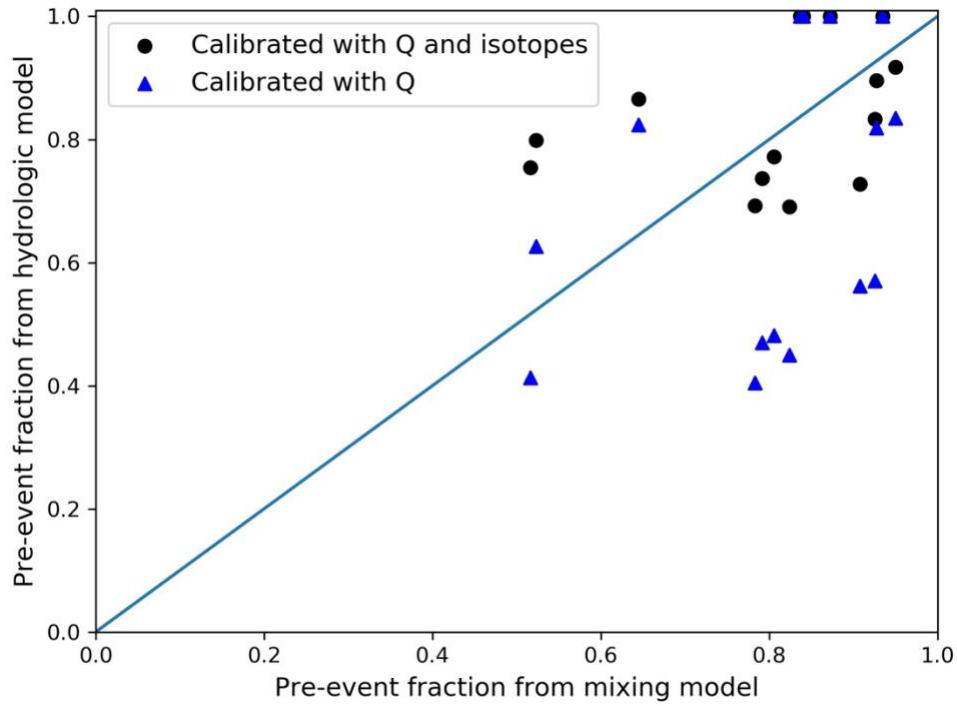

Figure 3.9. Pre-event water fraction estimated using the rainfall-runoff model vs the Bayesian mixing model in two different model calibration settings. The rainfall-runoff model is calibrated with streamflow in the first setting, and calibrated with streamflow and stable water isotope data in the second setting.

3.6. Appendix

Parameter	I_a	β	v_S	v_H	ρ	σ_ε	ρ_ε
Prior	$U[5, 20]$	$U[0.2, 0.95]$	$U[0.01, 3]$	$U[0.01, 3]$	$U[0.05, 0.095]$	$U[0.01, 0.5]$	$U[600, 4000]$
Proposal amplitude $Q(x) \sim U[x-a, x+a]$	a=0.075	a=0.04	a=0.015	a=0.015	a=0.045	a=0.03	a=25
Initial value	8.0	0.4	0.8	0.15	0.06	0.05	2500

Parameter	S_{fast}	S_{slow}	K_{fast}	K_{slow}	γ_{fast}	γ_{slow}	L_{max}
Prior	$U[0, 500]$	$U[100, 10000]$	$U[1e^{-4}, 0.1]$	$U[1e^{-7}, 1e^{-4}]$	$U[0.5, 2]$	$U[0.5, 2]$	$U[0, 0.2]$
Proposal amplitude $Q(x) \sim U[x-a, x+a]$	a=5	a=100	a=0.001	a=1e-6	a=0.015	a=0.015	a=0.002
Initial value	50	4000	0.003	5e-5	1	1	0.006

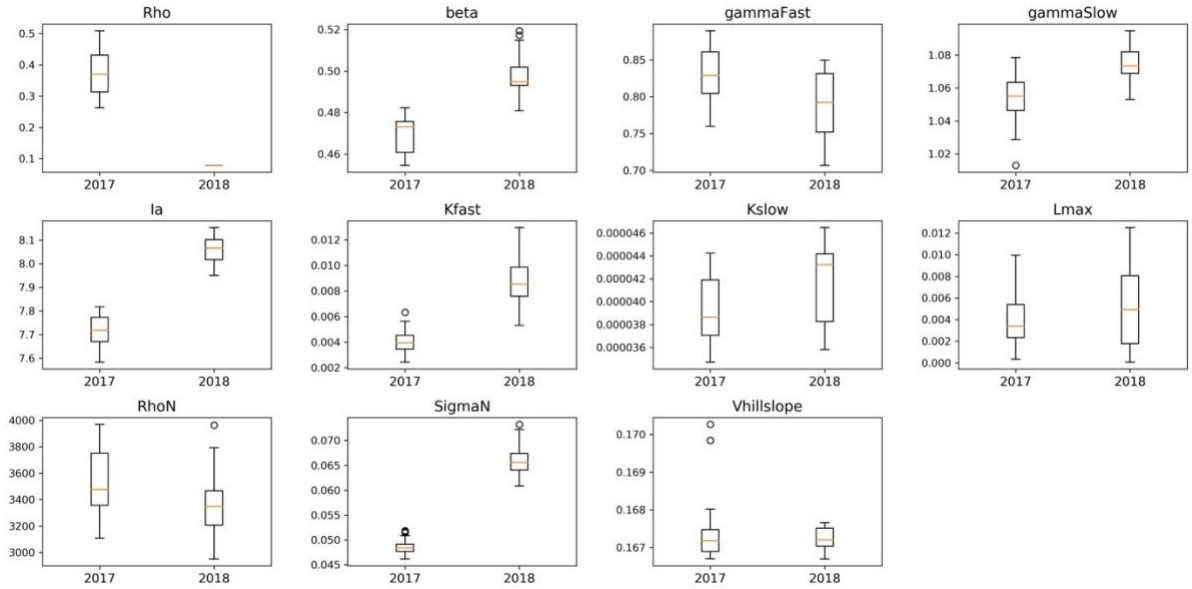

Figure 3.S1. Posterior distribution of the model parameters calibrated using streamflow and stable water isotope data for years 2017 and 2018.

Author contributions: The paper was written by HB with contributions from all coauthors. HB and LB formulated the conceptual underpinnings of the hydrological model. HB formulated the mixing model and LB formulated the hydrological model. GM and BS helped in framing the statistical and hydrological tests to evaluate the modeling framework and provided critical feedback during different phases of the project.

4. Ephemeral snowpack enhances winter groundwater recharge and low flow water supply

Harsh Beria, Joshua R. Larsen, Natalie C. Ceperley, Anthony Michelon, Bettina Schaefli

Current under review[3] in *Nature Climate Change.*

[3] Beria, H., Larsen, J. R., Ceperley, N. C., Michelon, A. and Schaefli, B.: Ephemeral snowpack enhances winter groundwater recharge and low flow water supply (in review), Nat. Clim. Chang.

Abstract

Snowmelt has been shown to be more efficient than rainfall at recharging groundwater across many world regions, with significant implications for water resources availability and ecosystem productivity in a warming climate. A key factor that has been largely ignored is the role of snow cover intermittency. Based on stable water isotope and discharge data from the Swiss Alps, we show that melt originating from ephemeral snowpacks enhances groundwater recharge compared to melt from seasonal snowpacks. We furthermore show that a 2.5 °C warmer climate will expand the regional footprint of ephemeral snowpacks, altering the partitioning of the water balance to increase cold season low flow supply to river networks at the expense of summer low flows, with ensuing negative consequences for freshwater ecosystems. This shift to a more ephemeral snow cover regime under a warmer climate is therefore of wider concern for water security and aquatic ecosystem resilience in snow influenced regions globally.

Keywords: stable water isotopes; mixing model; baseflow separation; climate change; degree-day snow model; hydrology;

4.1. Introduction

Seasonal snow covers over 30% of the Earth's land surface (Brodzik and Armstrong, 2017), and its contribution to the global economy has been estimated at more than a trillion dollars (Sturm et al., 2017). Snowmelt from mountainous regions sustain critical water supplies for agricultural irrigation, hydroelectric power generation and other domestic consumption for over one sixth of the global population (Barnett et al., 2005; Kapnick et al., 2018; Viviroli et al., 2007). For example, in the Western U.S., snowmelt accounts for more than 70% of the total summer runoff, which is expected to decrease by one-third by the end of the century (Li et al., 2017). In the Indian subcontinent, the ten major river basins that are home to over 1.9 billion people are fed by seasonal snow- and ice melt originating from the Hindu Kush Himalayan range (Wester et al., 2018). Snow accumulation in this important mountain range is projected to decline by up to 90% by 2100 (Wester et al., 2018), causing significant water stress in the entire region (Wester et al., 2018). However, the mechanisms by which these changes will propagate through the hydrological cycle in mountainous regions, especially the interplay between surface and subsurface partitioning of snowmelt, remains fundamentally unclear.

Snowmelt provides water supply to river basins beyond the melt season because of infiltration and recharge to groundwater storage and ensuing water release to the river network throughout the year (Pritchard, 2019). As climate warms, a smaller fraction of precipitation will fall as snow (Adam et al., 2009; Choi et al., 2010; Jenicek et al., 2018; Steger et al., 2013), and the duration and accumulation of seasonal snow cover are also likely to decrease (Huning and AghaKouchak, 2018; Zohner and Renner, 2019). A warmer world will also entail an earlier onset of snowmelt (Marty et al., 2017; Stewart et al., 2005), which in turn may reduce the hydrological buffering capacity of snowpacks (Clow, 2010; Dudley et al., 2017), thereby altering streamflow regimes (Milano et al., 2015), and translating into lower summer streamflow (Jenicek et al., 2016). The propagation of these changes across mountainous and especially alpine regions may negatively impact plant growth (Campbell, 2019), and increase the frequency of late summer and autumn droughts (Jenicek et al., 2018), examples of which have already begun to manifest in the Western US (Stewart et al., 2005) and Northern Europe (Hiscock et al., 2011).

Although the onset of snowmelt may be earlier with warming, the corresponding melt rates may be lower due to this melt occurring when solar radiation inputs are lower (Harpold and Brooks, 2018; Musselman et al., 2017). This effect will likely be accentuated in places where solar radiation limits snowmelt (Woods et al., 2019). In addition, enhanced winter warming is likely to make snowpacks at lower elevations more ephemeral (Petersky and Harpold, 2018), causing more intermittent melt during winter (Dong and Menzel, 2019). Ephemeral snowpacks have previously been defined as those persisting for less than 60 continuous days, with both their accumulation and melt occurring during the same (winter) season (Petersky and Harpold, 2018). In contrast, seasonal snowpacks accumulate during the winter season and melt during the spring season. With global warming, ephemeral snowpacks will most likely become more widespread at places where seasonal snowpacks currently prevail. The implications of such snow cover regime change remains poorly understood for meltwater cycling at landscape scale, especially for groundwater recharge and subsequent summer low flows, despite their significant economic and ecologic values (Damigos et al., 2017; Shah, 2008).

In light of this large knowledge gap, we analyze the interplay between snowmelt and groundwater recharge at catchment scale. Specifically, we examine how groundwater recharge varies across an elevation gradient in the Swiss Alps to ask 1) whether snowmelt is more effective at recharging groundwater than liquid precipitation and how this varies in space, and 2) how the dynamics of ephemeral versus seasonal snowpacks control the differences in groundwater recharge and low flow water supply. We first estimate the effectiveness of cold season (November - April) groundwater recharge in 8 headwater catchments (Figure 4.1) using stable water isotopes as a tracer and a Bayesian mixing model (Beria et al., 2020). We complement this with a baseflow recession analysis to quantify groundwater recharge for an extended set of 39 headwater catchments (Figure 4.1) spread across a large elevation gradient. Using a temperature-index snow model, we undertake a novel analysis of snowmelt and rainfall frequency and intensity to see how snow ephemerality relates to cold season low flow water supply. Finally, we examine the potential implications of a transition from seasonal to ephemeral snow regimes on cold season groundwater

recharge and low flow water supply, which has broader implications for many mountain environments undergoing these transitions.

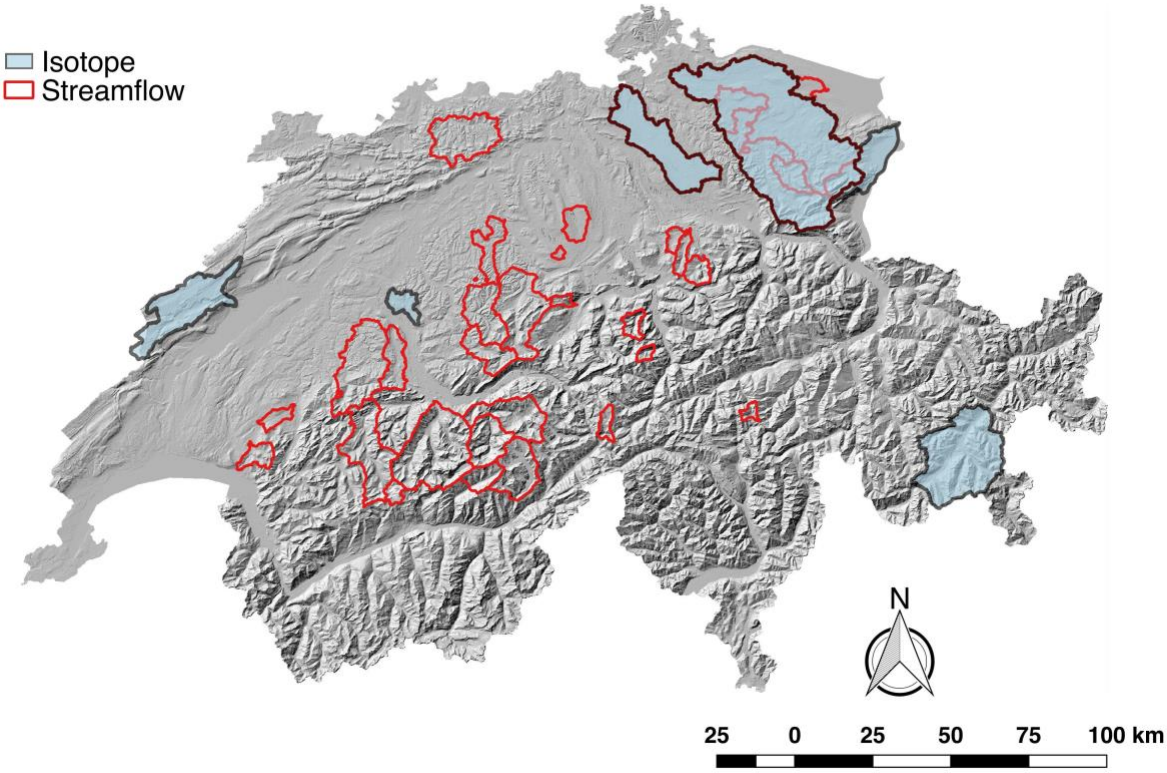

Figure 4.1. Map of Switzerland showing the headwater catchments used this study; in blue: catchments with isotopic data, in red: catchments with only streamflow data.

4.2. Results

All the groundwater systems analyzed have cold season recharge ratios greater than 1, indicating that cold season rain and snowmelt contribute disproportionately to groundwater recharge across pre-alpine and alpine mountain environments (Figure 4.2a). However, this cold season recharge effectiveness is 2 – 4 times higher in lower elevation catchments than in higher elevation catchments (Figure 4.2a). In the Swiss Alps these low elevation environments are typically characterized by ephemeral snowpacks (Morán-Tejeda et al., 2013). Since snowfall forms an increasingly diminishing fraction of the annual precipitation at lower elevations (4 - 6% in the two catchments located at 500 m a.s.l.), the uncertainty in the winter recharge ratio is also higher (Figure 4.2a).

Given the limited spatial extent of the groundwater isotope data, especially at mid-elevations, we expand on this analysis by considering baseflow as a proxy for groundwater recharge over the cold and warm seasons for 39 headwater catchments. Cold season recharge appears to be far more effective at supplying continuous low flow to streams at lower to mid-elevations (i.e. up to ~1500 m a.s.l.) (Figure 4.2b), which is consistent with the results from the isotope data.

Interestingly, the wide span in elevations included in this analysis highlights that the transition from ephemeral to seasonal snowpack is at mean catchment elevations of ~1500 m a.s.l., which is similar to the findings of previous studies in the Swiss Alps (Morán-Tejeda et al., 2013; Santos et al., 2018). For mean catchment elevations above 1500 m a.s.l., cold season recharge effectiveness is < 1 due to seasonal snowpack delaying the release of water until the warm season. This diminished cold season groundwater recharge at high elevations, in turn, results in very low winter baseflows that are typical in seasonal snow-dominated and glacial streamflow regimes (Milano et al., 2015).

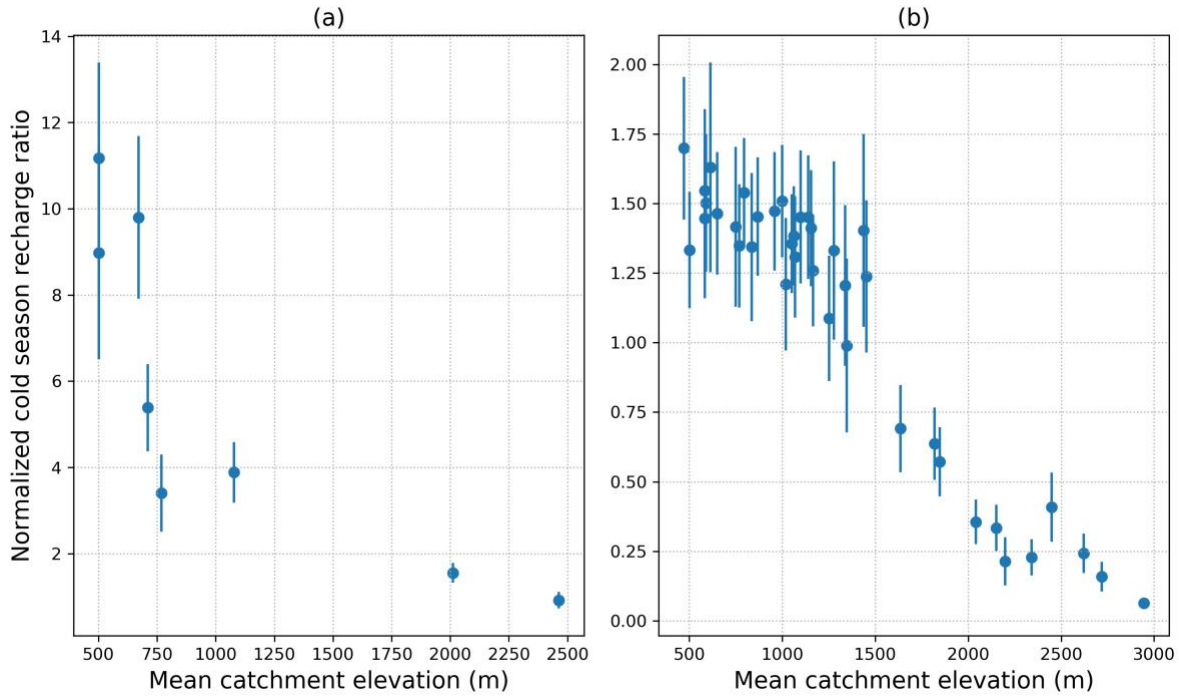

Figure 4.2. Fraction of groundwater recharged during the cold season (November - April) using (a) stable isotopes in groundwater and precipitation normalized by the fraction of

annual precipitation falling as snow, and (b) baseflow, where cold season recharge is expressed as cumulative cold season recharge / cumulative warm season recharge. The recharge ratio is normalized by the fraction of annual precipitation during the cold season and plotted against mean catchment elevation. The error bars represent one standard deviation of the normalized ratio.

An important limitation of the above analysis is that for lower elevation catchments the broader definition of cold season will cover the true winter period affected by snowfall and melt events (December to February), as well as months that generally no longer have snow events (November, March, April). In order to account for this effect, we now restrict the analysis to the true winter season (December – February) for catchments below 1500 m a.sl. This reveals a stronger decreasing trend in winter baseflow with increasing elevation (Figure 4.3a), boosting confidence in the interpretation that cold season groundwater recharge is more effective in low to mid-elevation catchments. We further interrogate this dynamic with a temporal analysis of maximum yearly winter baseflow computed for all observed years across the catchments with ephemeral snowpack (mean elevation < 1500 m a.s.l.) (Figure 4.3b). In this case, normalized maximum winter baseflow also tends to increase in years with lower total snowfall, even within the same catchment. This suggests that within the range of ephemeral snow conditions, increasing the degree of snow ephemerality also increases groundwater recharge effectiveness and cold season low flow water supply.

In order to explore why ephemeral snowpack is more effective at recharging groundwater, we consider the combined melt and rain (equivalent precipitation, PEQ) event frequency and intensity. Interestingly, we find PEQ events have a stable frequency up to the elevation threshold of ephemeral snow at ~1500 m a.s.l. (Figure 4.4a). This is due to continuous accumulation and melt of ephemeral snowpacks during the cold season within this elevation band. Above this elevation threshold, the lack of winter melt and the development of seasonal snowpacks steadily decreases the frequency of PEQ events at higher elevations during the cold season (Figure 4.4a).

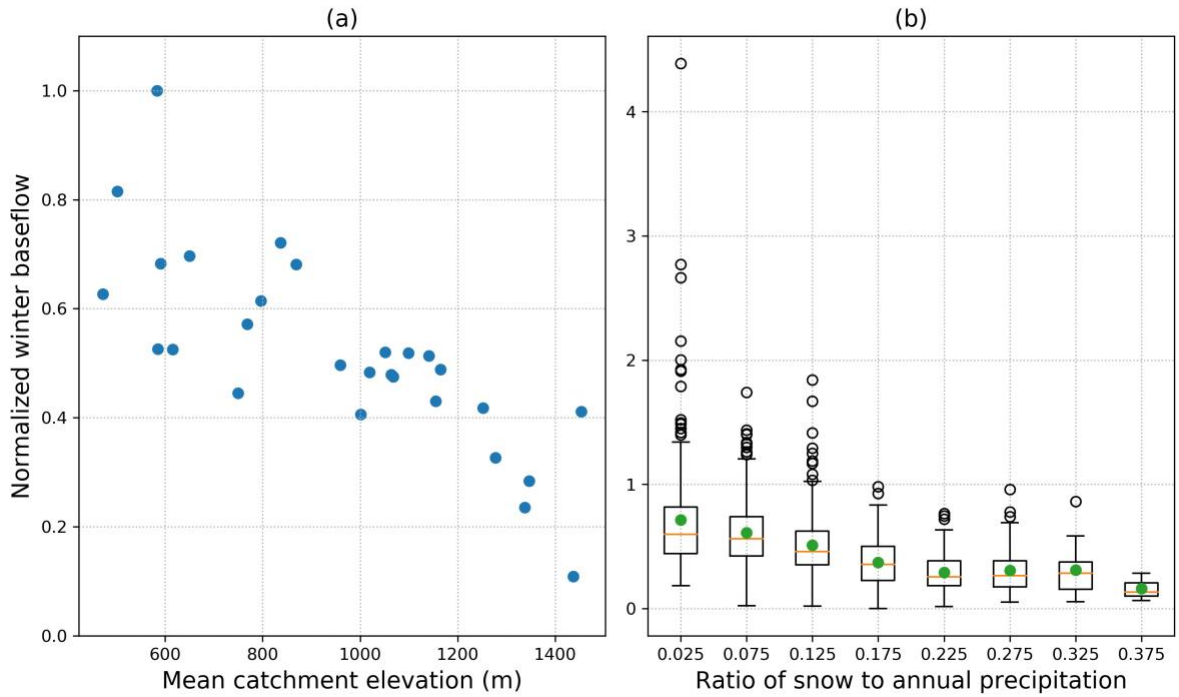

Figure 4.3. Maximum winter (December – February) baseflow normalized by average daily winter precipitation plotted against (a) mean catchment elevation and (b) annual snowfall ratio for all ephemeral snow catchments (mean elevation < 1500 m a.s.l.). In boxplot (b), data for all the 39 catchments are combined together and binned in 0.05 increments of the annual snow fraction. The boxplot spans from 25th to 75th percentile value, and the whiskers extends up to 1.5 times of the interquartile range. The orange line shows the median value and the green dot shows the mean value in the given bin range. The y-axis scales are different for the two subplots.

In contrast, the intensity of cold season PEQ events is parabolic and increases with elevation up to the ephemeral snow elevation threshold (~1500 m a.s.l.) before abruptly decreasing again under seasonal snow conditions (Figure 4.4c). Within the ephemeral snow range, this increase in PEQ intensity with elevation reflects the increase in accumulated snow depths available for melt. Thus, it appears that decreasing equivalent precipitation intensity (Figure 4.4c) plays a critical role in increasing groundwater recharge efficiency (Figure 4.3a). In other words, catchments with more ephemeral snowpacks experience a higher number of liquid water input events during the colder season compared to catchments with seasonal snowpacks. These events are more effective at recharging groundwater because of lower melt rates. In any case, it is clear that during the cold season the product of PEQ frequency

and intensity, which is equivalent to total meltwater, is higher under ephemeral snowpack conditions, implying greater amounts of available meltwater for groundwater recharge. In addition to these dynamics, largely dormant or less active vegetation transpiration during the cold season also facilitates more meltwater travelling beyond the root zone (Jeton et al., 1996) to recharge groundwater storages.

During the warmer season, the number of PEQ events (Figure 4.4b) and their intensity (Figure 4.4d) generally increase with elevation. As a result, for catchments with seasonal snowpack that melt during the warm season, the amount of meltwater available for infiltration into the subsurface also increases with elevation. However, a larger fraction of this infiltration may be partitioned to transpiration rather than groundwater recharge (Tashie et al., 2019), but this depends on how vegetation dynamics change with elevation (Rumpf et al., 2018). A recent analysis suggests higher elevation vegetation in the Swiss Alps are less dependent on cold season snowmelt (Allen et al., 2019), however further work is required to quantitatively link seasonal vegetation and recharge dynamics.

To examine the potential impact of warming temperatures on groundwater recharge, we apply a uniform increase of 2.5 °C to the air temperature time-series in all catchments. This warming scenario increases the elevation transition from ephemeral to seasonal snow conditions from the current ~1500 m a.s.l. threshold to ~2000 m a.s.l. in the future (Figures 4.4a, 4.4c). Interestingly, the number of cold season melt events increase only slightly in ephemeral snowpacks (elevations up to 1500 m a.s.l.), but much more significantly at higher elevations (>1500 m a.s.l.) (Figure 4.4a). Cold season melt intensity decreases slightly with warming at elevations < 1500 m a.s.l., and increases significantly at elevations > 1800 m a.s.l. (Figure 4.4c). In contrast, warming decreases both the frequency and intensity of events for catchments > 1500 m a.s.l. (Figures 4.4b, 4.4d). It is important to note that this analysis does not take into account changes in the magnitude and timing of precipitation that may accompany any increase in air temperature.

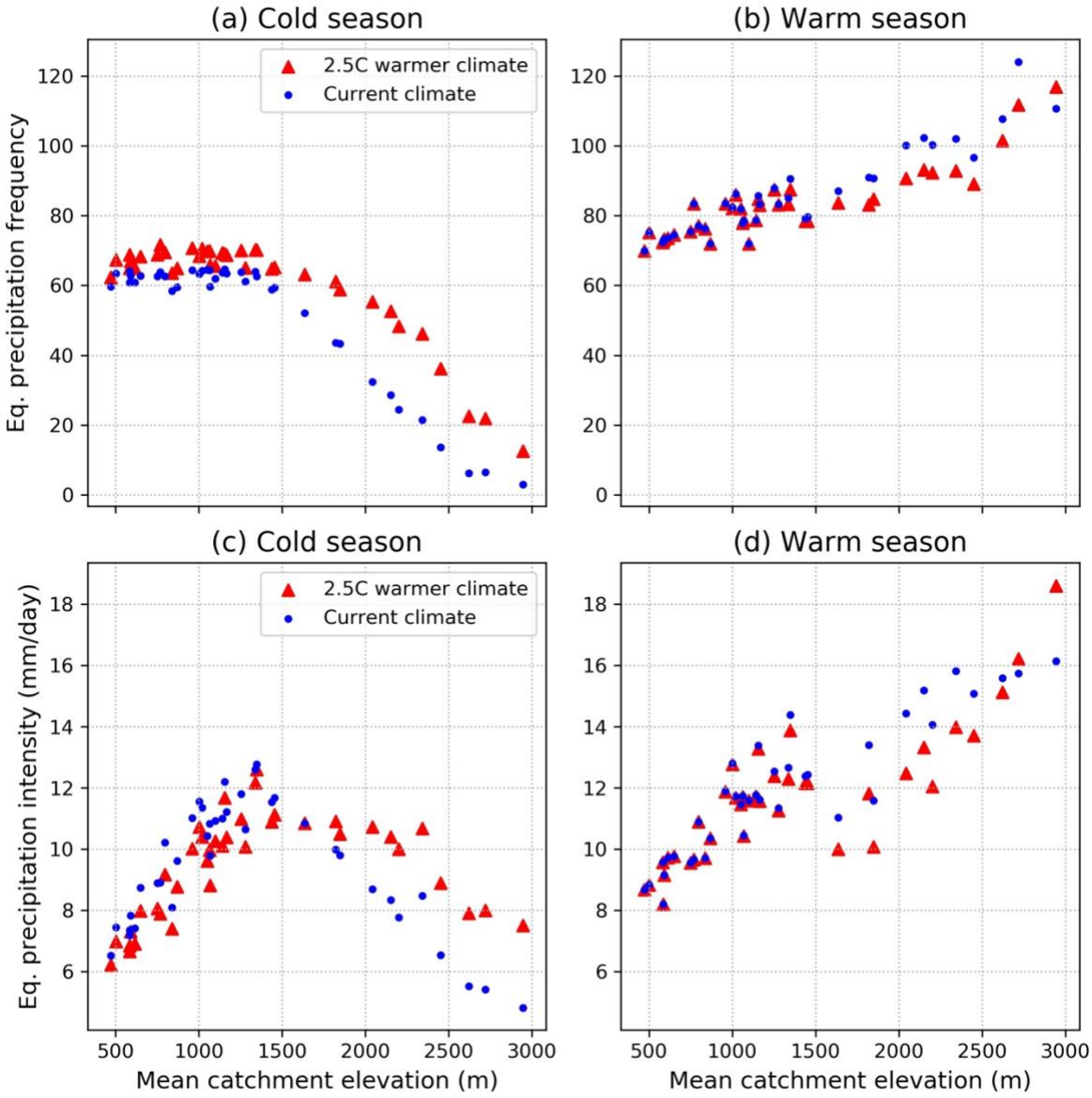

Figure 4.4. (a,b) Frequency and (c,d) average intensity of equivalent precipitation (rainfall + snowmelt) events in (a,c) cold (November - April) and (b,d) warm season (May - October) for the current and a 2.5 °C warmer climate plotted against mean catchment elevation for 39 catchments spread across Switzerland. Average intensity is computed for days when the equivalent precipitation is over a 1 mm/day threshold.

4.3. Discussion

Previous research investigating the interrelation between snowmelt and groundwater recharge have mainly focused on changes in snowmelt rates under climate warming (Barnhart et al., 2016), thereby neglecting potential changes in snowmelt frequency and snowpack

regime, i.e. a transition from seasonal to ephemeral snowpacks. Understanding this transition is, however, key to anticipating future groundwater recharge dynamics in snow-influenced environments because meltwater sourced from ephemeral snowpacks is far more efficient in recharging groundwater than when sourced from a seasonal snowpack (Figure 4.2). Additionally, increasingly ephemeral snowpack conditions, typically characterized by lower melt intensities, further enhance groundwater recharge (Figures 4.3, 4.4c). This suggests that for soils with sufficient antecedent water content, which is the case during the cold season in temperate mountain environments like the Swiss Alps, more diffuse and low intensity melt provides greater opportunity for meltwater to percolate into the subsoil and recharge groundwater, a process which has also been indirectly implicated in the Southwest US (Earman et al., 2006) and more recently in two Russian river basins (Makarieva et al., 2019).

Although vegetation dynamics are also an important determinant of groundwater recharge (Carroll et al., 2019; Tashie et al., 2019), these have not been considered in this study. This is because ephemeral snowpacks mostly melt during winters, when catchment vegetation has little transpiration activity, especially at higher elevations where vegetation density is already quite low. It can therefore be assumed that a larger fraction of infiltrating meltwater can travel beyond the root zone, increasing the effectiveness of this cold season groundwater recharge. Furthermore, with a warming of 2.5 °C we anticipate ephemeral snowpacks to expand from the current elevation limit of ~1500 m a.s.l. to ~2000 m a.s.l. in the Swiss Alps (Figures 4.4a, 4.4c), which will incorporate catchments with large areas of lower density (or absent) vegetation, further increasing groundwater recharge effectiveness of melt from ephemeral snowpacks at these elevations.

The likely impact of warming on the seasonal distribution of meltwater and the subsequent impact on water resources in mountain environments is largely unknown. We speculate that an increasing shift to melt supplied from ephemeral snowpacks during the winter months under a warmer climate will mean an overall increase in the magnitude of groundwater recharge in catchments that are currently at the boundary of ephemeral and seasonal snow regimes. In our analysis of the Swiss Alps, the current boundary of ~1500 m a.s.l. can expand up to ~2000 m a.s.l. with a 2.5 °C increase in air temperature (Figure 4.5). The exact magnitude of the resulting increase in groundwater recharge is difficult to estimate and lies beyond the

scope of this study. However, it is useful to investigate the implications of such a shift in the seasonal transfer of water assuming the annual water balance remains similar in the future, with the caveat that some long term changes in the overall water balance are possible as rain increases at the expense of snow (Berghuijs et al., 2014).

Looking at the long-term average seasonal low flow water supply relationships for the Swiss Alps, we find that higher winter baseflow (December – February) is generally associated with lower summer baseflow (Appendix Figure 4.S1), but interestingly there is no relationship with spring baseflow (Appendix Figure 4.S1). Thus, as higher elevation catchments transition from a seasonal to an ephemeral snow regime, it is reasonable to expect that increased winter baseflow will translate into decreased summer baseflow (Jenicek et al., 2016, 2018). This potential transition to higher winter baseflow at the expense of lower summer flows has important implications for water resources and ecosystems. Lower summer flows reduces the amount of hydropower production (Schaefli, 2015). For aquatic ecosystems, the net primary productivity may decline as a greater proportion of low flows will be supplied under colder conditions when metabolic activity is much lower. In addition, diminished summer low flows in the same catchments will limit aquatic habitat availability when productivity is higher (Ulseth et al., 2018).

This work highlights that the future of ephemeral snowpacks require greater research attention, as their changing regional distribution will have important consequences for water resources availability in mountain environments. Although many existing studies have examined the links between snow and groundwater recharge with a strong focus on seasonal snow cover, a more detailed understanding of regional-scale effects of a warming climate on snow and water resources calls for an analysis of the full range of snow cover regimes (Clark et al., 2011; Trujillo and Molotch, 2014). Our work shows that changes in these snow cover regimes can shift the partitioning of catchment water balances, which will be of wider concern for future water and ecosystem protection measures in snow influenced regions globally.

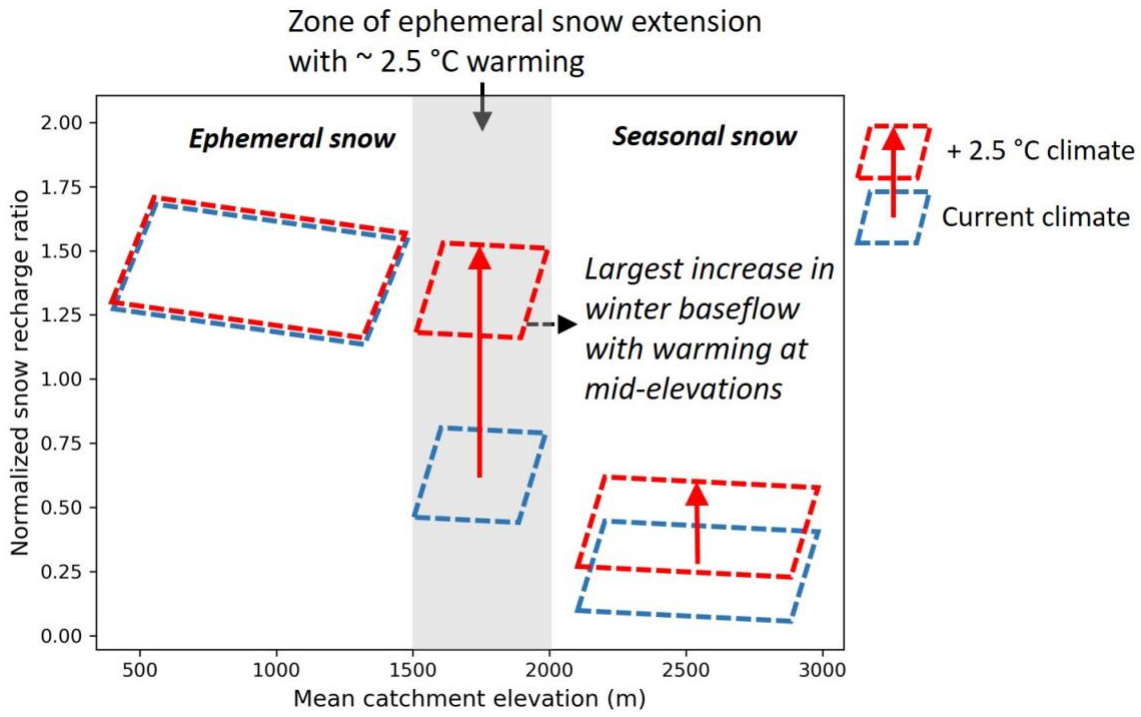

Figure 4.5. Re-conceptualization of Figure 4.2b demonstrates the proposed increase in the fraction of cold season groundwater recharge and low flow water supply, especially for mid-elevation mountainous catchments under a warming climate due to the expansion of ephemeral snow conditions.

4.4. Methods

Data. Isotope ratios in precipitation and groundwater in Switzerland were obtained from the Global Network for Isotopes in Precipitation (GNIP) maintained by the International Atomic Energy Agency (IAEA), and from the Swiss National Network on Groundwater (NAQUA) maintained by the Swiss Federal Office for the Environment (FOEN). IAEA under the GNIP program collects monthly composite precipitation samples at 19 stations in Switzerland and analyzes the isotopic composition of hydrogen (δ^2H) and oxygen ($\delta^{18}O$), with the samples dating from 1966 to present. This data contains precipitation phase labels (e.g.: rain, snow, mixed, etc.), which are however not used here since close to 50% of the samples have no label. FOEN under the TREND module of NAQUA collected monthly groundwater isotopes at 50 sites during 2007 - 2013. For the present study, seven of these sites were found to be within headwater catchments and therefore appropriate for our analysis.

Due to the limited data availability from mountain catchments, we also included an additional data point from a high elevation alpine catchment (Vallon de Nant, mean catchment elevation 2000 m a.sl.), located in the Vaud Alps in South-west of Switzerland (Figure 4.1) (Ceperley et al., 2018; Michelon, 2017). Isotope ratios in rain, snowpack and groundwater were sampled across an elevation gradient from February 2016 to September 2017 (Michelon et al., 2020b).

Daily gridded precipitation and temperature data (resolution 1 km x 1 km) were obtained from the Swiss Federal Office of Meteorology and Climatology (MeteoSwiss) (MeteoSwiss, 2016, 2017). Daily streamflow data was also obtained for 39 Swiss catchments with undisturbed streamflow from the FOEN, with catchment areas ranging from 1 to 378 km^2 (FOEN, 2012), and mean elevation ranging from 500 to 3000 m a.s.l. We used the common time period 1961 – 2015 for the analysis. The mean annual precipitation computed from the gridded meteorological data varies from 850 to 2700 mm/year. Applying an air temperature threshold approach (see section on *Snow model* below), snowfall is estimated to vary from 3% to 73% of the annual precipitation.

Mixing model. The Bayesian mixing model HydroMix (Beria et al., 2020) is used to estimate the 'cold season recharge ratio' using stable water isotopes. Cold season recharge ratio is defined as the fraction of groundwater recharged from precipitation originating during the cold season (November – April), normalized by the proportion of annual precipitation that falls as snow. For the characterization of the two sources for the mixing model (i.e. snowfall and rainfall), only monthly isotopic ratios are available from the GNIP database, and accordingly, precipitation phase attribution is approximate. Here, precipitation isotopes collected during the warmer months (May to October) are treated as rain samples, while the remainder are considered cold season samples that have varying degrees of snow influence. Similar representations of recharge seasonality have been used by previous isotopic studies (Beria et al., 2018; Jasechko et al., 2014, 2017; Simpson et al., 1970; Winograd et al., 1998).

Baseflow extraction. Baseflow is considered as the minimum observed daily streamflow over a 20-day moving window, which is the equivalent of a low pass filter (Spongberg, 2000). The resulting baseflow time series is further summarized in terms of the maximum baseflow per

season and per year. The obtained maximum baseflow value per season provides a measure for the responsiveness of groundwater storage to all liquid inputs (rain and snowmelt) during that season and is assumed to be a proxy for groundwater recharge. The extracted maximum seasonal baseflow values are furthermore normalized by total season precipitation to make the values comparable across catchments.

Snow model. Catchment-average snowfall is estimated from area-averaged precipitation and air temperature time series by applying a linear transition from 100% snowfall at temperatures below -1 °C to 100% rainfall at temperatures above 1 °C (Jennings and Molotch, 2019). To obtain estimates of snowmelt, a simple snowpack evolution model is used. The snow water equivalent (SWE) of the snowpack (h_s) is computed as:

$$\frac{dh_s(t)}{dt} = P_s(t) - M_s(t), \qquad 4.1$$

where P_s [mm d^{-1}] is snowfall at time step t (daily time step) and M_s [mm d^{-1}] is snowmelt, which is computed using a degree-day approach (Hock, 2003):

$$M_s(t) = \begin{cases} a_s(T(t) - T_m), & \text{if } T(t) > T_m \\ 0 & \text{otherwise} \end{cases}, \qquad 4.2$$

where a_s [mm °C^{-1}d^{-1}] is the degree-day factor and T_m is the snowmelt temperature threshold (set to 0 °C). The total liquid water input to the subsurface resulting from melt and rainfall is termed as equivalent precipitation (PEQ). Such a simple degree-day melt estimation method has been shown to be very effective at capturing melt rates in temperate climates (Ohmura, 2001). In hydrological applications, degree-day factors are usually calibrated on observed streamflow (Schaefli et al., 2014); here we set a_s =2.5 [mm °C^{-1}d^{-1}] for the sake of simplicity, a value that is commonly obtained for snow dominated catchments.

To analyze snow melt effects on groundwater recharge, we consider the stochastic streamflow modelling framework developed by Botter et al., (2007). In this framework streamflow is considered to be the result of censored stochastic rainfall inputs, where average streamflow is the product of average rainfall on rainy days and the frequency of streamflow

generating events (Santos et al., 2018; Schaefli et al., 2013). In the context of the present study, the input process of interest is PEQ. For the estimation of PEQ frequency and intensity, we consider only days with PEQ > 1 mm.

4.5. Appendix

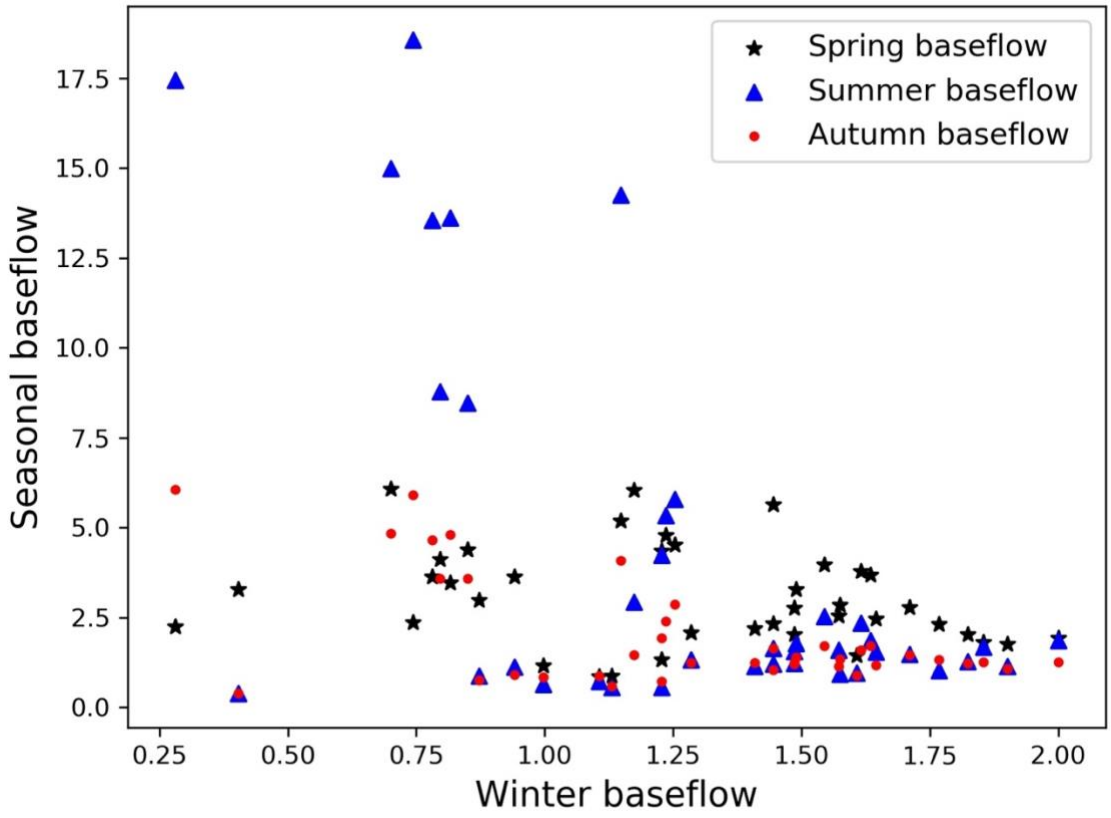

Figure 4.S1. Winter baseflow plotted against spring, summer and autumn baseflows for all the 39 catchments spread across Switzerland.

Author contributions: The paper was written by HB with contributions from all co-authors. HB and BS formulated the hypothesis of this study with substantial inputs from JRL. Data related to Vallon de Nant were collected and archived by AM and NCC who also provided critical feedback during the data analysis and writing phase of this study.

Concluding remarks

The key objective of this project was to use naturally occurring environmental tracers such as stable water isotopes, along with other hydrometeorological variables to improve the understanding of snow hydrological processes in the Swiss Alps. In order to achieve this, I first did a comprehensive review on how stable water isotopes have been used in snow hydrology within existing literature, described in the first chapter. This review provides insights into how different snow hydrologic processes modify the isotopic ratio of precipitation, and revealed that stable water isotopes can be used to trace the journey of a snow particle along its entire hydrologic life cycle. These insights led to the development of a novel mixing modeling framework, described in the second chapter, where hydrologic metrics, such as the proportion of streamflow derived from snowmelt, can be estimated using stable water isotopes. The mixing model was shown to be robust in different hydrological scenarios, while also addressing common field limitations such as that of small samples sizes.

Such mixing models and other hydrograph separation methods have been previously used to estimate a number of hydrologically relevant metrics such as pre-event water fraction, proportion of snow recharging groundwater, etc. However, these metrics have not been used within a hydrological model. Consequently, in the third chapter, a novel hydrologic modeling framework was developed where metrics such as pre-event water fraction are directly used to calibrate rainfall-runoff model, along with streamflow. Incorporating stable water isotopes within the model domain significantly improves the representation of dominant hydrologic processes occurring in mountainous landscapes, allowing for more reliable hydrological predictions.

In the final chapter, I develop a new modeling framework to show that climate change may increase groundwater recharge in the Swiss Alps, especially in regions where the nature of snowpack is intermittent or is likely to become more intermittent in the future because of a warming climate. This finding is based on two distinct datasets (streamflow and stable water isotopes) collected over different parts of Switzerland, and is explained using a novel

analytical framework that quantifies groundwater recharge as a function of frequency and intensity of rainfall and snowmelt.

I now summarize the main questions posed in this thesis along with a short answer for each of them.

Summary

Obj. 1: To identify ways in which stable water isotopes have been used in snow hydrology

Stable water isotopes have mainly been used to better characterize different snow hydrologic processes such as metamorphism, sublimation, interception, and melt; and how these processes modify the isotopic composition of snowpack and snowmelt. Snow metamorphism homogenizes snowpack isotopic composition, reducing the variability in isotopic composition from the onset of snowfall to the final snowmelt. Also, snowmelt during the early melt season is more depleted in heavier isotopes which in due course of the melt season, becomes more enriched. Snow sublimation enriches the isotopic composition of the residual snowpack in heavier isotopes, having a similar effect as evaporation. Also, the fact that there is a general seasonality trend in precipitation isotope ratio can be leveraged to examine seasonal dependence of stream runoff or groundwater recharge.

Obj. 2: Develop a mixing model that works with the common limitations in isotope hydrology

A Bayesian mixing model was developed which gives reliable results for mixing applications with small sample sizes (<20-30 samples), which is especially useful in data scarce environments. The mixing model was rigorously tested with a number of synthetic and real case studies. Composite likelihood functions were introduced that allow weighting samples by their relative amounts and address a very important and often overlooked bias which arises due to unweighted mixing. Finally, due to the flexible modeling framework, additional model parameters that account for source modification processes (such as sublimation, interception, etc.) can be easily incorporated in this model.

Obj. 3: Develop a novel approach of integrating stable water isotopes within continuous hydrological model

A novel coupling framework was developed where pre-event water fraction estimates derived from the Bayesian mixing model (described in Chapter 2) are directly used to calibrate a semi-distributed conceptual rainfall-runoff model. The model was rigorously tested over two summers at Vallon de Nant catchment. This unique modeling approach allows to explicitly parameterize celerity and velocity behavior of a catchment.

Obj. 4: To quantify the impact of climate change on groundwater recharge in the Swiss Alps

The role of snow cover ephemerality (or intermittency) on groundwater recharge was explored within the Swiss Alps. Using a combination of different data sources (isotopic and streamflow) spread across the Swiss Alps, it was found that climate change will lead to increase in groundwater recharge. The increase in groundwater recharge might lead to lower summer flows in river networks, which will then decrease the net ecosystem productivity and reduce the habitat availability for the marine ecosystem.

Potential topics for future research

Most of this work relied on stable isotope ratio of $^{18}O/^{16}O$ and $^{2}H/^{1}H$ in water. With recent technological advancements, $^{17}O/^{16}O$ measurements have also become more widely available. However, $^{17}O/^{16}O$ has not been used in isotope hydrology. $^{17}O/^{16}O$ is known to be relatively insensitive to temperature, but sensitive to humidity (Angert et al., 2004; Berman et al., 2013), which means O17-excess can be used with d-excess to constrain kinetic processes like evaporation and sublimation. This hypothesis should be tested in future research, to see if $^{17}O/^{16}O$ can be used to better constrain sublimation or evaporation processes.

One of the key novelties of this work is the conceptualization of a piston-flow parameter that constrains both the celerity and velocity behavior of catchments, and promises to be a potential catchment hydrologic signature. Future research should test this hypothesis over a larger number of catchments, and link the piston flow parameter with geomorphological attributes of a catchment.

Another major finding of this thesis is the impact that ephemeral snowpacks have on groundwater recharge dynamics in the Swiss Alps. The regional footprint of such ephemeral snowpacks is projected to increase globally because of higher winter air temperatures in a warmer climate (Petersky and Harpold, 2018). Consequently, future work should explore the impact of this change on groundwater recharge in other parts of the world.

References

Adam, J. C., Hamlet, A. F. and Lettenmaier, D. P.: Implications of global climate change for snowmelt hydrology in the twenty-first century, Hydrol. Process., 23(7), 962–972, doi:10.1002/hyp.7201, 2009.

Addor, N., Nearing, G., Prieto, C., Newman, A. J., Le Vine, N. and Clark, M. P.: A Ranking of Hydrological Signatures Based on Their Predictability in Space, Water Resour. Res., 54(11), 8792–8812, doi:10.1029/2018WR022606, 2018.

Akers, P. D., Welker, J. M. and Brook, G. A.: Reassessing the role of temperature in precipitation oxygen isotopes across the eastern and central United States through weekly precipitation-day data, Water Resour. Res., 53(9), 7644–7661, doi:10.1002/2017WR020569, 2017.

Ala-aho, P., Tetzlaff, D., McNamara, J. P., Laudon, H., Kormos, P. and Soulsby, C.: Modeling the isotopic evolution of snowpack and snowmelt: Testing a spatially distributed parsimonious approach, Water Resour. Res., 53(7), 5813–5830, doi:10.1002/2017WR020650, 2017.

Allen, S. T., Keim, R. F., Barnard, H. R., McDonnell, J. J. and Renée Brooks, J.: The role of stable isotopes in understanding rainfall interception processes: a review, Wiley Interdiscip. Rev. Water, 4(1), e1187, doi:10.1002/wat2.1187, 2016.

Allen, S. T., Kirchner, J. W. and Goldsmith, G. R.: Predicting spatial patterns in precipitation isotope (δ2H and δ18O) seasonality using sinusoidal isoscapes, Geophys. Res. Lett., 45(10), 4859–4868, doi:10.1029/2018GL077458, 2018.

Allen, S. T., Kirchner, J. W., Braun, S., Siegwolf, R. T. W. and Goldsmith, G. R.: Seasonal origins of soil water used by trees, Hydrol. Earth Syst. Sci., 23(2), 1199–1210, doi:10.5194/hess-23-1199-2019, 2019.

Ammann, L., Fenicia, F. and Reichert, P.: A likelihood framework for deterministic hydrological models and the importance of non-stationary autocorrelation, Hydrol. Earth Syst. Sci., 23(4), 2147–2172, doi:10.5194/hess-23-2147-2019, 2019.

Angert, A., Cappa, C. D. and DePaolo, D. J.: Kinetic 17O effects in the hydrologic cycle: Indirect evidence and implications1 1Associate editor: J. Horita, Geochim. Cosmochim. Acta, 68(17), 3487–3495, doi:10.1016/j.gca.2004.02.010, 2004.

Ayala, A., Pellicciotti, F., MacDonell, S., McPhee, J. and Burlando, P.: Patterns of glacier ablation across North-Central Chile: Identifying the limits of empirical melt models under sublimation-favorable conditions, Water Resour. Res., 53(7), 5601–5625, doi:10.1002/2016WR020126, 2017.

Bai, P., Liu, X. and Liu, C.: Improving hydrological simulations by incorporating GRACE data for model calibration, J. Hydrol., 557, 291–304, doi:10.1016/j.jhydrol.2017.12.025, 2018.

Barbeta, A. and Peñuelas, J.: Relative contribution of groundwater to plant transpiration estimated with stable isotopes, Sci. Rep., 7(1), 10580, doi:10.1038/s41598-017-09643-x, 2017.

Barnett, T. P., Adam, J. C. and Lettenmaier, D. P.: Potential impacts of a warming climate on water availability in snow-dominated regions, Nature, 438(7066), 303–309 [online] Available from: http://dx.doi.org/10.1038/nature04141, 2005.

Barnhart, T. B., Molotch, N. P., Livneh, B., Harpold, A. A., Knowles, J. F. and Schneider, D.: Snowmelt rate dictates streamflow, Geophys. Res. Lett., 43(15), 8006–8016, doi:10.1002/2016GL069690, 2016.

Benettin, P., Rinaldo, A. and Botter, G.: Tracking residence times in hydrological systems: forward and backward formulations, Hydrol. Process., 29(25), 5203–5213, doi:10.1002/hyp.10513, 2015.

Benettin, P., Soulsby, C., Birkel, C., Tetzlaff, D., Botter, G. and Rinaldo, A.: Using SAS functions and high-resolution isotope data to unravel travel time distributions in headwater catchments, Water Resour. Res., 53(3), 1864–1878, doi:10.1002/2016WR020117, 2017a.

Benettin, P., Bailey, S. W., Rinaldo, A., Likens, G. E., McGuire, K. J. and Botter, G.: Young runoff fractions control streamwater age and solute concentration dynamics, Hydrol. Process., 31(16), 2982–2986, doi:10.1002/hyp.11243, 2017b.

Beniston, M., Farinotti, D., Stoffel, M., Andreassen, L. M., Coppola, E., Eckert, N., Fantini, A., Giacona, F., Hauck, C., Huss, M., Huwald, H., Lehning, M., López-Moreno, J.-I., Magnusson, J., Marty, C., Moran-Tejéda, E., Morin, S., Naaim, M., Provenzale, A., Rabatel, A., Six, D., Stötter, J., Strasser, U., Terzago, S. and Vincent, C.: The European mountain cryosphere: A review of past, current and future issues, Cryosph. Discuss., 2017, 1–60, doi:10.5194/tc-2016-290, 2017.

Berghuijs, W. R., Woods, R. A. and Hrachowitz, M.: A precipitation shift from snow towards rain leads to a decrease in streamflow, Nat. Clim. Chang., 4(7), 583–586,

doi:10.1038/nclimate2246, 2014.

Beria, H., Larsen, J. R., Ceperley, N. C., Michelon, A., Vennemann, T. and Schaefli, B.: Understanding snow hydrological processes through the lens of stable water isotopes, Wiley Interdiscip. Rev. Water, 5(6), e1311, doi:10.1002/wat2.1311, 2018.

Beria, H., Larsen, J. R., Michelon, A., Ceperley, N. C. and Schaefli, B.: Data for the manuscript "HydroMix v1.0: a new Bayesian mixing framework for attributing uncertain hydrological sources," , doi:10.5281/ZENODO.3475429, 2019.

Beria, H., Larsen, J. R., Michelon, A., Ceperley, N. C. and Schaefli, B.: HydroMix v1.0: a new Bayesian mixing framework for attributing uncertain hydrological sources, Geosci. Model Dev., 13(5), 2433–2450, doi:10.5194/gmd-13-2433-2020, 2020.

Berman, E. S. F., Levin, N. E., Landais, A., Li, S. and Owano, T.: Measurement of δ18O, δ17O, and 17O-excess in Water by Off-Axis Integrated Cavity Output Spectroscopy and Isotope Ratio Mass Spectrometry, Anal. Chem., 85(21), 10392–10398, doi:10.1021/ac402366t, 2013.

Bershaw, J., Penny, S. M. and Garzione, C. N.: Stable isotopes of modern water across the Himalaya and eastern Tibetan Plateau: Implications for estimates of paleoelevation and paleoclimate, J. Geophys. Res. Atmos., 117(D2), doi:10.1029/2011JD016132, 2012.

Beven, K. and Freer, J.: Equifinality, data assimilation, and uncertainty estimation in mechanistic modelling of complex environmental systems using the GLUE methodology, J. Hydrol., 249(1–4), 11–29, doi:10.1016/S0022-1694(01)00421-8, 2001.

Beven, K. J.: Rainfall-runoff modelling: the primer, Second Edi., John Wiley & Sons., 2011.

Biederman, J. A., Harpold, A. A., Gochis, D. J., Ewers, B. E., Reed, D. E., Papuga, S. A. and Brooks, P. D.: Increased evaporation following widespread tree mortality limits streamflow response, Water Resour. Res., 50(7), 5395–5409, doi:10.1002/2013WR014994, 2014a.

Biederman, J. A., Brooks, P. D., Harpold, A. A., Gochis, D. J., Gutmann, E., Reed, D. E., Pendall, E. and Ewers, B. E.: Multiscale observations of snow accumulation and peak snowpack following widespread, insect-induced lodgepole pine mortality, Ecohydrology, 7(1), 150–162, doi:10.1002/eco.1342, 2014b.

Birkel, C. and Soulsby, C.: Advancing tracer-aided rainfall-runoff modelling: A review of progress, problems and unrealised potential, Hydrol. Process., 29(25), 5227–5240, doi:10.1002/hyp.10594, 2015.

Birkel, C., Duvert, C., Correa, A., Munksgaard, N. C., Maher, D. T. and Hutley, L. B.: Tracer-Aided Modeling in the Low-Relief, Wet-Dry Tropics Suggests Water Ages and DOC Export Are Driven by Seasonal Wetlands and Deep Groundwater, Water Resour. Res., 56(4), e2019WR026175, doi:10.1029/2019WR026175, 2020.

Blake, W. H., Boeckx, P., Stock, B. C., Smith, H. G., Bodé, S., Upadhayay, H. R., Gaspar, L., Goddard, R., Lennard, A. T., Lizaga, I., Lobb, D. A., Owens, P. N., Petticrew, E. L., Kuzyk, Z. Z. A., Gari, B. D., Munishi, L., Mtei, K., Nebiyu, A., Mabit, L., Navas, A. and Semmens, B. X.: A deconvolutional Bayesian mixing model approach for river basin sediment source apportionment, Sci. Rep., 8(1), 13073, doi:10.1038/s41598-018-30905-9, 2018.

Blöschl, G., Hall, J., Parajka, J., Perdigão, R. A. P., Merz, B., Arheimer, B., Aronica, G. T., Bilibashi, A., Bonacci, O., Borga, M., Čanjevac, I., Castellarin, A., Chirico, G. B., Claps, P., Fiala, K., Frolova, N., Gorbachova, L., Gül, A., Hannaford, J., Harrigan, S., Kireeva, M., Kiss, A., Kjeldsen, T. R., Kohnová, S., Koskela, J. J., Ledvinka, O., Macdonald, N., Mavrova-Guirguinova, M., Mediero, L., Merz, R., Molnar, P., Montanari, A., Murphy, C., Osuch, M., Ovcharuk, V., Radevski, I., Rogger, M., Salinas, J. L., Sauquet, E., Šraj, M., Szolgay, J., Viglione, A., Volpi, E., Wilson, D., Zaimi, K. and Živković, N.: Changing climate shifts timing of European floods, Science (80-.)., 357(6351), 588–590, doi:10.1126/science.aan2506, 2017.

Bokhorst, S., Pedersen, S. H., Brucker, L., Anisimov, O., Bjerke, J. W., Brown, R. D., Ehrich, D., Essery, R. L. H., Heilig, A., Ingvander, S., Johansson, C., Johansson, M., Jónsdóttir, I. S., Inga, N., Luojus, K., Macelloni, G., Mariash, H., McLennan, D., Rosqvist, G. N., Sato, A., Savela, H., Schneebeli, M., Sokolov, A., Sokratov, S. A., Terzago, S., Vikhamar-Schuler, D., Williamson, S., Qiu, Y. and Callaghan, T. V: Changing Arctic snow cover: A review of recent developments and assessment of future needs for observations, modelling, and impacts, Ambio, 45(5), 516–537, doi:10.1007/s13280-016-0770-0, 2016.

Botter, G., Porporato, A., Rodriguez-Iturbe, I. and Rinaldo, A.: Basin-scale soil moisture dynamics and the probabilistic characterization of carrier hydrologic flows: Slow, leaching-prone components of the hydrologic response, Water Resour. Res., 43(2), doi:10.1029/2006WR005043, 2007.

Botter, G., Bertuzzo, E. and Rinaldo, A.: Catchment residence and travel time distributions: The master equation, Geophys. Res. Lett., 38(11), doi:10.1029/2011GL047666, 2011.

Boughton, W. C.: A review of the USDA SCS curve number method, Soil Res., 27(3), 511–523

[online] Available from: https://doi.org/10.1071/SR9890511, 1989.

Bowen, G. J. and Good, S. P.: Incorporating water isoscapes in hydrological and water resource investigations, Wiley Interdiscip. Rev. Water, 2(2), 107–119, doi:10.1002/wat2.1069, 2015.

Branger, F. and McMillan, H. K.: Deriving hydrological signatures from soil moisture data, Hydrol. Process., 34(6), 1410–1427, doi:10.1002/hyp.13645, 2020.

Brodzik, M. J. and Armstrong, R.: Northern Hemisphere EASE-Grid 2.0 Weekly Snow Cover and Sea Ice Extent, Version 4, NASA Natl. Snow Ice Data Cent. Distrib. Act. Arch. Cent., doi:10.5067/P7O0HGJLYUQU, 2017.

Brown, R. D. and Mote, P. W.: The Response of Northern Hemisphere Snow Cover to a Changing Climate, J. Clim., 22(8), 2124–2145, doi:10.1175/2008JCLI2665.1, 2009.

Brunengo, M. J.: A method of modeling the frequency characteristics of daily snow amount for stochastic simulation of rain-on-snowmelt events, in Proceedings of the Western Snow Conference, pp. 110–121, Western Snow Conference, Sacramento, California., 1990.

Brunner, M. I., Sikorska, A. E. and Seibert, J.: Bivariate analysis of floods in climate impact assessments, Sci. Total Environ., 616–617, 1392–1403, doi:10.1016/j.scitotenv.2017.10.176, 2018.

Burns, D. A. and McDonnell, J. J.: Effects of a beaver pond on runoff processes: comparison of two headwater catchments, J. Hydrol., 205(3), 248–264, doi:10.1016/S0022-1694(98)00081-X, 1998.

Burns, D. A., McDonnell, J. J., Hooper, R. P., Peters, N. E., Freer, J. E., Kendall, C. and Beven, K.: Quantifying contributions to storm runoff through end-member mixing analysis and hydrologic measurements at the Panola Mountain Research Watershed (Georgia, USA), Hydrol. Process., 15(10), 1903–1924, doi:10.1002/hyp.246, 2001.

Buttle, J. M., Vonk, A. M. and Taylor, C. H.: Applicability of isotopic hydrograph separation in a suburban basin during snowmelt, Hydrol. Process., 9(2), 197–211, doi:10.1002/hyp.3360090206, 1995.

Campbell, D. R.: Early snowmelt projected to cause population decline in a subalpine plant, Proc. Natl. Acad. Sci., 116(26), 12901 LP – 12906, doi:10.1073/pnas.1820096116, 2019.

Capell, R., Tetzlaff, D. and Soulsby, C.: Can time domain and source area tracers reduce uncertainty in rainfall-runoff models in larger heterogeneous catchments?, Water

Resour. Res., 48(9), doi:10.1029/2011WR011543, 2012.

Carpenter, B., Gelman, A., Hoffman, M. D., Lee, D., Goodrich, B., Betancourt, M., Brubaker, M. A., Guo, J., Li, P. and Riddell, A.: Stan : A Probabilistic Programming Language, J. Stat. Softw., 76(1), doi:10.18637/jss.v076.i01, 2017.

Carroll, R. W. H., Deems, J. S., Niswonger, R., Schumer, R. and Williams, K. H.: The Importance of Interflow to Groundwater Recharge in a Snowmelt-Dominated Headwater Basin, Geophys. Res. Lett., 46(11), 5899–5908, doi:10.1029/2019GL082447, 2019.

Casson, N. J., Eimers, M. C. and Watmough, S. A.: Sources of nitrate export during rain-on-snow events at forested catchments, Biogeochemistry, 120(1), 23–36, doi:10.1007/s10533-013-9850-4, 2014.

Cayuela, C., Latron, J., Geris, J. and Llorens, P.: Spatio-temporal variability of the isotopic input signal in a partly forested catchment: Implications for hydrograph separation, Hydrol. Process., 33(1), 36–46, doi:10.1002/hyp.13309, 2019.

Ceballos, G., Ehrlich, P. R. and Dirzo, R.: Biological annihilation via the ongoing sixth mass extinction signaled by vertebrate population losses and declines, Proc. Natl. Acad. Sci., 114(30), E6089 LP-E6096, doi:10.1073/pnas.1704949114, 2017.

Ceperley, N., Michelon, A., Escoffier, N., Mayoraz, G., Boix Canadell, M., Horgby, A., Hammer, F., Antoniazza, G., Schaefli, B., Lane, S., Rickenmann, D. and Boss, S.: Salt gauging and stage-discharge curve, Avançon de Nant, outlet Vallon de Nant catchment, data set accessible at https://zenodo.org/record/1154798#.Wm7pvjQiG1s, , doi:10.5281/zenodo.1154798, 2018.

Cervi, F., Corsini, A., Doveri, M., Mussi, M., Ronchetti, F. and Tazioli, A.: Characterizing the Recharge of Fractured Aquifers: A Case Study in a Flysch Rock Mass of the Northern Apennines (Italy), in Engineering Geology for Society and Territory, vol. 3, edited by G. Lollino, M. Arattano, M. Rinaldi, O. Giustolisi, J.-C. Marechal, and G. E. Grant, pp. 563–567, Springer International Publishing, Cham., 2015.

Chen, X., Liang, S., Cao, Y., He, T. and Wang, D.: Observed contrast changes in snow cover phenology in northern middle and high latitudes from 2001–2014, , 5, 16820 [online] Available from: http://dx.doi.org/10.1038/srep16820, 2015.

Choi, G., Robinson, D. A. and Kang, S.: Changing Northern Hemisphere Snow Seasons, J. Clim., 23(19), 5305–5310, doi:10.1175/2010JCLI3644.1, 2010.

Choularton, T. W. and Perry, S. J.: A model of the orographic enhancement of snowfall by the

seeder-feeder mechanism, Q. J. R. Meteorol. Soc., 112(472), 335–345, doi:10.1002/qj.49711247204, 1986.

Claassen, H. C. and Downey, J. S.: A Model for Deuterium and Oxygen 18 Isotope Changes During Evergreen Interception of Snowfall, Water Resour. Res., 31(3), 601–618, doi:10.1029/94WR01995, 1995.

Clark, I. D. and Fritz, P.: Environmental isotopes in hydrogeology, CRC press., 1997.

Clark, M. P., Hendrikx, J., Slater, A. G., Kavetski, D., Anderson, B., Cullen, N. J., Kerr, T., Örn Hreinsson, E. and Woods, R. A.: Representing spatial variability of snow water equivalent in hydrologic and land-surface models: A review, Water Resour. Res., 47(7), doi:10.1029/2011WR010745, 2011.

Clow, D. W.: Changes in the Timing of Snowmelt and Streamflow in Colorado: A Response to Recent Warming, J. Clim., 23(9), 2293–2306, doi:10.1175/2009jcli2951.1, 2010.

Colbeck, S. C.: Analysis of Hydrologic Response to Rain-on-Snow, DTIC Document., 1975.

Colbeck, S. C.: An overview of seasonal snow metamorphism, Rev. Geophys., 20(1), 45–61, doi:10.1029/RG020i001p00045, 1982.

Comola, F.: Stochastic modeling of snow transport and hydrologic response in alpine terrain, EPFL PP - Lausanne., 2017.

Comola, F., Kok, J. F., Gaume, J., Paterna, E. and Lehning, M.: Fragmentation of wind-blown snow crystals, Geophys. Res. Lett., 44(9), 4195–4203, doi:10.1002/2017GL073039, 2017.

Cooper, L. W.: Chapter 4 - Isotopic Fractionation in Snow Cover A2 - KENDALL, CAROL, in Isotope Tracers in Catchment Hydrology, edited by J. J. B. T.-I. T. in C. H. McDONNELL, pp. 119–136, Elsevier, Amsterdam., 1998.

Craig, H.: Isotopic Variations in Meteoric Waters, Science (80-.)., 133(3465), 1702 LP – 1703 [online] Available from: http://science.sciencemag.org/content/133/3465/1702.abstract, 1961.

Damigos, D., Tentes, G., Balzarini, M., Furlanis, F. and Vianello, A.: Revealing the economic value of managed aquifer recharge: Evidence from a contingent valuation study in Italy, Water Resour. Res., 53(8), 6597–6611, doi:10.1002/2016WR020281, 2017.

Dansgaard, W.: Stable isotopes in precipitation, Tellus, 16(4), 436–468, doi:10.1111/j.2153-3490.1964.tb00181.x, 1964.

Delavau, C. J., Stadnyk, T. and Holmes, T.: Examining the impacts of precipitation isotope input (δ18Oppt) on distributed, tracer-aided hydrological modelling, Hydrol. Earth Syst. Sci.,

21(5), 2595–2614, doi:10.5194/hess-21-2595-2017, 2017.

Dembélé, M., Hrachowitz, M., Savenije, H. H. G., Mariéthoz, G. and Schaefli, B.: Improving the Predictive Skill of a Distributed Hydrological Model by Calibration on Spatial Patterns With Multiple Satellite Data Sets, Water Resour. Res., 56(1), e2019WR026085, doi:10.1029/2019WR026085, 2020.

Dewalle, D. R. and Swistock, B. R.: Differences in oxygen-18 content of throughfall and rainfall in hardwood and coniferous forests, Hydrol. Process., 8(1), 75–82, doi:10.1002/hyp.3360080106, 1994.

Dietermann, N. and Weiler, M.: Spatial distribution of stable water isotopes in alpine snow cover, Hydrol. Earth Syst. Sci., 17(7), 2657–2668, doi:10.5194/hess-17-2657-2013, 2013.

Diggle, P. J. and Ribeiro, P. J.: Bayesian Inference in Gaussian Model-based Geostatistics, Geogr. Environ. Model., 6(2), 129–146, doi:10.1080/1361593022000029467, 2002.

Dingman, S. L.: Physical Hydrology, 2nd ed., Prentice-Hall, New Jersey., 2002.

Dong, C. and Menzel, L.: Recent snow cover changes over central European low mountain ranges, Hydrol. Process., 0(0), doi:10.1002/hyp.13586, 2019.

Dozier, J., Bair, E. H. and Davis, R. E.: Estimating the spatial distribution of snow water equivalent in the world's mountains, Wiley Interdiscip. Rev. Water, 3(3), 461–474, doi:10.1002/wat2.1140, 2016.

Dudley, R. W., Hodgkins, G. A., McHale, M. R., Kolian, M. J. and Renard, B.: Trends in snowmelt-related streamflow timing in the conterminous United States, J. Hydrol., 547, 208–221, doi:10.1016/j.jhydrol.2017.01.051, 2017.

Earman, S., Campbell, A. R., Phillips, F. M. and Newman, B. D.: Isotopic exchange between snow and atmospheric water vapor: Estimation of the snowmelt component of groundwater recharge in the southwestern United States, J. Geophys. Res. Atmos., 111(D9), doi:10.1029/2005JD006470, 2006.

Ehleringer, J. R. and Dawson, T. E.: Water uptake by plants: perspectives from stable isotope composition, Plant. Cell Environ., 15(9), 1073–1082, doi:10.1111/j.1365-3040.1992.tb01657.x, 1992.

Eiriksson, D., Whitson, M., Luce, C. H., Marshall, H. P., Bradford, J., Benner, S. G., Black, T., Hetrick, H. and McNamara, J. P.: An evaluation of the hydrologic relevance of lateral flow in snow at hillslope and catchment scales, Hydrol. Process., 27(5), 640–654, doi:10.1002/hyp.9666, 2013.

Essery, R., Li, L. and Pomeroy, J.: A distributed model of blowing snow over complex terrain, Hydrol. Process., 13(14–15), 2423–2438, doi:10.1002/(SICI)1099-1085(199910)13:14/15<2423::AID-HYP853>3.0.CO;2-U, 1999.

Evans, S. L., Flores, A. N., Heilig, A., Kohn, M. J., Marshall, H.-P. and McNamara, J. P.: Isotopic evidence for lateral flow and diffusive transport, but not sublimation, in a sloped seasonal snowpack, Idaho, USA, Geophys. Res. Lett., 43(7), 3298–3306, doi:10.1002/2015GL067605, 2016.

Evaristo, J., McDonnell, J. J., Scholl, M. A., Bruijnzeel, L. A. and Chun, K. P.: Insights into plant water uptake from xylem-water isotope measurements in two tropical catchments with contrasting moisture conditions, Hydrol. Process., 30(18), 3210–3227, doi:10.1002/hyp.10841, 2016.

Evaristo, J., McDonnell, J. J. and Clemens, J.: Plant source water apportionment using stable isotopes: A comparison of simple linear, two-compartment mixing model approaches, Hydrol. Process., 31(21), 3750–3758, doi:10.1002/hyp.11233, 2017.

Fayad, A., Gascoin, S., Faour, G., López-Moreno, J. I., Drapeau, L., Page, M. Le and Escadafal, R.: Snow hydrology in Mediterranean mountain regions: A review, J. Hydrol., 551, 374–396, doi:10.1016/j.jhydrol.2017.05.063, 2017a.

Fayad, A., Gascoin, S., Faour, G., Fanise, P., Drapeau, L., Somma, J., Fadel, A., Al Bitar, A. and Escadafal, R.: Snow observations in Mount Lebanon (2011–2016), Earth Syst. Sci. Data, 9(2), 573–587, doi:10.5194/essd-9-573-2017, 2017b.

Feng, X., Taylor, S., Renshaw, C. E. and Kirchner, J. W.: Isotopic evolution of snowmelt 1. A physically based one-dimensional model, Water Resour. Res., 38(10), 35–38, doi:10.1029/2001WR000814, 2002.

FOEN: Subdivision de la Suisse en bassins versants, EZGG-CH. Subdivision de la Suisse en bassins versants topographiques, édition 2012, Swiss Federal Office for the Environment, FOEN, Bern., 2012.

Fossheim, M., Primicerio, R., Johannesen, E., Ingvaldsen, R. B., Aschan, M. M. and Dolgov, A. V.: Recent warming leads to a rapid borealization of fish communities in the Arctic, Nat. Clim. Chang., 5(7), 673–677, doi:10.1038/nclimate2647, 2015.

Frei, A., Tedesco, M., Lee, S., Foster, J., Hall, D. K., Kelly, R. and Robinson, D. A.: A review of global satellite-derived snow products, Adv. Sp. Res., 50(8), 1007–1029, doi:10.1016/j.asr.2011.12.021, 2012.

Freudiger, D., Kohn, I., Stahl, K. and Weiler, M.: Large-scale analysis of changing frequencies of rain-on-snow events with flood-generation potential, Hydrol. Earth Syst. Sci., 18(7), 2695–2709, doi:10.5194/hess-18-2695-2014, 2014.

Friedman, I., Redfield, A. C., Schoen, B. and Harris, J.: The variation of the deuterium content of natural waters in the hydrologic cycle, Rev. Geophys., 2(1), 177–224, doi:10.1029/RG002i001p00177, 1964.

Friedman, I., Benson, C. and Gleason, J.: Isotopic changes during snow metamorphism, Stable Isot. Geochemistry A Tribut. to Samuel Epstein, Special Pu, 211–221, 1991.

Friedman, I., Smith, G. I., Gleason, J. D., Warden, A. and Harris, J. M.: Stable isotope composition of waters in southeastern California 1. Modern precipitation, J. Geophys. Res. Atmos., 97(D5), 5795–5812, doi:10.1029/92JD00184, 1992.

Frisbee, M. D., Phillips, F. M., Campbell, A. R. and Hendrickx, J. M. H.: Modified passive capillary samplers for collecting samples of snowmelt infiltration for stable isotope analysis in remote, seasonally inaccessible watersheds 1: laboratory evaluation, Hydrol. Process., 24(7), 825–833, doi:10.1002/hyp.7523, 2010a.

Frisbee, M. D., Phillips, F. M., Campbell, A. R., Hendrickx, J. M. H. and Engle, E. M.: Modified passive capillary samplers for collecting samples of snowmelt infiltration for stable isotope analysis in remote, seasonally inaccessible watersheds 2: field evaluation, Hydrol. Process., 24(7), 834–849, doi:10.1002/hyp.7524, 2010b.

Galewsky, J., Steen-Larsen, H. C., Field, R. D., Worden, J., Risi, C. and Schneider, M.: Stable isotopes in atmospheric water vapor and applications to the hydrologic cycle, Rev. Geophys., 54(4), 809–865, doi:10.1002/2015RG000512, 2016.

Gascoin, S., Lhermitte, S., Kinnard, C., Bortels, K. and Liston, G. E.: Wind effects on snow cover in Pascua-Lama, Dry Andes of Chile, Adv. Water Resour., 55, 25–39, doi:10.1016/j.advwatres.2012.11.013, 2013.

Gassman, P. W., Reyes, M. R., Green, C. H. and Arnold, J. G.: The soil and water assessment tool: Historical development, applications, and future research directions, Trans. ASABE, 50(4), 1211–1250, 2007.

Gat, J. R.: Oxygen and hydrogen isotopes in the hydrologic cycle, Annu. Rev. Earth Planet. Sci., 24(1), 225–262, doi:10.1146/annurev.earth.24.1.225, 1996.

Gat, J. R. and Tzur, Y.: Modification of the isotopic composition of rainwater by processes which occur before groundwater recharge, International Atomic Energy Agency (IAEA),

Vienna, Austria., 1967.

Gaume, J., Chambon, G., Eckert, N. and Naaim, M.: Influence of weak-layer heterogeneity on snow slab avalanche release: application to the evaluation of avalanche release depths, J. Glaciol., 59(215), 423–437, doi:10.3189/2013JoG12J161, 2013.

Gelman, A. and Rubin, D. B.: Inference from Iterative Simulation Using Multiple Sequences, Stat. Sci., 7(4), 457–472, doi:10.1214/ss/1177011136, 1992.

Genereux, D.: Quantifying uncertainty in tracer-based hydrograph separations, Water Resour. Res., 34(4), 915–919, doi:10.1029/98WR00010, 1998.

Genereux, D. P., Wood, S. J. and Pringle, C. M.: Chemical tracing of interbasin groundwater transfer in the lowland rainforest of Costa Rica, J. Hydrol., 258(1–4), 163–178, doi:10.1016/S0022-1694(01)00568-6, 2002.

Gerdel, R. W.: The dynamics of liquid water in deep snow-packs, Eos, Trans. Am. Geophys. Union, 26(1), 83–90, doi:10.1029/TR026i001p00083, 1945.

Glynn, P. W. and Iglehart, D. L.: Importance Sampling for Stochastic Simulations, Manage. Sci., 35(11), 1367–1392, doi:10.1287/mnsc.35.11.1367, 1989.

Good, S. P., Noone, D., Kurita, N., Benetti, M. and Bowen, G. J.: D/H isotope ratios in the global hydrologic cycle, Geophys. Res. Lett., 42(12), 5042–5050, doi:10.1002/2015GL064117, 2015.

Guan, B., Waliser, D. E., Ralph, F. M., Fetzer, E. J. and Neiman, P. J.: Hydrometeorological characteristics of rain-on-snow events associated with atmospheric rivers, Geophys. Res. Lett., 43(6), 2964–2973, doi:10.1002/2016GL067978, 2016.

Gustafson, J. R., Brooks, P. D., Molotch, N. P. and Veatch, W. C.: Estimating snow sublimation using natural chemical and isotopic tracers across a gradient of solar radiation, Water Resour. Res., 46(12), doi:10.1029/2009WR009060, 2010.

Halder, J., Decrouy, L. and Vennemann, T. W.: Mixing of Rhône River water in Lake Geneva (Switzerland–France) inferred from stable hydrogen and oxygen isotope profiles, J. Hydrol., 477(Supplement C), 152–164, doi:10.1016/j.jhydrol.2012.11.026, 2013.

Harder, P. and Pomeroy, J. W.: Hydrological model uncertainty due to precipitation-phase partitioning methods, Hydrol. Process., 28(14), 4311–4327, doi:10.1002/hyp.10214, 2014.

Harman, C. J.: Time-variable transit time distributions and transport: Theory and application to storage-dependent transport of chloride in a watershed, Water Resour. Res., 51(1), 1–

30, doi:10.1002/2014WR015707, 2015.

Harpold, A. A. and Brooks, P. D.: Humidity determines snowpack ablation under a warming climate, Proc. Natl. Acad. Sci., 115(6), 1215 LP – 1220 [online] Available from: http://www.pnas.org/content/115/6/1215.abstract, 2018.

Harpold, A. A., Kaplan, M. L., Klos, P. Z., Link, T., McNamara, J. P., Rajagopal, S., Schumer, R. and Steele, C. M.: Rain or snow: hydrologic processes, observations, prediction, and research needs, Hydrol. Earth Syst. Sci., 21(1), 1–22, doi:10.5194/hess-21-1-2017, 2017a.

Harpold, A. A., Rajagopal, S., Crews, J. B., Winchell, T. and Schumer, R.: Relative Humidity Has Uneven Effects on Shifts From Snow to Rain Over the Western U.S., Geophys. Res. Lett., 44(19), 9742–9750, doi:10.1002/2017GL075046, 2017b.

Hastings, W. K.: Monte Carlo sampling methods using Markov chains and their applications, Biometrika, 57(1), 97–109, doi:10.1093/biomet/57.1.97, 1970.

Hedstrom, N. R. and Pomeroy, J. W.: Measurements and modelling of snow interception in the boreal forest, Hydrol. Process., 12(10–11), 1611–1625, doi:10.1002/(SICI)1099-1085(199808/09)12:10/11<1611::AID-HYP684>3.0.CO;2-4, 1998.

Herrera, C., Custodio, E., Chong, G., Lambán, L. J., Riquelme, R., Wilke, H., Jódar, J., Urrutia, J., Urqueta, H., Sarmiento, A., Gamboa, C. and Lictevout, E.: Groundwater flow in a closed basin with a saline shallow lake in a volcanic area: Laguna Tuyajto, northern Chilean Altiplano of the Andes, Sci. Total Environ., 541, 303–318, doi:10.1016/j.scitotenv.2015.09.060, 2016.

Hijmans, R. J., Cameron, S. E., Parra, J. L., Jones, P. G. and Jarvis, A.: Very high resolution interpolated climate surfaces for global land areas, Int. J. Climatol., 25(15), 1965–1978, doi:10.1002/joc.1276, 2005.

Hiscock, K., Sparkes, R. and Hodgson, A.: Evaluation of future climate change impacts on European groundwater resources, in Climate Change Effects on Groundwater Resources: A Global Synthesis of Findings and Recommendations, pp. 351–365., 2011.

Hock, R.: Temperature index melt modelling in mountain areas, J. Hydrol., 282(1–4), 104–115, doi:10.1016/S0022-1694(03)00257-9, 2003.

Hoeg, S., Uhlenbrook, S. and Leibundgut, C.: Hydrograph separation in a mountainous catchment — combining hydrochemical and isotopic tracers, Hydrol. Process., 14(7), 1199–1216, doi:10.1002/(SICI)1099-1085(200005)14:7<1199::AID-HYP35>3.0.CO;2-K, 2000.

Holko, L., Danko, M., Dóša, M., Kostka, Z., Šanda, M., Pfister, L. and Iffly, J. F.: Spatial and temporal variability of stable water isotopes in snow related hydrological processes, Die Bodenkultur, 64, 3–4, 2013.

Houze, R. A.: Orographic effects on precipitating clouds, Rev. Geophys., 50(1), doi:10.1029/2011RG000365, 2012.

Hrachowitz, M. and Clark, M. P.: HESS Opinions: The complementary merits of competing modelling philosophies in hydrology, Hydrol. Earth Syst. Sci., 21(8), 3953–3973, doi:10.5194/hess-21-3953-2017, 2017.

Hrachowitz, M., Savenije, H., Bogaard, T. A., Tetzlaff, D. and Soulsby, C.: What can flux tracking teach us about water age distribution patterns and their temporal dynamics?, Hydrol. Earth Syst. Sci., 17(2), 533–564, doi:10.5194/hess-17-533-2013, 2013.

Hrachowitz, M., Fovet, O., Ruiz, L. and Savenije, H. H. G.: Transit time distributions, legacy contamination and variability in biogeochemical 1/fα scaling: how are hydrological response dynamics linked to water quality at the catchment scale?, Hydrol. Process., 29(25), 5241–5256, doi:10.1002/hyp.10546, 2015.

Hrachowitz, M., Benettin, P., van Breukelen, B. M., Fovet, O., Howden, N. J. K., Ruiz, L., van der Velde, Y. and Wade, A. J.: Transit times—the link between hydrology and water quality at the catchment scale, Wiley Interdiscip. Rev. Water, 3(5), 629–657, doi:10.1002/wat2.1155, 2016.

van Huijgevoort, M. H. J., Tetzlaff, D., Sutanudjaja, E. H. and Soulsby, C.: Using high resolution tracer data to constrain water storage, flux and age estimates in a spatially distributed rainfall-runoff model, Hydrol. Process., 30(25), 4761–4778, doi:10.1002/hyp.10902, 2016a.

van Huijgevoort, M. H. J., Tetzlaff, D., Sutanudjaja, E. H. and Soulsby, C.: Visualization of spatial patterns of connectivity and runoff ages derived from a tracer-aided model, Hydrol. Process., 30(25), 4893–4895, doi:10.1002/hyp.10961, 2016b.

Huning, L. S. and AghaKouchak, A.: Mountain snowpack response to different levels of warming, Proc. Natl. Acad. Sci. U. S. A., 115(43), 10932–10937, doi:10.1073/pnas.1805953115, 2018.

Huss, M., Bookhagen, B., Huggel, C., Jacobsen, D., Bradley, R. S., Clague, J. J., Vuille, M., Buytaert, W., Cayan, D. R., Greenwood, G., Mark, B. G., Milner, A. M., Weingartner, R. and Winder, M.: Toward mountains without permanent snow and ice, Earth's Futur.,

5(5), 418–435, doi:10.1002/2016EF000514, 2017.

IAEA/WMO: Global Network of Isotopes in Precipitation. The GNIP Database, [online] Available from: http://www-naweb.iaea.org/napc/ih/IHS_resources_gnip.html, 2018.

Inouye, D., Yang, E., Allen, G. and Ravikumar, P.: A Review of Multivariate Distributions for Count Data Derived from the Poisson Distribution, Wiley Interdiscip. Rev. Comput. Stat., 9(3), e1398, doi:10.1002/wics.1398, 2017.

Isotta, F. A., Frei, C., Weilguni, V., Perčec Tadić, M., Lassègues, P., Rudolf, B., Pavan, V., Cacciamani, C., Antolini, G., Ratto, S. M., Munari, M., Micheletti, S., Bonati, V., Lussana, C., Ronchi, C., Panettieri, E., Marigo, G. and Vertačnik, G.: The climate of daily precipitation in the Alps: development and analysis of a high-resolution grid dataset from pan-Alpine rain-gauge data, Int. J. Climatol., 34(5), 1657–1675, doi:10.1002/joc.3794, 2013.

Jasechko, S. and Taylor, R. G.: Intensive rainfall recharges tropical groundwaters, Environ. Res. Lett., 10(12), 124015, doi:10.1088/1748-9326/10/12/124015, 2015.

Jasechko, S., Birks, S. J., Gleeson, T., Wada, Y., Fawcett, P. J., Sharp, Z. D., McDonnell, J. J. and Welker, J. M.: The pronounced seasonality of global groundwater recharge, Water Resour. Res., 50(11), 8845–8867, doi:10.1002/2014WR015809, 2014.

Jasechko, S., Wassenaar, L. I. and Mayer, B.: Isotopic evidence for widespread cold-season-biased groundwater recharge and young streamflow across central Canada, Hydrol. Process., 31(12), 2196–2209, doi:10.1002/hyp.11175, 2017.

Jayathilake, D. I. and Smith, T.: Predicting the temporal transferability of model parameters through a hydrological signature analysis, Front. Earth Sci., doi:10.1007/s11707-019-0755-y, 2019.

Jeelani, G., Bhat, N. A. and Shivanna, K.: Use of δ18O tracer to identify stream and spring origins of a mountainous catchment: A case study from Liddar watershed, Western Himalaya, India, J. Hydrol., 393(3), 257–264, doi:https://doi.org/10.1016/j.jhydrol.2010.08.021, 2010.

Jeelani, G., Saravana Kumar, U. and Kumar, B.: Variation of δ18O and δD in precipitation and stream waters across the Kashmir Himalaya (India) to distinguish and estimate the seasonal sources of stream flow, J. Hydrol., 481, 157–165, doi:https://doi.org/10.1016/j.jhydrol.2012.12.035, 2013.

Jenicek, M., Seibert, J., Zappa, M., Staudinger, M. and Jonas, T.: Importance of maximum snow

accumulation for summer low flows in humid catchments, Hydrol. Earth Syst. Sci., 20(2), 859–874, doi:10.5194/hess-20-859-2016, 2016.

Jenicek, M., Seibert, J. and Staudinger, M.: Modeling of Future Changes in Seasonal Snowpack and Impacts on Summer Low Flows in Alpine Catchments, Water Resour. Res., 54(1), 538–556, doi:10.1002/2017WR021648, 2018.

Jennings, K. S. and Molotch, N. P.: The sensitivity of modeled snow accumulation and melt to precipitation phase methods across a climatic gradient, Hydrol. Earth Syst. Sci. Discuss., 2019, 1–33, doi:10.5194/hess-2019-82, 2019.

Jeton, A. E., Dettinger, M. D. and Smith, J. L.: Potential effects of climate change on streamflow, eastern and western slopes of the Sierra Nevada, California and Nevada., 1996.

Jonas, T., Marty, C. and Magnusson, J.: Estimating the snow water equivalent from snow depth measurements in the Swiss Alps, J. Hydrol., 378(1), 161–167, doi:10.1016/j.jhydrol.2009.09.021, 2009.

Juras, R., Pavlásek, J., Vitvar, T., Šanda, M., Holub, J., Jankovec, J. and Linda, M.: Isotopic tracing of the outflow during artificial rain-on-snow event, J. Hydrol., 541, 1145–1154, doi:10.1016/j.jhydrol.2016.08.018, 2016.

Kapnick, S. B., Yang, X., Vecchi, G. A., Delworth, T. L., Gudgel, R., Malyshev, S., Milly, P. C. D., Shevliakova, E., Underwood, S. and Margulis, S. A.: Potential for western US seasonal snowpack prediction, Proc. Natl. Acad. Sci. U. S. A., 115(6), 1180–1185, doi:10.1073/pnas.1716760115, 2018.

Kaser, G., Grosshauser, M. and Marzeion, B.: Contribution potential of glaciers to water availability in different climate regimes, Proc. Natl. Acad. Sci. U. S. A., 107(47), 20223–20227, doi:10.1073/pnas.1008162107, 2010.

Katsushima, T., Yamaguchi, S., Kumakura, T. and Sato, A.: Experimental analysis of preferential flow in dry snowpack, Cold Reg. Sci. Technol., 85, 206–216, doi:10.1016/j.coldregions.2012.09.012, 2013.

Kattelmann, R.: Water release from a forested snowpack during rainfall, in Proceedings of the Vancouver Symposium., 1987.

Kavetski, D., Kuczera, G. and Franks, S. W.: Bayesian analysis of input uncertainty in hydrological modeling: 1. Theory, Water Resour. Res., 42(3), n/a-n/a, doi:10.1029/2005WR004368, 2006a.

Kavetski, D., Kuczera, G. and Franks, S. W.: Bayesian analysis of input uncertainty in hydrological modeling: 2. Application, Water Resour. Res., 42(3), n/a-n/a, doi:10.1029/2005WR004376, 2006b.

Kelleher, C., McGlynn, B. and Wagener, T.: Characterizing and reducing equifinality by constraining a distributed catchment model with regional signatures, local observations, and process understanding, Hydrol. Earth Syst. Sci., 21(7), 3325–3352, doi:10.5194/hess-21-3325-2017, 2017.

Kelleher, C., Ward, A., Knapp, J. L. A., Blaen, P. J., Kurz, M. J., Drummond, J. D., Zarnetske, J. P., Hannah, D. M., Mendoza-Lera, C., Schmadel, N. M., Datry, T., Lewandowski, J., Milner, A. M. and Krause, S.: Exploring Tracer Information and Model Framework Trade-Offs to Improve Estimation of Stream Transient Storage Processes, Water Resour. Res., 55(4), 3481–3501, doi:10.1029/2018WR023585, 2019.

Kendall, C. and McDonnell, J. J.: Isotope tracers in catchment hydrology, Elsevier., 1998.

Khatami, S., Peel, M. C., Peterson, T. J. and Western, A. W.: Equifinality and Flux Mapping: A New Approach to Model Evaluation and Process Representation Under Uncertainty, Water Resour. Res., 55(11), 8922–8941, doi:10.1029/2018WR023750, 2019.

Kirchner, J. W.: A double paradox in catchment hydrology and geochemistry, Hydrol. Process., 17(4), 871–874, doi:10.1002/hyp.5108, 2003.

Kirchner, J. W.: Getting the right answers for the right reasons: Linking measurements, analyses, and models to advance the science of hydrology, Water Resour. Res., 42(3), n/a-n/a, doi:10.1029/2005WR004362, 2006.

Kirchner, J. W.: Aggregation in environmental systems – Part 2: Catchment mean transit times and young water fractions under hydrologic nonstationarity, Hydrol. Earth Syst. Sci., 20(1), 299–328, doi:doi:10.5194/hess-20-299-2016, 2016.

Klaus, J. and McDonnell, J. J.: Hydrograph separation using stable isotopes: Review and evaluation, J. Hydrol., 505, 47–64, doi:10.1016/j.jhydrol.2013.09.006, 2013.

Koeniger, P., Hubbart, J. A., Link, T. and Marshall, J. D.: Isotopic variation of snow cover and streamflow in response to changes in canopy structure in a snow-dominated mountain catchment, Hydrol. Process., 22(4), 557–566, doi:10.1002/hyp.6967, 2008.

Kohfahl, C., Sprenger, C., Herrera, J. B., Meyer, H., Chacón, F. F. and Pekdeger, A.: Recharge sources and hydrogeochemical evolution of groundwater in semiarid and karstic environments: A field study in the Granada Basin (Southern Spain), Appl. Geochemistry,

23(4), 846–862, doi:10.1016/j.apgeochem.2007.09.009, 2008.

Körner, C., Jetz, W., Paulsen, J., Payne, D., Rudmann-Maurer, K. and Spehn, E.: A global inventory of mountains for bio-geographical applications; data sets available from https://ilias.unibe.ch/goto_ilias3_unibe_cat_1000515.html, last accessed 20 Aug 2017, Alp. Bot., 127(1), 1–15, doi:10.1007/s00035-016-0182-6, 2017.

Koutsouris, A. J. and Lyon, S. W.: Advancing understanding in data-limited conditions: estimating contributions to streamflow across Tanzania's rapidly developing Kilombero Valley, Hydrol. Sci. J., 63(2), 197–209, doi:10.1080/02626667.2018.1426857, 2018.

Kuczera, G. and Parent, E.: Monte Carlo assessment of parameter uncertainty in conceptual catchment models: the Metropolis algorithm, J. Hydrol., 211(1), 69–85, doi:10.1016/S0022-1694(98)00198-X, 1998.

Kunnath-Poovakka, A., Ryu, D., Renzullo, L. J. and George, B.: The efficacy of calibrating hydrologic model using remotely sensed evapotranspiration and soil moisture for streamflow prediction, J. Hydrol., 535, 509–524, doi:10.1016/j.jhydrol.2016.02.018, 2016.

Kuppel, S., Tetzlaff, D., Maneta, M. P. and Soulsby, C.: EcH2O-iso 1.0: water isotopes and age tracking in a process-based, distributed ecohydrological model, Geosci. Model Dev., 11(7), 3045–3069, doi:10.5194/gmd-11-3045-2018, 2018.

Lambán, L. J., Jódar, J., Custodio, E., Soler, A., Sapriza, G. and Soto, R.: Isotopic and hydrogeochemical characterization of high-altitude karst aquifers in complex geological settings. The Ordesa and Monte Perdido National Park (Northern Spain) case study, Sci. Total Environ., 506, 466–479, doi:10.1016/j.scitotenv.2014.11.030, 2015.

Lammers, R. B., Pundsack, J. W. and Shiklomanov, A. I.: Variability in river temperature, discharge, and energy flux from the Russian pan-Arctic landmass, J. Geophys. Res. Biogeosciences, 112(4), G04S59, doi:10.1029/2006JG000370, 2007.

Laudon, H. and Slaymaker, O.: Hydrograph separation using stable isotopes, silica and electrical conductivity: an alpine example, J. Hydrol., 201(1), 82–101, doi:10.1016/S0022-1694(97)00030-9, 1997.

Laudon, H., Hemond, H. F., Krouse, R. and Bishop, K. H.: Oxygen 18 fractionation during snowmelt: Implications for spring flood hydrograph separation, Water Resour. Res., 38(11), 10–40, doi:10.1029/2002WR001510, 2002.

Law, J. and Vandijk, D.: SUBLIMATION AS A GEOMORPHIC PROCESS - A REVIEW, Permafr.

Periglac. Process., 5(4), 237–249, doi:10.1002/ppp.3430050404, 1994.

Lechler, A. R. and Niemi, N. A.: The influence of snow sublimation on the isotopic composition of spring and surface waters in the southwestern United States: Implications for stable isotope-based paleoaltimetry and hydrologic studies, Geol. Soc. Am. Bull., 124(3–4), 318–334, doi:10.1130/B30467.1, 2012.

Lee, J.: A numerical study of isotopic evolution of a seasonal snowpack and its meltwater by melting rates, Geosci. J., 18(4), 503–510, doi:10.1007/s12303-014-0019-5, 2014.

Lee, J., Feng, X., Posmentier, E. S., Faiia, A. M. and Taylor, S.: Stable isotopic exchange rate constant between snow and liquid water, Chem. Geol., 260(1–2), 57–62, doi:10.1016/j.chemgeo.2008.11.023, 2009.

Lee, J., Feng, X., Faiia, A. M., Posmentier, E. S., Kirchner, J. W., Osterhuber, R. and Taylor, S.: Isotopic evolution of a seasonal snowcover and its melt by isotopic exchange between liquid water and ice, Chem. Geol., 270(1–4), 126–134, doi:10.1016/j.chemgeo.2009.11.011, 2010a.

Lee, J., Feng, X., Faiia, A., Posmentier, E., Osterhuber, R. and Kirchner, J.: Isotopic evolution of snowmelt: A new model incorporating mobile and immobile water, Water Resour. Res., 46(11), doi:10.1029/2009WR008306, 2010b.

Legates, D. R. and Willmott, C. J.: Mean seasonal and spatial variability in gauge-corrected, global precipitation, Int. J. Climatol., 10(2), 111–127, doi:10.1002/joc.3370100202, 1990.

Lehning, M., Löwe, H., Ryser, M. and Raderschall, N.: Inhomogeneous precipitation distribution and snow transport in steep terrain, Water Resour. Res., 44(7), doi:10.1029/2007WR006545, 2008.

Leslie, D. L., Welch, K. A. and Lyons, W. B.: A temporal stable isotopic (δ18O, δD, d-excess) comparison in glacier meltwater streams, Taylor Valley, Antarctica, Hydrol. Process., 31(17), 3069–3083, doi:10.1002/hyp.11245, 2017.

Lessels, J. S., Tetzlaff, D., Birkel, C., Dick, J. and Soulsby, C.: Water sources and mixing in riparian wetlands revealed by tracers and geospatial analysis, Water Resour. Res., 52(1), 456–470, doi:10.1002/2015WR017519, 2016.

Li, D., Wrzesien, M. L., Durand, M., Adam, J. and Lettenmaier, D. P.: How much runoff originates as snow in the western United States, and how will that change in the future?, Geophys. Res. Lett., 44(12), 6163–6172, doi:10.1002/2017GL073551, 2017.

Liston, G. E.: Representing Subgrid Snow Cover Heterogeneities in Regional and Global

Models, J. Clim., 17(6), 1381–1397, doi:10.1175/1520-0442(2004)017<1381:RSSCHI>2.0.CO;2, 2004.

Lopes, S. O. A. M., Stefan, U., P.W., J. G., Ilyas, M., Sebastian, R. E. and Pieter, V. der Z.: Hydrograph separation using tracers and digital filters to quantify runoff components in a semi-arid mesoscale catchment, Hydrol. Process., 32(10), 1334–1350, doi:10.1002/hyp.11491, 2018.

Lundberg, A., Granlund, N. and Gustafsson, D.: Towards automated 'Ground truth' snow measurements—a review of operational and new measurement methods for Sweden, Norway, and Finland, Hydrol. Process., 24(14), 1955–1970, doi:10.1002/hyp.7658, 2010.

Lyon, A.: Why are Normal Distributions Normal?, Br. J. Philos. Sci., 65(3), 621–649, doi:10.1093/bjps/axs046, 2013.

MacDonald, M. K., Pomeroy, J. W. and Pietroniro, A.: On the importance of sublimation to an alpine snow mass balance in the Canadian Rocky Mountains, Hydrol. Earth Syst. Sci., 14(7), 1401–1415, doi:10.5194/hess-14-1401-2010, 2010.

MacDonell, S., Kinnard, C., Molg, T., Nicholson, L. and Abermann, J.: Meteorological drivers of ablation processes on a cold glacier in the semi-arid Andes of Chile, Cryosphere, 7(5), 1513–1526, doi:10.5194/tc-7-1513-2013, 2013.

Mächler, E., Salyani, A., Walser, J.-C., Larsen, A., Schaefli, B., Altermatt, F. and Ceperley, N.: Water tracing with environmental DNA in a high-Alpine catchment, Hydrol. Earth Syst. Sci. Discuss., 2019, 1–30, doi:10.5194/hess-2019-551, 2019.

Maclean, R. A., English, M. C. and Schiff, S. L.: Hydrological and hydrochemical response of a small canadian shield catchment to late winter rain-on-snow events, Hydrol. Process., 9(8), 845–863, doi:10.1002/hyp.3360090803, 1995.

Makarieva, O., Nesterova, N., Post, D. A., Sherstyukov, A. and Lebedeva, L.: Warming temperatures are impacting the hydrometeorological regime of Russian rivers in the zone of continuous permafrost, Cryosph., 13(6), 1635–1659, doi:10.5194/tc-13-1635-2019, 2019.

Malhi, Y., Franklin, J., Seddon, N., Solan, M., Turner, M. G., Field, C. B. and Knowlton, N.: Climate change and ecosystems: threats, opportunities and solutions, Philos. Trans. R. Soc. B Biol. Sci., 375(1794), 20190104, doi:10.1098/rstb.2019.0104, 2020.

Marks, D., Winstral, A. and Seyfried, M.: Simulation of terrain and forest shelter effects on patterns of snow deposition, snowmelt and runoff over a semi-arid mountain catchment,

Hydrol. Process., 16(18), 3605–3626, doi:10.1002/hyp.1237, 2002.

Marty, C.: Regime shift of snow days in Switzerland, Geophys. Res. Lett., 35(12), doi:10.1029/2008GL033998, 2008.

Marty, C., Tilg, A.-M. and Jonas, T.: Recent Evidence of Large-Scale Receding Snow Water Equivalents in the European Alps, J. Hydrometeorol., 18(4), 1021–1031, doi:10.1175/jhm-d-16-0188.1, 2017.

Maule, C. P., Chanasyk, D. S. and Muehlenbachs, K.: Isotopic determination of snow-water contribution to soil water and groundwater, J. Hydrol., 155(1), 73–91, doi:10.1016/0022-1694(94)90159-7, 1994.

Mazurkiewicz, A. B., Callery, D. G. and McDonnell, J. J.: Assessing the controls of the snow energy balance and water available for runoff in a rain-on-snow environment, J. Hydrol., 354(1), 1–14, doi:https://doi.org/10.1016/j.jhydrol.2007.12.027, 2008.

McCabe, G. J., Hay, L. E. and Clark, M. P.: Rain-on-Snow Events in the Western United States, Bull. Am. Meteorol. Soc., 88(3), 319–328, doi:10.1175/BAMS-88-3-319, 2007.

McCabe, G. J., Wolock, D. M. and Austin, S. H.: Variability of runoff-based drought conditions in the conterminous United States, Int. J. Climatol., doi:10.1002/joc.4756, 2016.

Mcdonnell, J. J. and Beven, K.: Debates - The future of hydrological sciences: A (common) path forward? A call to action aimed at understanding velocities, celerities and residence time distributions of the headwater hydrograph, Water Resour. Res., 50(6), 5342–5350, doi:10.1002/2013WR015141, 2014.

McDonnell, J. J., McGuire, K., Aggarwal, P., Beven, K. J., Biondi, D., Destouni, G., Dunn, S., James, A., Kirchner, J., Kraft, P., Lyon, S., Maloszewski, P., Newman, B., Pfister, L., Rinaldo, A., Rodhe, A., Sayama, T., Seibert, J., Solomon, K., Soulsby, C., Stewart, M., Tetzlaff, D., Tobin, C., Troch, P., Weiler, M., Western, A., Wörman, A. and Wrede, S.: How old is streamwater? Open questions in catchment transit time conceptualization, modelling and analysis, Hydrol. Process., 24(12), 1745–1754, doi:10.1002/hyp.7796, 2010.

McMillan, H.: Linking hydrologic signatures to hydrologic processes: A review, Hydrol. Process., 34(6), 1393–1409, doi:10.1002/hyp.13632, 2020.

McMillan, H., Tetzlaff, D., Clark, M. and Soulsby, C.: Do time-variable tracers aid the evaluation of hydrological model structure? A multimodel approach, Water Resour. Res., 48(5), doi:10.1029/2011WR011688, 2012.

MeteoSwiss: Documentation of MeteoSwiss Grid-Data Products: Daily Precipitation (final

analysis): RhiresD, Zürich. [online] Available from: https://www.meteoswiss.admin.ch/content/dam/meteoswiss/fr/climat/le-climat-suisse-en-detail/doc/ProdDoc_RhiresD.pdf, 2016.

MeteoSwiss: Documentation of MeteoSwiss Grid-Data Products: Daily mean, minimum and maximum temperature, Zürich. [online] Available from: https://www.meteoswiss.admin.ch/content/dam/meteoswiss/de/service-und-publikationen/produkt/raeumliche-daten-temperatur/doc/ProdDoc_TabsD.pdf, 2017.

Metropolis, N. and Ulam, S.: The Monte Carlo Method, J. Am. Stat. Assoc., 44(247), 335–341, doi:10.1080/01621459.1949.10483310, 1949.

Michelon, A.: Weather dataset from Vallon de Nant, Switzerland, until July 2017, , doi:10.5281/ZENODO.1042473, 2017.

Michelon, A., Benoit, L., Beria, H., Ceperley, N. and Schaefli, B.: A 2-minute rainfall (12 locations) and discharge time series at the Vallon de Nant catchment, Switzerland, for 2017 and 2018 summer seasons, , doi:10.5281/ZENODO.3613841, 2020a.

Michelon, A., Benoit, L., Beria, H., Ceperley, N. and Schaefli, B.: On the value of high density rain gauge observations for small Alpine headwater catchments, Hydrol. Earth Syst. Sci. Discuss., 2020, 1–31, doi:10.5194/hess-2019-683, 2020b.

Milano, M., Reynard, E., Bosshard, N. and Weingartner, R.: Simulating future trends in hydrological regimes in Western Switzerland, J. Hydrol. Reg. Stud., 4, 748–761, doi:10.1016/j.ejrh.2015.10.010, 2015.

Morán-Tejeda, E., López-Moreno, J. I. and Beniston, M.: The changing roles of temperature and precipitation on snowpack variability in Switzerland as a function of altitude, Geophys. Res. Lett., 40(10), 2131–2136, doi:10.1002/grl.50463, 2013.

Moran, T. A., Marshall, S. J., Evans, E. C. and Sinclair, K. E.: Altitudinal Gradients of Stable Isotopes in Lee-Slope Precipitation in the Canadian Rocky Mountains, Arctic, Antarct. Alp. Res., 39(3), 455–467 [online] Available from: http://www.jstor.org/stable/20181717, 2007.

Moser, H. and Stichler, W.: Deuterium and oxygen-18 contents as an index of the properties of snow covers, Int. Assoc. Hydrol. Sci. Publ., 114, 122–135, 1974.

Mosquera, M. G., Segura, C. and Crespo, P.: Flow Partitioning Modelling Using High-Resolution Isotopic and Electrical Conductivity Data, Water, 10(7), doi:10.3390/w10070904, 2018.

Motoyama, H., Hirasawa, N., Satow, K. and Watanabe, O.: Seasonal variations in oxygen isotope ratios of daily collected precipitation and wind drift samples and in the final snow cover at Dome Fuji Station, Antarctica, J. Geophys. Res. Atmos., 110(D11), doi:10.1029/2004JD004953, 2005.

Mott, R., Schirmer, M., Bavay, M., Grünewald, T. and Lehning, M.: Understanding snow-transport processes shaping the mountain snow-cover, Cryosph., 4(4), 545–559, doi:10.5194/tc-4-545-2010, 2010.

Mountain, N., James, A. L. and Chutko, K.: Groundwater and surface water influences on streamflow in a mesoscale Precambrian Shield catchment, Hydrol. Process., 29(18), 3941–3953, doi:10.1002/hyp.10590, 2015.

Murakami, S.: A proposal for a new forest canopy interception mechanism: Splash droplet evaporation, J. Hydrol., 319(1), 72–82, doi:10.1016/j.jhydrol.2005.07.002, 2006.

Musselman, K. N., Clark, M. P., Liu, C., Ikeda, K. and Rasmussen, R.: Slower snowmelt in a warmer world, Nat. Clim. Chang., 7(3), 214–219, doi:10.1038/nclimate3225, 2017.

N'da, A. B., Bouchaou, L., Reichert, B., Hanich, L., Ait Brahim, Y., Chehbouni, A., Beraaouz, E. H. and Michelot, J.-L.: Isotopic signatures for the assessment of snow water resources in the Moroccan high Atlas mountains: contribution to surface and groundwater recharge, Environ. Earth Sci., 75(9), 755, doi:10.1007/s12665-016-5566-9, 2016.

Neal, R. M.: Annealed importance sampling, Stat. Comput., 11(2), 125–139, doi:10.1023/A:1008923215028, 2001.

Nijzink, R. C., Almeida, S., Pechlivanidis, I. G., Capell, R., Gustafssons, D., Arheimer, B., Parajka, J., Freer, J., Han, D., Wagener, T., Nooijen, R. R. P., Savenije, H. H. G. and Hrachowitz, M.: Constraining Conceptual Hydrological Models With Multiple Information Sources, Water Resour. Res., 54(10), 8332–8362, doi:10.1029/2017WR021895, 2018.

Nogués-Bravo, D., Araújo, M. B., Errea, M. P. and Martínez-Rica, J. P.: Exposure of global mountain systems to climate warming during the 21st Century, Glob. Environ. Chang., 17(3), 420–428, doi:https://doi.org/10.1016/j.gloenvcha.2006.11.007, 2007.

Nolin, A. W. and Daly, C.: Mapping "At Risk" Snow in the Pacific Northwest, J. Hydrometeorol., 7(5), 1164–1171, doi:10.1175/JHM543.1, 2006.

O'Driscoll, M. A., DeWalle, D. R., McGuire, K. J. and Gburek, W. J.: Seasonal 18O variations and groundwater recharge for three landscape types in central Pennsylvania, USA, J. Hydrol., 303(1), 108–124, doi:10.1016/j.jhydrol.2004.08.020, 2005.

Obradovic, M. M. and Sklash, M. G.: An isotopic and geochemical study of snowmelt runoff in a small arctic watershed, Hydrol. Process., 1(1), 15–30, doi:10.1002/hyp.3360010104, 1986.

Odusanya, A. E., Mehdi, B., Schürz, C., Oke, A. O., Awokola, O. S., Awomeso, J. A., Adejuwon, J. O. and Schulz, K.: Multi-site calibration and validation of SWAT with satellite-based evapotranspiration in a data-sparse catchment in southwestern Nigeria, Hydrol. Earth Syst. Sci., 23(2), 1113–1144, doi:10.5194/hess-23-1113-2019, 2019.

Oerter, E. J., Siebert, G., Bowling, D. R. and Bowen, G.: Soil water vapour isotopes identify missing water source for streamside trees, Ecohydrology, 21(4), e2083, doi:10.1002/eco.2083, 2019.

Ohmura, A.: Physical Basis for the Temperature-Based Melt-Index Method, J. Appl. Meteorol., 40(4), 753–761, doi:10.1175/1520-0450(2001)040<0753:PBFTTB>2.0.CO;2, 2001.

Palazzi, E., von Hardenberg, J. and Provenzale, A.: Precipitation in the Hindu-Kush Karakoram Himalaya: Observations and future scenarios, J. Geophys. Res., 118(1), 85–100, doi:10.1029/2012jd018697, 2013.

Parajka, J. and Blöschl, G.: The value of MODIS snow cover data in validating and calibrating conceptual hydrologic models, J. Hydrol., 358(3), 240–258, doi:https://doi.org/10.1016/j.jhydrol.2008.06.006, 2008.

Parnell, A. C., Inger, R., Bearhop, S. and Jackson, A. L.: Source partitioning using stable isotopes: coping with too much variation., PLoS One, 5(3), e9672, doi:10.1371/journal.pone.0009672, 2010.

Parton, W. J. and Logan, J. A.: A model for diurnal variation in soil and air temperature, Agric. Meteorol., 23, 205–216, doi:https://doi.org/10.1016/0002-1571(81)90105-9, 1981.

Pavlovskii, I., Hayashi, M. and Lennon, M. R.: Transformation of snow isotopic signature along groundwater recharge pathways in the Canadian Prairies, J. Hydrol., 563, 1147–1160, doi:10.1016/j.jhydrol.2017.09.053, 2018.

Pearce, A. J., Stewart, M. K. and Sklash, M. G.: Storm Runoff Generation in Humid Headwater Catchments: 1. Where Does the Water Come From?, Water Resour. Res., 22(8), 1263–1272, doi:10.1029/WR022i008p01263, 1986.

Peel, M. C., Finlayson, B. L. and McMahon, T. A.: Updated world map of the Köppen-Geiger climate classification, Hydrol. Earth Syst. Sci., 11(5), 1633–1644, doi:10.5194/hess-11-1633-2007, 2007.

Pellerin, B. A., Wollheim, W. M., Feng, X. and Vörösmarty, C. J.: The application of electrical conductivity as a tracer for hydrograph separation in urban catchments, Hydrol. Process., 22(12), 1810–1818, doi:10.1002/hyp.6786, 2007.

Penna, D., Ahmad, M., Birks, S. J., Bouchaou, L., Brenčič, M., Butt, S., Holko, L., Jeelani, G., Martínez, D. E., Melikadze, G., Shanley, J. B., Sokratov, S. A., Stadnyk, T., Sugimoto, A. and Vreča, P.: A new method of snowmelt sampling for water stable isotopes, Hydrol. Process., 28(22), 5637–5644, doi:10.1002/hyp.10273, 2014a.

Penna, D., Engel, M., Mao, L., Dell'Agnese, A., Bertoldi, G. and Comiti, F.: Tracer-based analysis of spatial and temporal variations of water sources in a glacierized catchment, Hydrol. Earth Syst. Sci., 18(12), 5271–5288, doi:10.5194/hess-18-5271-2014, 2014b.

Penna, D., Zuecco, G., Crema, S., Trevisani, S., Cavalli, M., Pianezzola, L., Marchi, L. and Borga, M.: Response time and water origin in a steep nested catchment in the Italian Dolomites, Hydrol. Process., 31(4), 768–782, doi:10.1002/hyp.11050, 2017.

Peters-Lidard, C. D., Hossain, F., Leung, L. R., McDowell, N., Rodell, M., Tapiador, F. J., Turk, F. J. and Wood, A.: 100 Years of Progress in Hydrology, Meteorol. Monogr., 59, 25.1-25.51, doi:10.1175/AMSMONOGRAPHS-D-18-0019.1, 2019.

Petersky, R. and Harpold, A.: Now you see it, now you don't: a case study of ephemeral snowpacks and soil moisture response in the Great Basin, USA, Hydrol. Earth Syst. Sci., 22(9), 4891–4906, doi:10.5194/hess-22-4891-2018, 2018.

Pomeroy, J. W., Gray, D. M., Hedstrom, N. R. and Janowicz, J. R.: Prediction of seasonal snow accumulation in cold climate forests, Hydrol. Process., 16(18), 3543–3558, doi:10.1002/hyp.1228, 2002.

Pritchard, H. D.: Asia's shrinking glaciers protect large populations from drought stress, Nature, 569(7758), 649–654, doi:10.1038/s41586-019-1240-1, 2019.

Rajib, A., Evenson, G. R., Golden, H. E. and Lane, C. R.: Hydrologic model predictability improves with spatially explicit calibration using remotely sensed evapotranspiration and biophysical parameters, J. Hydrol., 567, 668–683, doi:10.1016/j.jhydrol.2018.10.024, 2018.

Regan, S., Goodhue, R., Naughton, O. and Hynds, P.: Geospatial drivers of the groundwater δ18O isoscape in a temperate maritime climate (Republic of Ireland), J. Hydrol., 554, 173–186, doi:10.1016/j.jhydrol.2017.09.017, 2017.

Ren, W., Yao, T., Yang, X. and Joswiak, D. R.: Implications of variations in δ18O and δD in

precipitation at Madoi in the eastern Tibetan Plateau, Quat. Int., 313, 56–61, doi:10.1016/j.quaint.2013.05.026, 2013.

Rice, K. C. and Hornberger, G. M.: Comparison of hydrochemical tracers to estimate source contributions to peak flow in a small, forested, headwater catchment, Water Resour. Res., 34(7), 1755–1766, doi:10.1029/98WR00917, 1998.

Rinaldo, A., Marani, A. and Rigon, R.: Geomorphological dispersion, Water Resour. Res., 27(4), 513–525, doi:10.1029/90WR02501, 1991.

Rinaldo, A., Benettin, P., Harman, C. J., Hrachowitz, M., McGuire, K. J., van der Velde, Y., Bertuzzo, E. and Botter, G.: Storage selection functions: A coherent framework for quantifying how catchments store and release water and solutes, Water Resour. Res., 51(6), 4840–4847, doi:10.1002/2015WR017273, 2015.

Robinson, D. A., Dewey, K. F. and Heim, R. R.: Global Snow Cover Monitoring: An Update, Bull. Am. Meteorol. Soc., 74(9), 1689–1696, doi:10.1175/1520-0477(1993)074<1689:GSCMAU>2.0.CO;2, 1993.

Rodriguez-Iturbe, I., Porporato, A., Ridolfi, L., Isham, V. and Coxi, D. R.: Probabilistic modelling of water balance at a point: the role of climate, soil and vegetation, Proc. R. Soc. London. Ser. A Math. Phys. Eng. Sci., 455(1990), 3789 LP – 3805 [online] Available from: http://rspa.royalsocietypublishing.org/content/455/1990/3789.abstract, 1999.

Roques, C., Rupp, D. E. and Selker, J. S.: Improved streamflow recession parameter estimation with attention to calculation of − dQ/dt, Adv. Water Resour., 108, 29–43, doi:10.1016/J.ADVWATRES.2017.07.013, 2017.

Rose, T. P.: Stable isotope investigation of precipitation and recharge processes in central Nevada, Hydrol. Resour. Manag. Progr. Undergr. Test Area Proj. FY 2001–2002 Prog. Rep., 113, 2003.

Rössler, O., Froidevaux, P., Börst, U., Rickli, R., Martius, O. and Weingartner, R.: Retrospective analysis of a nonforecasted rain-on-snow flood in the Alps – a matter of model limitations or unpredictable nature?, Hydrol. Earth Syst. Sci., 18(6), 2265–2285, doi:10.5194/hess-18-2265-2014, 2014.

Rothfuss, Y. and Javaux, M.: Reviews and syntheses: Isotopic approaches to quantify root water uptake: a review and comparison of methods, Biogeosciences, 14(8), 2199–2224, doi:10.5194/bg-14-2199-2017, 2017.

Rumpf, S. B., Hülber, K., Klonner, G., Moser, D., Schütz, M., Wessely, J., Willner, W.,

Zimmermann, N. E. and Dullinger, S.: Range dynamics of mountain plants decrease with elevation, Proc. Natl. Acad. Sci., 115(8), 1848 LP – 1853, doi:10.1073/pnas.1713936115, 2018.

Salvatore, M., Leonardo, M., Fortunato, D. S. S., Caterina, S. and Leonardo, M.: Exploiting the use of physical information for the calibration of a lumped hydrological model, Hydrol. Process., 32(10), 1420–1433, doi:10.1002/hyp.11501, 2018.

Santos, A. C., Portela, M. M., Rinaldo, A. and Schaefli, B.: Analytical flow duration curves for summer streamflow in Switzerland, Hydrol. Earth Syst. Sci., 22(4), 2377–2389, doi:10.5194/hess-22-2377-2018, 2018.

Saxena, R. K.: Estimation of Canopy Reservoir Capacity and Oxygen-18 Fractionation in Throughfall in a Pine Forest, Hydrol. Res., 17(4–5), 251 LP – 260 [online] Available from: http://hr.iwaponline.com/content/17/4-5/251.abstract, 1986.

Schaefli, B.: Projecting hydropower production under future climates: a guide for decision-makers and modelers to interpret and design climate change impact assessments, Wiley Interdiscip. Rev. Water, 2(4), 271–289, doi:10.1002/wat2.1083, 2015.

Schaefli, B. and Kavetski, D.: Bayesian spectral likelihood for hydrological parameter inference, Water Resour. Res., 53(8), 6857–6884, doi:10.1002/2016WR019465, 2017.

Schaefli, B., Talamba, D. B. and Musy, A.: Quantifying hydrological modeling errors through a mixture of normal distributions, J. Hydrol., 332(3), 303–315, doi:10.1016/j.jhydrol.2006.07.005, 2007.

Schaefli, B., Rinaldo, A. and Botter, G.: Analytic probability distributions for snow-dominated streamflow, Water Resour. Res., 49(5), 2701–2713, doi:10.1002/wrcr.20234, 2013.

Schaefli, B., Nicótina, L., Imfeld, C., Da Ronco, P., Bertuzzo, E. and Rinaldo, A.: SEHR-ECHO v1.0: a Spatially Explicit Hydrologic Response model for ecohydrologic applications, Geosci. Model Dev., 7(6), 2733–2746, doi:10.5194/gmd-7-2733-2014, 2014.

Schlaepfer, D. R., Ewers, B. E., Shuman, B. N., Williams, D. G., Frank, J. M., Massman, W. J. and Lauenroth, W. K.: Terrestrial water fluxes dominated by transpiration: Comment, Ecosphere, 5(5), 1–9, doi:10.1890/ES13-00391.1, 2014.

Schmidhuber, J. and Tubiello, F. N.: Global food security under climate change, Proc. Natl. Acad. Sci., 104(50), 19703 LP – 19708, doi:10.1073/pnas.0701976104, 2007.

Schmieder, J., Hanzer, F., Marke, T., Garvelmann, J., Warscher, M., Kunstmann, H. and Strasser, U.: The importance of snowmelt spatiotemporal variability for isotope-based

hydrograph separation in a high-elevation catchment, Hydrol. Earth Syst. Sci., 20(12), 5015–5033, doi:10.5194/hess-20-5015-2016, 2016.

Schneebeli, M.: Development and stability of preferential flow paths in a layered snowpack, IAHS Publ. Proc. Reports-Intern Assoc Hydrol. Sci., 228, 89–96, 1995.

Scholl, M., Eugster, W. and Burkard, R.: Understanding the role of fog in forest hydrology: stable isotopes as tools for determining input and partitioning of cloud water in montane forests, Hydrol. Process., 25(3), 353–366, doi:10.1002/hyp.7762, 2011.

Scholl, M. A., Gingerich, S. B. and Tribble, G. W.: The influence of microclimates and fog on stable isotope signatures used in interpretation of regional hydrology: East Maui, Hawaii, J. Hydrol., 264(1–4), 170–184, doi:http://dx.doi.org/10.1016/S0022-1694(02)00073-2, 2002.

Schumann, A. H.: Thiessen PolygonThiessen polygon BT - Encyclopedia of Hydrology and Lakes, pp. 648–649, Springer Netherlands, Dordrecht ., 1998.

Schürch, M., Kozel, R., Schotterer, U. and Tripet, J.-P.: Observation of isotopes in the water cycle---the Swiss National Network (NISOT), Environ. Geol., 45(1), 1–11, doi:10.1007/s00254-003-0843-9, 2003.

Schweizer, J., Bruce Jamieson, J. and Schneebeli, M.: Snow avalanche formation, Rev. Geophys., 41(4), doi:10.1029/2002RG000123, 2003.

Shafii, M. and Tolson, B. A.: Optimizing hydrological consistency by incorporating hydrological signatures into model calibration objectives, Water Resour. Res., 51(5), 3796–3814, doi:10.1002/2014WR016520, 2015.

Shafii, M., Craig, J. R., Macrae, M. L., English, M. C., Schiff, S. L., Van Cappellen, P. and Basu, N. B.: Can Improved Flow Partitioning in Hydrologic Models Increase Biogeochemical Predictability?, Water Resour. Res., 55(4), 2939–2960, doi:10.1029/2018WR024487, 2019.

Shah, T.: India's Master Plan for Groundwater Recharge: An Assessment and Some Suggestions for Revision, Econ. Polit. Wkly., 43(51), 41–49 [online] Available from: http://www.jstor.org/stable/40278311, 2008.

Shanley, J. B., Kendall, C., Albert, M. R. and Hardy, J. P.: Chemical and isotopic evolution of a layered eastern U.S. snowpack and its relation to stream-water composition, Biogeochem. Seas. snow-covered catchments. Proc. Symp. Boulder, 1995, 228, 329–338 [online] Available from: http://pubs.er.usgs.gov/publication/70018881, 1995.

Simpson, E. S., Thorud, D. B. and Friedman, I.: Distinguishing seasonal recharge to groundwater by deuterium analysis in southern Arizona, in World Water Balance: Proceedings of the Reading Symposium, vol. 3, pp. 623–633., 1970.

Singh, P., Spitzbart, G., Hübl, H. and Weinmeister, H. W.: Hydrological response of snowpack under rain-on-snow events: a field study, J. Hydrol., 202(1), 1–20, doi:10.1016/S0022-1694(97)00004-8, 1997.

Smith, T., Marshall, L. and Sharma, A.: Modeling residual hydrologic errors with Bayesian inference, J. Hydrol., 528, 29–37, doi:10.1016/j.jhydrol.2015.05.051, 2015.

Sodemann, H. and Zubler, E.: Seasonal and inter-annual variability of the moisture sources for Alpine precipitation during 1995–2002, Int. J. Climatol., 30(7), 947–961, doi:10.1002/joc.1932, 2010.

Son, K. and Sivapalan, M.: Improving model structure and reducing parameter uncertainty in conceptual water balance models through the use of auxiliary data, Water Resour. Res., 43(1), doi:10.1029/2006WR005032, 2007.

Soulsby, C., Malcolm, R., Helliwell, R., Ferrier, R. C. and Jenkins, A.: Isotope hydrology of the Allt a' Mharcaidh catchment, Cairngorms, Scotland: implications for hydrological pathways and residence times, Hydrol. Process., 14(4), 747–762, doi:10.1002/(SICI)1099-1085(200003)14:4<747::AID-HYP970>3.0.CO;2-0, 2000.

Soulsby, C., Tetzlaff, D. and Hrachowitz, M.: Tracers and transit times: windows for viewing catchment scale storage?, Hydrol. Process., 23(24), 3503–3507, doi:10.1002/hyp.7501, 2009.

Soulsby, C., Tetzlaff, D. and Hrachowitz, M.: Are transit times useful process-based tools for flow prediction and classification in ungauged basins in montane regions?, Hydrol. Process., 24(12), 1685–1696, doi:10.1002/hyp.7578, 2010.

Soulsby, C., Birkel, C., Geris, J., Dick, J., Tunaley, C. and Tetzlaff, D.: Stream water age distributions controlled by storage dynamics and nonlinear hydrologic connectivity: Modeling with high-resolution isotope data, Water Resour. Res., 51(9), 7759–7776, doi:10.1002/2015WR017888, 2015.

Soulsby, C., Braun, H., Sprenger, M., Weiler, M. and Tetzlaff, D.: Influence of forest and shrub canopies on precipitation partitioning and isotopic signatures, Hydrol. Process., 31(24), 4282–4296, doi:10.1002/hyp.11351, 2017.

Spongberg, M. E.: Spectral analysis of base flow separation with digital filters, Water Resour.

Res., 36(3), 745–752, doi:10.1029/1999WR900303, 2000.

Stadnyk, T. A., Delavau, C., Kouwen, N. and Edwards, T. W. D.: Towards hydrological model calibration and validation: simulation of stable water isotopes using the isoWATFLOOD model, Hydrol. Process., 27(25), 3791–3810, doi:10.1002/hyp.9695, 2013.

Steger, C., Kotlarski, S., Jonas, T. and Schär, C.: Alpine snow cover in a changing climate: a regional climate model perspective, Clim. Dyn., 41(3), 735–754, doi:10.1007/s00382-012-1545-3, 2013.

Stewart, I. T., Cayan, D. R. and Dettinger, M. D.: Changes toward Earlier Streamflow Timing across Western North America, J. Clim., 18(8), 1136–1155, doi:10.1175/JCLI3321.1, 2005.

Stichler, W., Schotterer, U., Fröhlich, K., Ginot, P., Kull, C., Gäggeler, H. and Pouyaud, B.: Influence of sublimation on stable isotope records recovered from high-altitude glaciers in the tropical Andes, J. Geophys. Res. Atmos., 106(D19), 22613–22620, doi:10.1029/2001JD900179, 2001.

Stock, B. C., Jackson, A. L., Ward, E. J., Parnell, A. C., Phillips, D. L. and Semmens, B. X.: Analyzing mixing systems using a new generation of Bayesian tracer mixing models, edited by D. Nelson, PeerJ, 6, e5096, doi:10.7717/peerj.5096, 2018.

Stoffel, M., Wyżga, B., Niedźwiedź, T., Ruiz-Villanueva, V., Ballesteros-Cánovas, J. A. and Kundzewicz, Z. W.: Floods in Mountain Basins BT - Flood Risk in the Upper Vistula Basin, edited by Z. W. Kundzewicz, M. Stoffel, T. Niedźwiedź, and B. Wyżga, pp. 23–37, Springer International Publishing, Cham., 2016.

Stott, P.: How climate change affects extreme weather events, Science (80-.)., 352(6293), 1517–1518, doi:10.1126/science.aaf7271, 2016.

Strahler, A. N.: HYPSOMETRIC (AREA-ALTITUDE) ANALYSIS OF EROSIONAL TOPOGRAPHY, GSA Bull., 63(11), 1117–1142, doi:10.1130/0016-7606(1952)63[1117:HAAOET]2.0.CO;2, 1952.

Sturm, M.: White water: Fifty years of snow research in WRR and the outlook for the future, Water Resour. Res., 51(7), 4948–4965, doi:10.1002/2015WR017242, 2015.

Sturm, M., Holmgren, J. and Liston, G. E.: A seasonal snow cover classification-system for local to global applications, J. Clim., 8(5), 1261–1283, doi:10.1175/1520-0442(1995)008<1261:asscc>2.0.co;2, 1995.

Sturm, M., Goldstein, M. A. and Parr, C.: Water and life from snow: A trillion dollar science question, Water Resour. Res., 53(5), 3534–3544, doi:10.1002/2017WR020840, 2017.

Surfleet, C. G. and Tullos, D.: Variability in effect of climate change on rain-on-snow peak flow events in a temperate climate, J. Hydrol., 479, 24–34, doi:10.1016/j.jhydrol.2012.11.021, 2013.

Sutanudjaja, E. H., van Beek, L. P. H., de Jong, S. M., van Geer, F. C. and Bierkens, M. F. P.: Calibrating a large-extent high-resolution coupled groundwater-land surface model using soil moisture and discharge data, Water Resour. Res., 50(1), 687–705, doi:10.1002/2013WR013807, 2014.

Tashie, A., Scaife, C. I. and Band, L. E.: Transpiration and subsurface controls of streamflow recession characteristics, Hydrol. Process., 33(19), 2561–2575, doi:10.1002/hyp.13530, 2019.

Tashie, A., Pavelsky, T. and Emanuel, R. E.: Spatial and Temporal Patterns in Baseflow Recession in the Continental United States, Water Resour. Res., 56(3), e2019WR026425, doi:10.1029/2019WR026425, 2020.

Taylor, S., Feng, X., Kirchner, J. W., Osterhuber, R., Klaue, B. and Renshaw, C. E.: Isotopic evolution of a seasonal snowpack and its melt, Water Resour. Res., 37(3), 759–769, doi:10.1029/2000WR900341, 2001.

Taylor, S., Feng, X., Williams, M. and McNamara, J.: How isotopic fractionation of snowmelt affects hydrograph separation, Hydrol. Process., 16(18), 3683–3690, doi:10.1002/hyp.1232, 2002.

Tetzlaff, D., Birkel, C., Dick, J., Geris, J. and Soulsby, C.: Storage dynamics in hydropedological units control hillslope connectivity, runoff generation, and the evolution of catchment transit time distributions, Water Resour. Res., 50(2), 969–985, doi:10.1002/2013WR014147, 2014.

Tetzlaff, D., Buttle, J., Carey, S. K., McGuire, K., Laudon, H. and Soulsby, C.: Tracer-based assessment of flow paths, storage and runoff generation in northern catchments: a review, Hydrol. Process., 29(16), 3475–3490, doi:10.1002/hyp.10412, 2015.

Thornton, J. M., Mariethoz, G. and Brunner, P.: A 3D geological model of a structurally complex Alpine region as a basis for interdisciplinary research, Sci. Data, 5, 180238, doi:10.1038/sdata.2018.238, 2018.

Trujillo, E. and Molotch, N. P.: Snowpack regimes of the Western United States, Water Resour. Res., 50(7), 5611–5623, doi:10.1002/2013wr014753, 2014.

Tunaley, C., Tetzlaff, D., Birkel, C. and Soulsby, C.: Using high resolution isotope data and

alternative calibration strategies for a tracer-aided runoff model in a nested catchment, Hydrol. Process., 31(22), 3962–3978, doi:10.1002/hyp.11313, 2017.

Uehara, Y. and Kume, A.: Canopy Rainfall Interception and Fog Capture by Pinus pumila Regal at Mt. Tateyama in the Northern Japan Alps, Japan, Arctic, Antarct. Alp. Res., 44(1), 143–150, doi:10.1657/1938-4246-44.1.143, 2012.

Ulseth, A. J., Bertuzzo, E., Singer, G. A., Schelker, J. and Battin, T. J.: Climate-Induced Changes in Spring Snowmelt Impact Ecosystem Metabolism and Carbon Fluxes in an Alpine Stream Network, Ecosystems, 21(2), 373–390, doi:10.1007/s10021-017-0155-7, 2018.

Unnikrishna, P. V, McDonnell, J. J. and Kendall, C.: Isotope variations in a Sierra Nevada snowpack and their relation to meltwater, J. Hydrol., 260(1–4), 38–57, doi:10.1016/S0022-1694(01)00596-0, 2002.

Vaché, K. B. and McDonnell, J. J.: A process-based rejectionist framework for evaluating catchment runoff model structure, Water Resour. Res., 42(2), doi:10.1029/2005WR004247, 2006.

Varin, C., Reid, N. and Firth, D.: AN OVERVIEW OF COMPOSITE LIKELIHOOD METHODS, Stat. Sin., 21(1), 5–42 [online] Available from: http://www.jstor.org/stable/24309261, 2011.

Vasdekis, V. G. S., Rizopoulos, D. and Moustaki, I.: Weighted pairwise likelihood estimation for a general class of random effects models, Biostatistics, 15(4), 677–689, doi:10.1093/biostatistics/kxu018, 2014.

Viviroli, D., Durr, H. H., Messerli, B., Meybeck, M. and Weingartner, R.: Mountains of the world, water towers for humanity: Typology, mapping, and global significance, Water Resour. Res., 43(7), doi:W0744710.1029/2006wr005653, 2007.

Vrugt, J. A., Gupta, H. V, Bouten, W. and Sorooshian, S.: A Shuffled Complex Evolution Metropolis algorithm for optimization and uncertainty assessment of hydrologic model parameters, Water Resour. Res., 39(8), doi:10.1029/2002WR001642, 2003.

Wagnon, P., Ribstein, P., Kaser, G. and Berton, P.: Energy balance and runoff seasonality of a Bolivian glacier, Glob. Planet. Change, 22, 49–58, 1999.

Wang, L., van Meerveld, H. J. and Seibert, J.: When should stream water be sampled to be most informative for event-based, multi-criteria model calibration?, Hydrol. Res., 48(3), doi:10.2166/nh.2017.197, 2017.

Wang, L., von Freyberg, J., van Meerveld, I., Seibert, J. and Kirchner, J. W.: What is the best time to take stream isotope samples for event-based model calibration?, J. Hydrol., 577,

123950, doi:10.1016/J.JHYDROL.2019.123950, 2019.

Weijs, S. V, Mutzner, R. and Parlange, M. B.: Could electrical conductivity replace water level in rating curves for alpine streams?, Water Resour. Res., 49(1), 343–351, doi:10.1029/2012WR012181, 2013.

Weingartner, R., Barben, M. and Spreafico, M.: Floods in mountain areas—an overview based on examples from Switzerland, J. Hydrol., 282(1), 10–24, doi:https://doi.org/10.1016/S0022-1694(03)00249-X, 2003.

Wels, C., Cornett, R. J. and Lazerte, B. D.: Hydrograph separation: A comparison of geochemical and isotopic tracers, J. Hydrol., 122(1), 253–274, doi:10.1016/0022-1694(91)90181-G, 1991a.

Wels, C., Taylor, C. H., Cornett, R. J. and Lazerte, B. D.: Streamflow generation in a headwater basin on the precambrian shield, Hydrol. Process., 5(2), 185–199, doi:10.1002/hyp.3360050206, 1991b.

Wen, R., Tian, L., Weng, Y., Liu, Z. and Zhao, Z.: The altitude effect of δ 18O in precipitation and river water in the Southern Himalayas, Chinese Sci. Bull., 57(14), 1693–1698, doi:10.1007/s11434-012-4992-7, 2012.

Wester, P., Mishra, A., Mukherji, A. and Shrestha, A. B.: The Hindu Kush Himalaya Assessment, edited by P. Wester, A. Mishra, A. Mukherji, and A. B. Shrestha, Springer International Publishing., 2018.

Wever, N., Comola, F., Bavay, M. and Lehning, M.: Simulating the influence of snow surface processes on soil moisture dynamics and streamflow generation in an alpine catchment, Hydrol. Earth Syst. Sci., 21(8), 4053–4071, doi:10.5194/hess-21-4053-2017, 2017.

Willmott, C. J., Rowe, C. M. and Mintz, Y.: Climatology of the terrestrial seasonal water cycle, J. Climatol., 5(6), 589–606, 1985.

Winograd, I. J., Riggs, A. C. and Coplen, T. B.: The relative contributions of summer and cool-season precipitation to groundwater recharge, Spring Mountains, Nevada, USA, Hydrogeol. J., 6(1), 77–93, doi:10.1007/s100400050135, 1998.

Woods, R., Larsen, J. R., Schaefli, B. and Ceperley, N. C.: In a Warming World, Is Snowmelt Slower or Faster? Geophysical Research Abstracts,Vol. 21, EGU2019-9606 . Oral presentation, in EGU General Assembly, Vienna. [online] Available from: https://meetingorganizer.copernicus.org/EGU2019/EGU2019-9606.pdf, 2019.

Woods, R. A.: Analytical model of seasonal climate impacts on snow hydrology: Continuous

snowpacks, Adv. Water Resour., 32(10), 1465–1481, doi:10.1016/j.advwatres.2009.06.011, 2009.

Yang, D., Marsh, P. and Ge, S.: Heat flux calculations for Mackenzie and Yukon Rivers, Polar Sci., 8(3), 232–241, doi:10.1016/j.polar.2014.05.001, 2014.

Zappa, M., Vitvar, T., Rücker, A., Melikadzé, G., Bernhard, L., David, V., Jans-Singh, M., Zhukova, N. and Sanda, M.: A Tri-national program for estimating the link between snow resources and hydrological droughts, Proc. Int. Assoc. Hydrol. Sci., 369, 25–30, doi:10.5194/piahs-369-25-2015, 2015.

Zhu, X., Wu, T., Zhao, L., Yang, C., Zhang, H., Xie, C., Li, R., Wang, W., Hu, G., Ni, J., Du, Y., Yang, S., Zhang, Y., Hao, J., Yang, C., Qiao, Y. and Shi, J.: Exploring the contribution of precipitation to water within the active layer during the thawing period in the permafrost regions of central Qinghai-Tibet Plateau by stable isotopic tracing, Sci. Total Environ., 661, 630–644, doi:10.1016/J.SCITOTENV.2019.01.064, 2019.

Zohner, C. M. and Renner, S. S.: Ongoing seasonally uneven climate warming leads to earlier autumn growth cessation in deciduous trees, Oecologia, doi:10.1007/s00442-019-04339-7, 2019.

Zongxing, L., Qi, F., Wei, L., Tingting, W., Xiaoyan, G., Zongjie, L., Yan, G., Yanhui, P., Rui, G., Bing, J., Yaoxaun, S. and Chuntan, H.: The stable isotope evolution in Shiyi glacier system during the ablation period in the north of Tibetan Plateau, China, Quat. Int., 380, 262–271, doi:10.1016/j.quaint.2015.02.013, 2015.